



UNIVERSITAT  
POLITÈCNICA  
DE VALÈNCIA



ESCUELA TÉCNICA  
SUPERIOR INGENIEROS  
INDUSTRIALES VALENCIA

**Academic year:**

## **Appreciations**

Firstly, I would like to thank my tutor Mr. Alberto José Campillo Fernández for giving me the opportunity to work with him and to perform my studies for my end of degree project in the "Centro de Biomateriales e Ingeniería Tisular" (CBIT) in the "Universidad Politécnica de Valencia" (UPV).

I would also like to thank everyone involved in the CBIT for their support throughout my stay, for having helped me to resolve problems when needed and having helped me advance in my education both in the investigation field as well as in my general education. I would like to specially thank Laura Teruel Bioscá, the laboratory technician present in the CBIT, for having taught me how many of the systems and machines I have worked with function.

I would also like to thank the Electron Microscopy Service of the Technical University of Valencia for having let me use their facilities in our investigation.

Finally, I would like to thank everyone who has been there to support me throughout my career and life, namely my family, friends, teachers, trainers and anybody who has been there to teach, correct, help, motivate and support me both in the good and bad situations through which I have gone through.

---



## Resumen

El presente Trabajo Final de Grado pretende crear un material híbrido basado en la policaprolactona - que se ha usado ampliamente como biomaterial biodegradable - reforzado con óxido de grafeno, con el objetivo de dotar al sistema de mayor versatilidad para poder anclar moléculas de interés biológico a la par que poder ajustar sus propiedades físico-químicas a voluntad. Asimismo, los materiales se han sometido a un proceso de degradación acelerada en diferentes pH con objeto de conocer su cinética de degradación.

Para ello, se ha sintetizado una serie de híbridos variando la cantidad de óxido de grafeno, GO. El efecto de la incorporación de diferentes cantidades de GO en función del tiempo de degradación se estudió a través de varias técnicas de caracterización, como la pérdida de peso, el grado de hinchamiento, así como las propiedades morfológicas y térmicas. Asimismo, se analizó mediante rayos X la cristalinidad de las muestras.

A través del estudio de la pérdida de peso se pudo observar que la degradación fue mucho más rápida en medio básico, pH 13, que en medio ácido, pH 1. Los cambios morfológicos de las muestras fueron estudiados a través de microscopía electrónica de barrido observándose una degradación más rápida en las muestras sometidas a pH 13. Las propiedades térmicas de los materiales fueron analizadas mediante calorimetría diferencial de barrido (DSC) con la que se obtuvo información sobre la cristalinidad de las muestras y el pico de la temperatura de fusión en función de la cantidad de GO, tiempo de degradación y pH.

---



## Resum

El present Treball Final de Grau preten crear un material híbrid basat en la policaprolactona - que s'ha emprat amplament com biomaterial biodegradable - reforçat en oxid de grafeno, en l'objectiu de dotar al sistema de major versatilitat per a poder ancorar molècules d'interès biològic al par que poder ajustar les seues propietats físico-químiques a voluntat. Aixina mateixa, els materials s'han somes a un proces de degradació accelerada en diferents pH en objecte de coneixer la seua cinètica de degradació.

Per a això, s'ha sintetitzat una serie d'híbrids variant la quantitat d'oxid de grafeno, GO. L'efecte de l'incorporació de diferents quantitats de GO en funció del temps de degradació s'estudià a través de varies tècniques de caracterisació, com la pèrdua de pes, el grau d'unflament, aixina com les propietats morfològiques i tèrmiques. Aixina mateixa, s'analitzà mitjançant raigs X la cristalinidat de les mostres.

A través de l'estudi de la pèrdua de pes se pogué observar que la degradació fon molt més ràpida en mig bàsic, pH 13, que en mig àcid, pH 1. Els canvis morfològics de les mostres foren estudiats a través de microscòpia electrònica d'agranat observant-se una degradació més ràpida en les mostres someses a pH 13. Les propietats tèrmiques dels materials foren analitzades mitjançant calorimetria diferencial d'agranat (DSC) en la que s'obtingué informació sobre la cristalinidat de les mostres i el bec de la temperatura de fusió en funció de la quantitat de GO, temps de degradació i PH.

---



## **Abstract**

The present End of Degree Project aims to create a hybrid material based on Poly( $\epsilon$ -caprolactone) - which has been widely used as a biodegradable biomaterial - reinforced with graphene oxide, with the aim of providing the system with greater versatility when anchoring molecules of biological interest, as well as being able to adjust its physico-chemical properties at will. Also, the materials have undergone an accelerated degradation process at different pH values in order to know their degradation kinetics.

In order to do so, a series of hybrids have been synthesized by varying the amount of graphene oxide, GO. The effect of the incorporation of different amounts of GO as a function of degradation time was studied through several characterization techniques, such as weight loss and degree of swelling, along with their morphological and thermal properties. Likewise, the crystallinity of the samples were analyzed by X-ray.

Through the study of weight loss it was observed that the degradation was much faster in basic medium, pH 13, than in acid medium, pH 1. The morphological changes of the samples were studied through scanning electron microscopy, and a faster degradation in the samples subjected to pH 13 was observed. The thermal properties of the materials were analyzed by differential scanning calorimetry (DSC) through which information on the crystallinity of the samples and the peak of the melting temperature in function of the amount of GO, degradation time and pH, were observed.

---





# DESCRIPTIVE MEMORY INDEX

I.	DESCRIPTIVE MEMORY .....	1
1	INTRODUCTION .....	1
1.1	Background .....	1
1.1.1	Biodegradable polymers .....	4
1.1.2	Synthetic Biodegradable Polymers.....	8
1.1.3	Carbonaceous Materials as fillers.....	14
1.1.4	PCL/GO Biocomposites .....	18
1.1.5	Degradation Mechanisms .....	23
1.2	Motivation.....	33
1.3	Justification .....	33
2	OBJECTIVES.....	34
3	POLICIES.....	35
4	Extension of Applications and Range of Solutions .....	37
4.1	Experiment Design .....	37
4.2	Materials .....	37
4.2.1	Poly( $\epsilon$ -caprolactone)/GO hybrids .....	37
4.2.2	Degradation solutions .....	37
4.3	Synthesis .....	38
4.4	Degradation study .....	43
4.5	Characterization .....	46
4.5.1	Weight Loss and Equilibrium Water Content .....	46
4.5.2	Scanning Electron Microscopy (SEM).....	47
4.5.3	Differential Scanning Calorimetry (DSC).....	48
4.5.4	X-Ray Diffraction (XRD).....	49
5	PRESENTATION AND ANALYSIS OF THE RESULTS .....	50
5.1	Synthesized Materials .....	50
5.2	Characterization Study.....	50
5.2.1	Weight Loss - Equilibrium Water Content.....	50
5.2.2	Visual examination and scanning electron microscopy (SEM).....	57
5.2.3	DSC .....	67

---

5.2.4	X-Ray Diffraction.....	74
6	CONCLUSIONS .....	76
7	REFERENCES .....	78
II.	ATTACHMENTS .....	88
1	About the obtaining of the hybrid materials.....	88
1.1.1	Selection of a suitable solvent .....	88
1.1.2	Trial and error experiments previous to the final synthesis technique .....	90
1.1.3	Scanning Electron Microscopy (SEM) images .....	94
1.1.4	Differential Scanning Calorimetry (DSC) Graphs. ....	100

# I. DESCRIPTIVE MEMORY

## 1 INTRODUCTION

### 1.1 Background

For many years biodegradable materials and biocomposite hybrids have been widely studied due to the many advantages and possibilities they offer in the branch of biomedical science. The great achievements made in biomedical science in the past decades, and the possibilities they have to offer, have sparked the interest of both the public and researchers alike. The great step forward in the branch of biomedical science is greatly due to the discovery of biopolymers, which have proven to have a good biocompatibility with the human organism, as well as a wide range of properties which can give rise to a large amount of applications.

In biomedicine, a biomaterial can be defined as “any substance or combination of substances, with a natural or synthetic origin, designed to act interfacially with biological systems with the objective of evaluating, treating, increasing or substituting any tissue, organ or function in the human organism” (Williams, 1999). The essential property of a biomaterial is its biocompatibility, which is "the ability of a material to perform with an appropriate host response in a specific application" (Williams, 1999). In other words, this is the capability of the material to mimic the properties of the biological surroundings of its host, so that the host accepts the biomedical implant without rejecting it and causing infections or inflammations. When working with biomaterials it is essential to know two fundamental aspects of their behaviour when implanted: the effects of the implant on the organism, and the effects of the organism on the implant. In general, a biomaterial must comply with the following properties(Nair & Laurencin, 2007):

- The material must not contain components which are soluble in the organism unless it is intended to fulfil a specific need, for example, in the liberation of drugs.
- The organism must not degrade the implant unless said degradation is intentional, for example, in biodegradable sutures.
- The implant must be sterilized and free of bacteria and endotoxins adhered onto the walls of the cells of the bacteria.
- The material must be biocompatible, being this context extendable to the carcinogenic potential of the material, as well as the interaction it has with the immunologic system of which it will take part.
- The physical and mechanical properties of the polymer must be the most appropriate for the finality and application of the implant. For example, a substituted tendon must have an adequate tension modulus, a dialysis membrane must have the necessary permeability, and a hip joint implant must have a low friction coefficient. The polymers must maintain their properties for their expected lifespans, even when they have started to degrade.

Polymers used for medical-surgical applications can usually be classified into different families depending on their properties and origin. Firstly, they can be classified in terms of how much time the implant must maintain its functionality as an implant, in other words, from a biodegradation point of view.

- There are those biomaterials which must have a permanent character when working as an implant, such as systems and devices used to partially or fully substitute tissues or organs destroyed as a consequence of an illness or trauma. These polymers are called biostable and are considered biocompatible, but not biodegradable.
- Secondly there are those polymers which are considered degradable and are used for temporary applications. These implants must maintain their functionality adequately during a certain period of time, due to the capability of the human organism to cure and regenerate a damaged area or tissue. As the material is biocompatible, it is accepted by the host and it starts to degrade a certain time after its implantation giving rise to non-toxic products that can be eliminated or metabolized by the organism.

Although the previous classification of polymers gives us an idea of the properties and possible applications of a material, biopolymers tend to be classified into those which have a natural origin - animal, plant and microbial - and those which are created artificially, called synthetic polymers (Hull & Clyne, 1996) (Nair & Laurencin, 2006). Table 1 below summarizes the classification of biodegradable polymers in terms of their origin.

Table 1. Classification of biodegradable polymers, adapted from (Mansur, Curti, & other, 2013).

Natural Polymers		Synthetic Polymers	
Sub-classification	Examples	Sub-classification	Examples
1. Plant origin		1. Aliphatic polyesters	
1.1 Polysaccharides	Cellulose, Starch, Alginate	1.1 Glycol and dicarbonic acid polycondensates	Poly(ethylene succinate), Poly(butylene terephthalate)
2. Animal origin		1.2 Polylactides	Polyglycolide, Polylactides
2.1 Polysaccharides	Chitin (Chitosan), Hyaluronate	1.3 Polylactones	Poly( <i>ε</i> -caprolactone)
2.2 Proteins	Collagen (Gelatin), Albumin	1.4 Miscellaneous	Poly(butylene terephthalate)
3. Microbe origin		2. Polyols	Poly(vinyl alcohol)
3.1 Polyesters	Poly(3-hydroxyalkanoate)	3. Polycarbonates	Poly(ester carbonate)
3.2 Polysaccharides	Hyaluronate	4. Miscellaneous	Polyanhydrides, Poly( <i>α</i> -cyanoacrylate)s, Polyphosphazenes, Poly(orthoesters)

In the past two decades significant advances have been achieved in the branch of biomedicine with the discovery of a wide range of biomaterials with a great biodegradability and biocompatibility. Biomaterials such as Poly(L-lactide) and Poly( $\epsilon$ -caprolactone) (PCL) have been widely used in a great variety of biomedical applications such as drug delivery systems, bone fixation devices (Figure 1.1a), vascular grafts (Figure 1.1b), gene delivery systems and tissue engineering (Guo, Glavas, & others, 2013). Taking

into account the diversity and complexity of the possible applications that a biopolymer can have, a wide range of biomaterials have been, and continue to be synthesized.

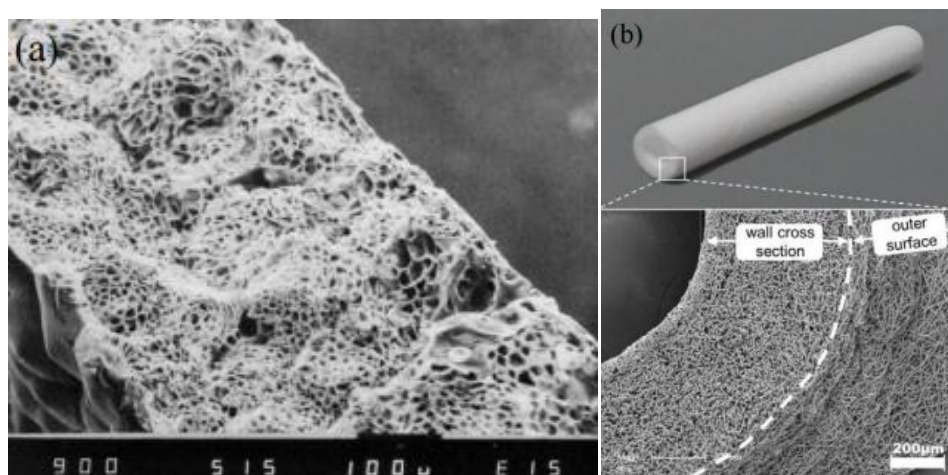


Figure 1 (a) SEM (scanning electron microscope) of the outer surface of a Poly(L-lactide) membrane developed to cover bone deficiencies (Meinig, Rahn, & others, 1996), and (b), a vascular graft made of electrospun Polycaprolactone micro and nano-fibres (Valence, Tille, & other, 2012).

This requirement is the primary motivation in the development of biocomposites. To enhance the properties of the original polymer, they can be modified to create copolymers or biocomposites. The so-called hybrid biocomposite materials consist of a polymeric matrix reinforced with a filler of a different nature (Hull & Clyne, An introduction to Composite materials., 1996) which can enhance certain properties of the original polymer and compensate for its deficiencies in certain applications. This results in a hybrid material with new or improved properties which can give rise to very interesting, and possibly innovative applications. Lately, there has been a huge interest in the development of hybrids with the use of nanomaterials such as nano-clays, hydroxyapatite and carbonaceous materials as fillers. (Tjong, 2012) (Gaharwar, Sant, & other, 2013).

In the present article the incorporation of graphene oxide (GO) into a Poly( $\epsilon$ -caprolactone) (PCL) matrix to form a PCL/GO hybrid is going to be studied. PCL is a biodegradable polymer with a synthetic origin which has been used in a broad range of applications such as sutures, wound dressings, contraceptive and bone fixation devices, dentistry, and most recently, tissue engineering and 3D printing (He, Kilsby, & other, 2013) (Woodroof & Hutmacher, 2010). The incorporation of GO into the PCL matrix seeks to significantly enhance the mechanical properties of the material, as well as potentially providing an anchor point for bioactive substances due to GO's relative ease to react with these substances through its functional groups.

### 1.1.1 Biodegradable polymers

In the last decades of the twentieth century there was a shift in the use of biostable polymers of a permanent character to those which are hydrolytically and enzymatically degradable. Following this trend, in the next few decades many of the prosthetic devices of a permanent character used for temporary therapeutic applications will be replaced by biodegradable devices that can assist the body in repairing and regenerating the damaged tissue. The major factor which is influencing this change is the long-term biocompatibility issues which arise with plenty of the existing, permanent character implants in use nowadays, along with technical and moral issues which arise in relation with revision surgeries. Another reason for this change is the arrival of new, innovative biomedical technologies such as tissue engineering, regeneration medicine, gene therapy, controlled drug delivery and bionanotechnology, which need a biodegradable platform to build on (Nair & Laurencin, 2007).

Polymeric degradable materials can undergo degradation through the cleavage of hydrolytically or enzymatically sensitive bonds present in their chain leading to the disintegration of the polymer (Katti & Laurencin, 2002). Both natural and synthetic polymers can undergo said degradation under both mechanisms, although most naturally occurring polymers undergo enzymatic degradation (Nair & Laurencin, 2007).

Natural biopolymers are complex, heterogeneous and difficultly characterizable and processable materials. Due to the origin of these polymers (obtained from living beings such as plants, animals, seaweed or even fungi), the use of natural biopolymers seems like the best option for biomedical applications due to their excellent biocompatibility and bioactivity, ability to present receptor-binding ligands to cells, susceptibility to cell-triggered proteolytic degradation and natural remodeling. Despite this, some fundamental disadvantages of natural polymers also arise from their bioactivity, namely a strong immunogenic response associated with most of the polymers, the complexities associated with their purification and the possibility of disease transmission. Furthermore, there is a considerable variation in properties from batch to batch, and the rate of *in vivo* degradation of enzymatically degradable polymers can vary considerably depending on the site of implantation. The degradation is affected by the availability and concentration of enzymes, which can be very variable inside the human organism, hindering problems when designing an application for the polymer. Chemical modification can also influence the rate of degradation and properties of the polymer. Functional groups can be introduced in the monomer units or directly into the polymeric chains to grant the polymer with new useful properties (Nair & Laurencin, 2006) (Barbucci, 2002)(Nair & Laurencin, 2007).

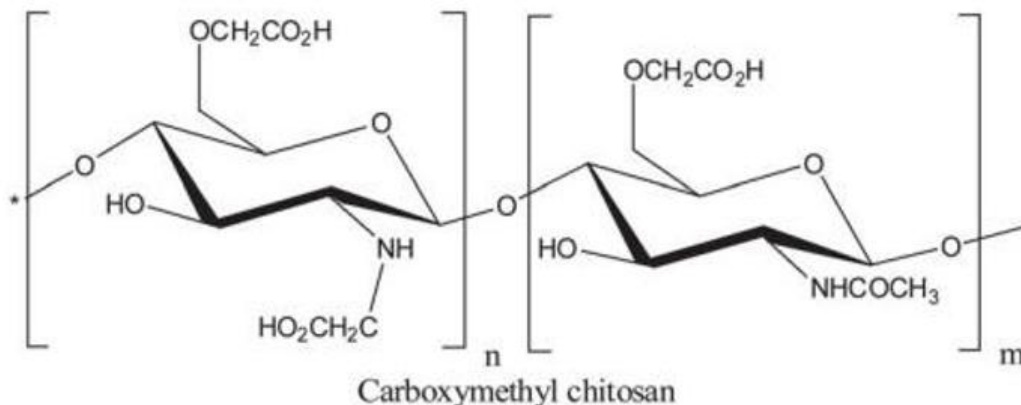


Figure 2. Structure of a natural biopolymer (chitosan) functionalized for nanomedicine applications, adapted from (Mansur, Curti, & other, 2013).



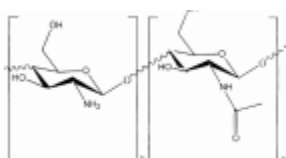
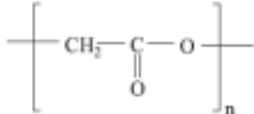
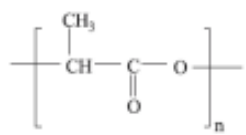
Polysaccharides and proteins are naturally occurring biopolymers which are typically used for biomedical applications (Tian, Tang, & other, 2012). Polysaccharides are high molecular weight polymeric carbohydrates composed of one or more monosaccharide repetition units (Schuerch, 1972). Some of the advantages that polysaccharides offer for biomedical uses is their low cost, high availability, high diversity in its structure and the presence of functional groups of interest in their polymeric chain (Khan & Ahmad, 2013) (Li, Leung, & other, 2010). Proteins are high molecular weight polymers which consist of repetition units of amino acids attached via peptide linkages (Nair & Laurencin, 2006). An attractive property of both proteins and polysaccharides, particularly the latter, is their ability to absorb water (swellability), which makes them ideal for the creation of hydrogels (Nair & Laurencin, 2006) (Lindblad Margaretha, Sjöberg, & other, 2007) (Leone & Barbucci, 2009).

Many of the problems associated with natural biopolymers can be usually fixed by the creation of the so-called synthetic polymers, which are generally synthesized from monomer units to satisfy specific applications. Synthetic biomaterials have a more predictable behaviour and more consistent properties between batches than natural biopolymers (Nair & Laurencin, 2006) (Barbucci, 2002). This is due to the fact that synthetic polymers are man-made and are created through certain reactions or procedures from monomer units to create polymer chains, so their final structure, and therefore properties, are more consistent and predictable. Hydrolytically degradable polymers are generally preferred as implants compared to enzymatically degradable polymers because their degradation changes very slightly from site-to-site and between patients, resulting in a more predictable behaviour. In general, synthetic polymers have attracted the attention since their first implantation in the 1960's due to their predictive erosion kinetics as drug/gene delivery vehicles or as scaffolds for tissue engineering (Nair & Laurencin, 2006).

In Table 2 below the most commonly used polymers in biomedical applications are described.



Table 2: The most commonly used polymers in biomedical applications, as adapted from (Sayyar, 2014).

Polymer	Major applications	Major advantages/disadvantages
<p>Collagen</p>  <p>Triple helix of various proteins.</p>	Development of suture materials and biomedical devices.	High risk of infection and inflammation, high cost, variable physico-chemical and degradation properties.
<p>Gelatin</p> <p>An irreversibly hydrolyzed form of collagen.</p>	Tissue engineering, development of hydrogels.	Excellent swelling properties.
<p>Alginate</p> 	Development of hydrogels drug and cell delivery devices and wound healing patches, tissue engineering.	Poor enzymatic degradability, cellular adhesion and mechanical properties
<p>Chitosan</p> 	Artificial skin, tissue engineering, drug delivery, development of hydrogels, wound healing applications.	Hemostatic properties, excellent swelling properties.
<p>Poly(glycolic acid) (PGA)</p> 	Suture anchors, medical devices, drug delivery, tissue engineering	Low processability (high melting point and low solubility in organic solvents), high degradation rate.
<p>Poly lactides</p> 	Orthopaedic implants, drug delivery	Slow degradation rate and high melting point.



### 1.1.2 Synthetic Biodegradable Polymers

As mentioned previously, the use of synthetic polymers is ever-growing due to the fact that many of the problems which arise from the use of biologically derived polymers can be avoided by using an appropriate synthetic polymer. Furthermore, the properties of a synthesized polymer are much more predictable and therefore possible applications are much easier to design. Since biopolymers with diverse specific properties are needed for *in vivo* applications because of the diversity and complexity of *in vivo* environments (Tian, Tang, & other, 2012), the use of synthetic polymers seems perfect for this purpose. Aliphatic polyesters are the most common synthetic polymers used in biomedicine, although there are plenty more which have also proven to have a huge potential in this field.

#### Aliphatic Polyesters.

Aliphatic polyesters have been present in the biomedical field for various decades. The synthesis of polyesters can be done through the polycondensation of diacids, diols and hydroxi acids or by polymerization through ring opening of cyclic diesters, lactones, glycolides and lactides (Nair & Laurencin, 2006) (Barbucci, 2002) (Okada, 2002). Some polyesters can also be synthesized through bacterial bioprocessing (Lenz & Marchessault, 2004). The initial aliphatic polyesters showed little desirable properties such as a low hydrolytic stability, low fusion temperatures and low molecular weights. Their low hydrolytic stability was taken advantage of when they started being used in applications such as absorbable stitches (Kulkarni, Moore, & other, 1971). As new synthesis techniques and catalytical systems emerged it was possible to create polyesters with a larger molecular weight and with a much narrower molecular weight distribution (Kricheldorf & Langanke, 2002) (Bhaw-Luximon, Jhurry, & other, 2001) (Jedlinski, Walach, & other, 1991).

Monomers such as lactide, glycolide and caprolactone are some of the most commonly used monomers for the synthesis of aliphatic polyesters, such as Poly(caprolactone).

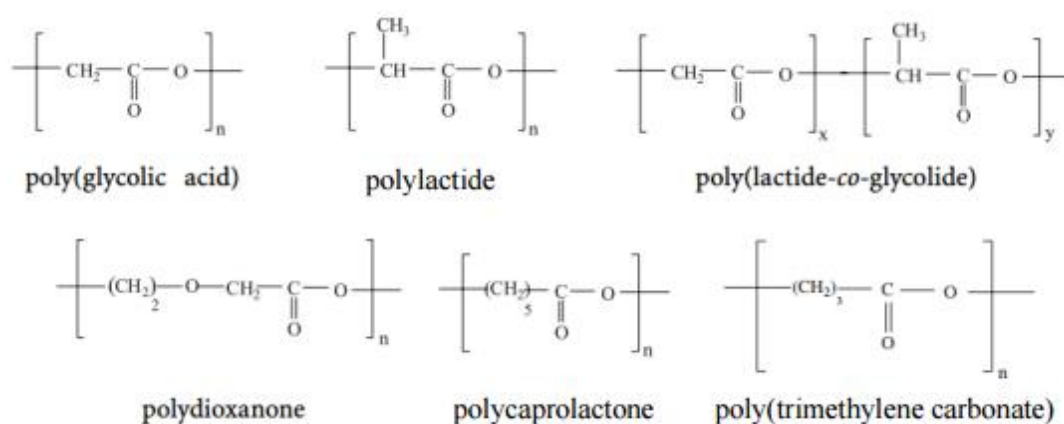


Figure 3: Structure of common aliphatic polyesters, as adapted from (Sayyar, 2014).

### 1.1.2.1 Poly( $\epsilon$ -caprolactone) (PCL)

In the early 1930's, Carothers group synthesized PCL (it was one of the earliest polymers to be synthesized) due to the necessity of identifying polymers which could be degraded by enzymatic pathways (Hill, Carothers, & other, 1934) (Huang S. , 1985). It is a semi-crystalline aliphatic polyester which is suitable for biomedical applications because it is biocompatible and biodegradable (Dash & Konkimalla, 2012).

It is a polymer, which together with its co-polymers and hybrid biocomposites, can have a broad range of applications, as shown in figure 4. It has mainly been studied for its use in controlled drug delivery systems and tissue engineering applications (Dash & Konkimalla, 2012).

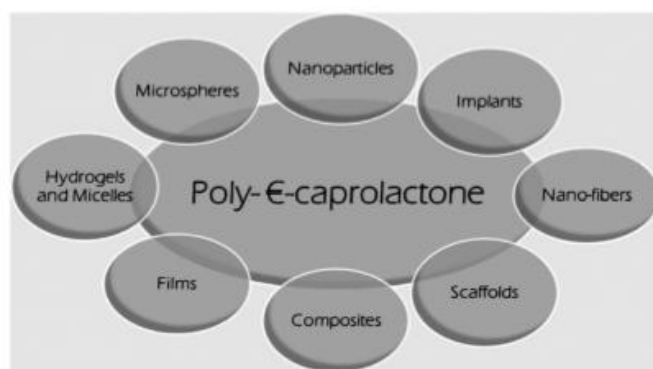


Figure 4: Various applications which can be given to PCL and its co-polymers, as adapted from (Dash & Konkimalla, 2012).

PCL can be synthesized by various reaction pathways. Its polymerization can be accomplished through cationic, anionic, radical and co-ordination mechanisms, and the final properties of the polymer such as molecular distribution, molecular weight, end group composition and the chemical structure are all affected by the synthesis mechanism pathway (Okada, 2002). The most commonly used synthesis techniques to obtain PCL are the ROP (ring-opening polymerization) of the cheap cyclic monomer  $\epsilon$ -caprolactone and via free radical ring-opening polymerization of 2-methylene-1-3-dioxepane (Pitt C. , 1990). The synthesis reactions can be catalyzed with the use of stannous octoate and the molecular weight of the resulting polymer can be controlled using low molecular weight alcohols (Storey & Taylor, 1996).

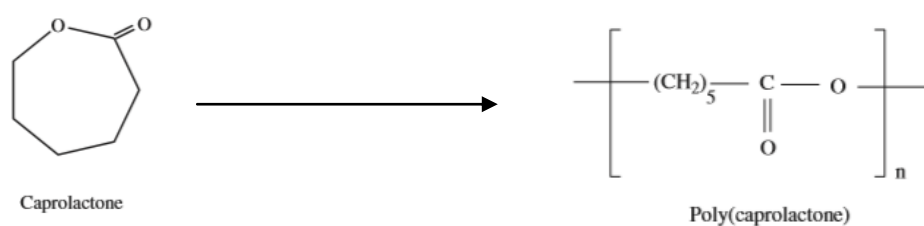


Figure 5. Synthesis of PCL through ROP of  $\epsilon$ -caprolactone, as adapted from (Nair & Laurencin, 2007).

PCL has a low glass transition temperature ( $T_g \approx -60^\circ\text{C}$ ), which permits the amorphous phase to exhibit a high chain flexibility at body temperature, granting the polymer chains with a high molecular mobility (Harrison & Jenkins, 2004). Due to its semi-crystalline nature, which grants an easy formability at low temperatures, it has a melting point between 59 and 64°C ( $T_m \approx 60^\circ\text{C}$ ) (Woodroof & Hutmacher, 2010). Another property which makes PCL unusual is its high thermal stability compared to other aliphatic polyesters. These usually have a decomposition temperature ( $T_d$ ) which ranges between 235 and 255°C, whilst PCL has a  $T_d$  of 350°C (Suggs & Mikos, 1996). Due to these thermal properties, PCL exists in a rubbery state at room temperature (Zein, Hutmacher, & other, 2002) and has flexible mechanical attributes (Young's modulus, elasticity, tensile strength, elongation at break) which make it suitable for uses such as wound dressing, contraceptive pills, sutures and dentistry (Woodroof & Hutmacher, 2010) (Estelle, Vidaurre, & other, 2008). As reported by Gunatillake et al., PCL has low tensile strength (approx. 23MPa) but an extremely high elongation at breakage (>700%) (Gunatillake, Mayadunne, & other, 2006). Zein et al. report similar properties, although their results vary probably due to the difference in molecular weight. Their results revealed that solid PCL ( $M_w = 44,000$ ) has a tensile strength of 16MPa, tensile modulus of 400MPa, flexural modulus of 500MPa, elongation at yield of 7.0% and elongation at break at 80%. (Zein, Hutmacher, & other, 2002).

The average molecular weight of PCL samples usually vary from 3000 to 80,000g/mol (although it can have higher molecular weights, as is the case of the PCL used in this project). The molecular weight of the polymer affects both its crystallinity and its degradation process (Hayashi, 1994). The crystallinity of PCL decreases as the molecular weight increases, because when the size of the molecular chains increases, they find it harder to pack themselves into crystalline formations (Woodroof & Hutmacher, 2010).

PCL can be degraded by two mechanisms under physiological conditions. It can either be degraded by enzymatic degradation, or by hydrolytic degradation, which takes place due to the existence of hydrolytically labile aliphatic ester bonds. However, the rate of degradation of high molecular weight PCL is rather slow (3-4 years) due to its hydrophobic properties and significant degree of crystallinity (Nair & Laurencin, 2007) (Harrison & Jenkins, 2004).

One of the advantages which PCL presents over other commercially available polymers is its high processability due to its ease to dissolve in a broad range of organic solvents at room temperature. It is capable of dissolving in solvents such as chloroform, benzene, toluene and dichloromethane. On the other hand, it is incapable of dissolving in polar solvents such as alcohols, petroleum ethers and diethyl ether, and is only partially soluble in acetone, dimethylformamide and acetonitrile (Coulembier, Degée, & other, 2006).

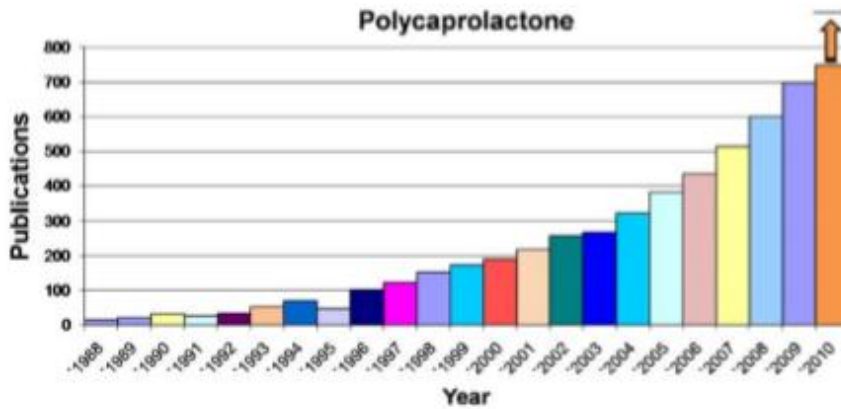
PCL became a popular polymer of interest because it presented numerous advantages over other available polymers at the time. Firstly, the ease through which it can be shaped and manufactured make it ideal for the creation of materials with convenient pore sizes which are useful for tissue in-growth. Furthermore, it has versatile degradation kinetics and

mechanical properties, and has the capacity of releasing drugs contained within its matrix, rendering it suitable as an appropriate drug delivery vehicle. In fact, as a result of its slow degradation, non-toxic properties and high permeability, PCL was originally investigated for its use as a long-term drug/vaccine delivery vehicle (Nair & Laurencin, 2007). As a result, during the 1970's and 1980's, PCL and its copolymers were used in a number of drug-delivery devices (Woodroof & Hutmacher, 2010). The large time span which is necessary for PCL to degrade facilitated drug release for long time periods, whilst uniform drug distribution occurred in the matrix due to its compatibility with an extensive number of drugs (Dash & Konkimalla, 2012). For example, the long-term contraceptive device called Capronor®, which releases Levonorgestrel, is based on this polymer (Nair & Laurencin, 2007).

After years of investigation, PCL has been found to be compatible with naturally occurring polymers such as hydroxy apatite (HA) and chitosan (Wan, Lu, & other, 2009), and synthetic polymers such as poly(ethylene glycol) (PEG) (Chen & Cai, 2010) (Cai, Chang, & other, 2008), poly(urethane) (PU) (Gorna & Gogolewski, 2002) and poly(vinyl alcohol) (PVA) (Sheikh, Barakat, & other, 2009). The modifications made by the copolymerization satisfy the required biophysical properties for most of the formulation currently used in drug delivery. Furthermore, through the addition of functional groups to the polymer chain a higher hydrophilicity, adhesion or biocompatibility can be obtained, all of which facilitate favourable cell responses (Woodroof & Hutmacher, 2010).

However, PCL was put aside for the next two decades in favour of other biodegradable polymers such as poly(lactides) and poly(glycolides). These biopolymers enabled encapsulated drugs to be released within days or weeks with a complete resorption between two to four months posterior to implantation. Furthermore, professionals from the medical device and the drug-delivery industry found that polymers which degraded faster also had less disadvantages linked with the long-term degradation and intracellular resorption pathways (Woodroof & Hutmacher, 2010).

In addition, the mechanical properties of neat PCL are not suitable for high load-bearing applications. Therefore, the medical device industry discarded the use of PCL for the replacement of implants made of metal (screws, nails and plates) in favour of other polymers (Woodroof & Hutmacher, 2010). However, in the past two decades the birth of a new field called tissue engineering has resparked the interest of scientists. The increase in the publications of PCL articles in the past decades can be appreciated in Figure 6 below.



Figure

6. Publications which contain PCL in the field of biomaterials and tissue engineering from 1988 to April 2010. Projected 2010 data is also included. Sourced from Web of Science and adapted from (Woodroof & Hutmacher, 2010).

This resurgence, which has made PCL broadly studied in the past decade for tissue engineering, has stemmed because of its excellent biocompatibility, and the fact that it possesses superior rheological and viscoelastic properties over many of its resorbable-polymer counterparts. Due to these properties, devices based on PCL can be easily manufactured and shaped into an extensive range of structures such as scaffolds, nanospheres, nanofibers, etc., as depicted in Figure 7 below. (Nair & Laurencin, 2007) (Dash & Konkimalla, 2012) (Luciani, Coccoli, & other, 2008) (Lee, Kim, & other, 2003) (Marrazzo, Maio, & other, 2008) (Huang, Oizumi, & other, 2007) (Zein, Hutmacher, & other, 2002). Furthermore, PCL has proved to be an ideal material for tissue engineering due to its non-toxic nature and the discovery that it is cyto-compatible with various body tissues (Dash & Konkimalla, 2012). To top all these advantages off, it has relatively cheap production routes in comparison with other aliphatic polyesters, which make its use in biomedical applications extremely beneficial (Woodroof & Hutmacher, 2010).

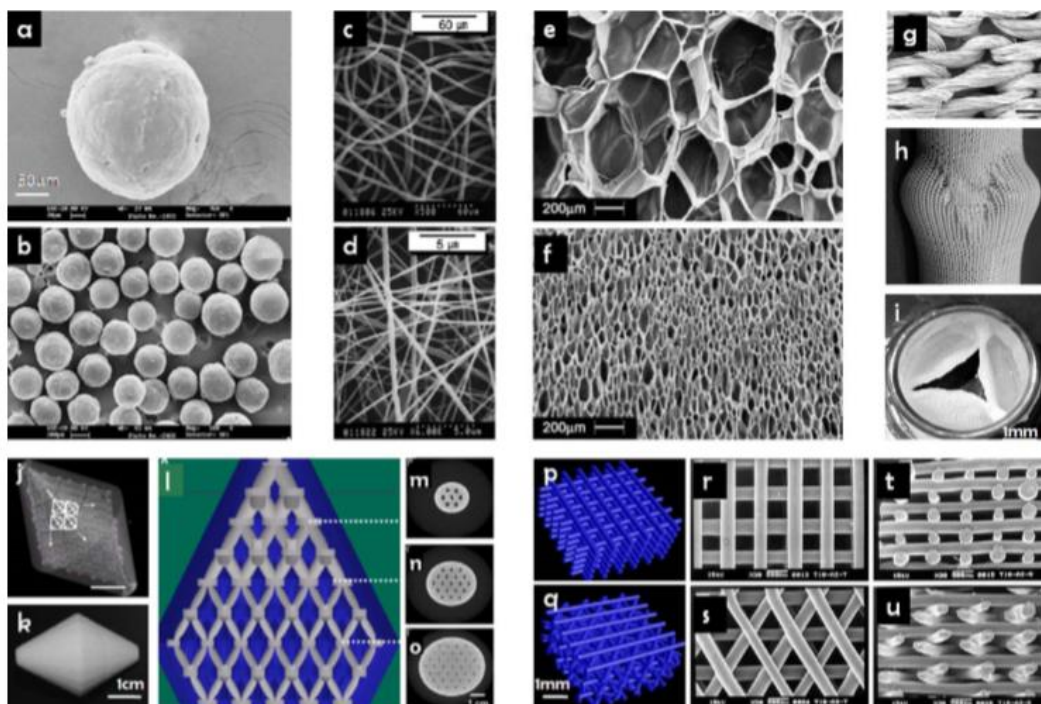


Figure 7. Structures made from PCL: (a,b) Nanospheres, (c,d) nanofibres, (e,f) Foams, (g,h,j) Knitted textiles, (j-o) selective laser sintered scaffold, (p-u) Fused deposition modelled scaffolds, as adapter from (Woodroof & Hutmacher, 2010).

Various materials based on copolymers which contain PCL have been investigated and created in order to improve the slow degradation rate of neat PCL and its properties. The mechanical problems which limited its use in high load bearing applications could be fixed by creating co-polymerical matrices with other polymers. For example, Chiari et al. demonstrated that the copolymerization of PCL with hydroxy apatite (HA) could produce a composite matrix capable of being used as a potential meniscus substitute (Chiari, Koller, & other, 2006). A huge advantage of PCL is that it has the ability to create miscible blends with a broad spectrum of polymers. The mixtures created with different polymers with other desirable properties can modify PCL's physical, mechanical and chemical properties and enhance its behaviour depending on the expected application of the newly created material. In fact, modifying the chemical structure of polymers indirectly alters other crucial properties such as ionic charge, solubility, crystallinity, and degradation patterns, creating polymers with more desirable characteristics for tissue engineering and drug release vehicles (Nair & Laurencin, 2007). Blends of polymers have been created in search of transformed mechanical and degradation properties along with greatly enhanced mechanical properties for their use in tissue engineering in the form of scaffolds, fibers and films. Nowadays, it is commonly used in the preparation of scaffolds for bone and cartilage tissue engineering, and a handful of polymers have been investigated with the objective of altering the thermal, rheological and biophysical properties of PCL depending on its expected use (Dash & Konkimalla, 2012).

There have been investigations that have studied the addition of calcium phosphate based ceramics to PCL matrices as appropriate scaffolds for bone tissue engineering (Mondrinos,



Dembzynski, & other, 2006). Components with higher degradation rates have been produced by the co-polymerization of ' $\epsilon$ -caprolactone' with DL-lactide (Nair & Laurencin, 2007). In a similar manner, fibers with a decreased stiffness than those created with neat poly-glycolide were created through the blending of ' $\epsilon$ -caprolactone' and glycolide, and are commercially available as a monofilament suture called MONACRYL® (Nair & Laurencin, 2007).

### **1.1.3 Carbonaceous Materials as fillers**

A wide range of biomaterials have been created and used to create structures for biomedical applications. However, it is hard to find a polymer that meets all the requirements for developing the perfect material for a certain biomedical application. As a solution to this problem researchers have developed co-polymers - which have been mentioned previously - and biocomposite hybrids, which are typically composed of a biodegradable matrix and a filler, which is used to compensate for the deficiencies of the matrix (Hull & Clyne, 1996). For example, pure polymers tend to be ductile and of a flexible nature, whilst ceramics are considered as stiff and brittle materials. The combination of polymers with ceramics or other fillers can help overcome the disparity in the mechanical properties which exists between the mentioned materials and the natural load-bearing tissues. The mechanical attributes of a polymer, for example the poor mechanical properties of PCL, may be improved with the addition of a ceramic phase, whilst the toughness and ductility of ceramics can be altered by the incorporation of a polymeric phase. Hybrid biocomposites, particularly those composed of polymers and carbonaceous materials, are a perfect example of the optimization of both substances, since the blending of both can grant beneficial properties for devices aimed for biomedical purposes by improving the insufficient characteristics of a single material (Lam, Hutmacher, & other, 2008). The major fillers used to improve the properties of biomaterials are Nano-clays, hydroxyapatite and carbonaceous materials (Tjong, 2012) (Gaharwar, Sant, & other, 2013). With the discovery of biocomposite hybrids, a new dimension of mechanical, physical and chemical properties can be pioneered.

In this article the carbonaceous material graphene oxide is going to be studied as the filler for a PCL biodegradable matrix.

Carbonaceous materials have been extensively employed in the fields of energy, electronics, and biomedicine (Rao, Sood, & others, 2009) (Matthew, Vincent, & others, 2009). Materials such as carbon nanotubes (CNT's), fullerenes, graphite, graphene oxide (GO) and graphene have recently attracted the attention of researchers as composite fillers for biomedical applications due to their unique physicochemical, electrical, thermal, and biological properties (Sayyar, 2014) (Jing, Mi, & others, 2014) (Rao, Sood, & others, 2009) (Matthew, Vincent, & others, 2009) (Chen, Müller, & others, 2008) (Liu, Robinson, & others, 2008). The building block of carbonaceous materials is a single layer of  $sp^2$  hybridized carbon atoms covalently bonded in a honeycomb two-dimensional lattice known as graphene (Sayyar, 2014). Stacked layers of graphene make graphite, graphene

can be rolled up to make CNT's or wrapped into spheres to form fullerenes, as shown in figure 8. All the mentioned carbonaceous fillers owe their properties to graphene.

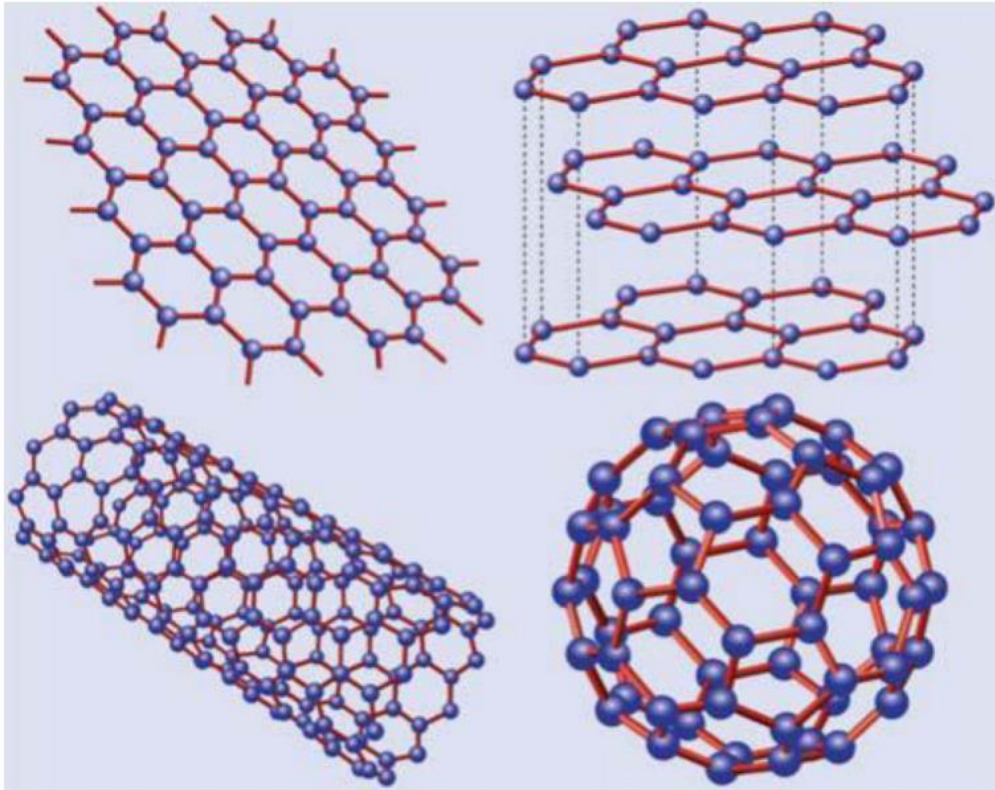


Figure 8: (a) Graphene and other well-known forms of carbon that all derive from graphene: (b) graphite, (c) CNT and (d) fullerene, as adapted from (Tapas, Sambhu, & others, 2010).

### 1.1.3.1 Graphene oxide

Advantageous properties which are attributed to GO such as an excellent flexibility, large Young's modulus, and a low cost compared to CNT's make it an exceptionally good reinforcement for hybrid biocomposites (Song, Gao, & others, 2015). Furthermore, since GO sheets consist of heavily oxygenated graphene which contain functional groups such as hydroxyl, epoxide, diols, ketones and carboxyls, they can considerably improve the van der Waals forces and be more compatible with organic polymers (Tapas, Sambhu, & others, 2010). GO exists as a two-dimensional solid in bulk form which contains strong covalent bonding within its layers. The sheets, or layers, are held together by weak interactions caused by hydrogen-bonding which occurs between intercalated water molecules (Kai, Hirota, & others, 2008).

Graphene oxide (GO) is typically synthesized by the oxidation of graphite using oxidants such as sulphuric acid ( $H_2SO_4$ ), nitric acid ( $HNO_3$ ) and potassium permanganate ( $KMnO_4$ ) using a method described by Hummers and Offeman in 1958 (Hummers W, 1958), which is known as the "Hummers method". However, there are other methods in existence which can be used for the preparation of GO: the method described by Brodie (Brodie EA, 1860), Hummers (Hummers W, 1958), and Staudenmeier (Staudenmaier, 1898). When GO is

synthesized, it continues being a layered structure, but is much lighter in colour than graphite due to the loss of electronic conjugation brought about by the oxidation (Stankovich, y otros, 2007). The carbon sheets in GO contain hydrophilic hydroxyl and epoxy groups located on  $sp^3$  hybridized carbon on the basal plane as well as carbonyl and carboxyl groups situated at the sheet edges on  $sp^2$  hybridized carbon. The functional groups act as reactive sites that can be used for performing a variety of surface modifications on GO as well as developing GO reinforced composites (Sayyar, 2014). These functional groups can give GO beneficial properties as a composite filler over hydroxyapatite (HAp), nanoclays, and other fillers because molecules of interest can be incorporated to them.

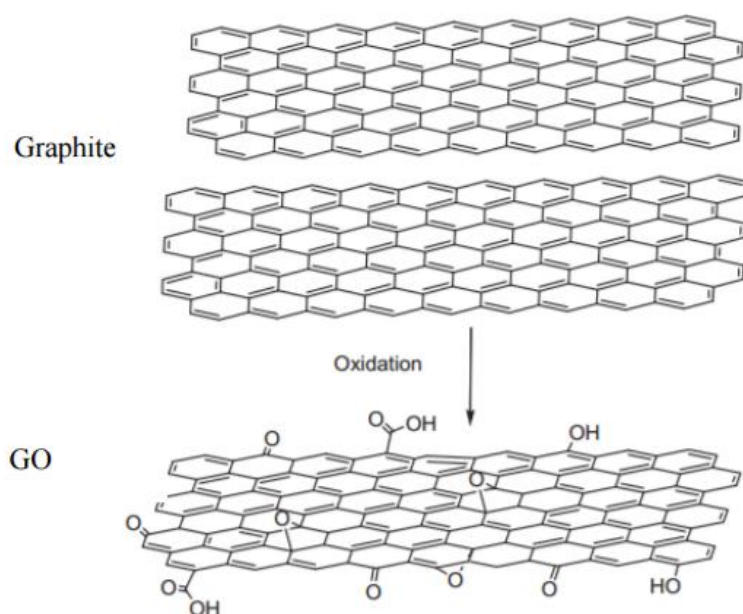


Figure 9: Schematic of oxidation from graphite to GO as adapted from (Sayyar, 2014).

Due to the presence of these functional groups, GO is a highly hydrophilic material which is stable with uniform dispersion in a few polar solvents by electrostatic repulsion (Paredes & Villar-Rodil, 2008) and strong interactions occur between the surface-oxygenated functionalities in GO nanosheets and polymer matrices (Jing & Ming, 2014). Therefore, it is possible to prepare a stable homogenous dispersion of GO in water and some organic solvents that contain mostly single layer sheets, since the graphene oxide can readily swell and disperse in water (Stankovic, Dikin, & others, 2006). In figure 10 the dispersion of GO in water and another 13 organic solvents is studied. It can be observed that GO disperses in some, and is incapable of doing so in others. In all, GO is considered a promising biomaterial for regulating cell behaviours (Chen, Müller, & others, 2008) (Shi & Chang, 2012), enhancing the mechanical properties of the polymer matrices (Kai, Hirota, & others, 2008), as well as loading and releasing drugs or genes (Liu, Robinson, & others, 2008), because of its excellent biocompatibility.

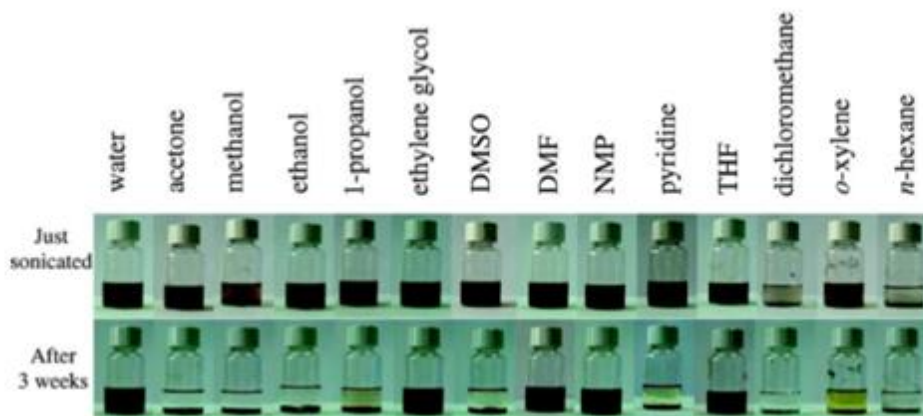


Figure 10: Digital pictures of GO dispersion in water and 13 organic solvents after 1 hour of bath ultrasonication, as adapted from (Paredes & Villar-Rodil, 2008).

The great interest which has arisen from graphene and GO biocomposites is due to their superior properties. These properties can be harnessed to improve the thermal and mechanical properties of polymers by introducing these fillers into a polymeric matrix. Furthermore, the use of GO as a biomaterial is also encouraging because of its excellent biocompatibility (Song, Gao, & others, 2015). Studies have shown that GO and graphene are not only biocompatible but they can also be beneficial in cell growth (Sayyar, 2014). It is worth noting that there was an uncertainty in GO biocompatibility, but reports demonstrated that the toxicity of GO and its effects on cells was dose-dependent and that a low concentration of the substance can exhibit positive effects on cellular behaviours (Correa-Duarte, Wagner, & other, 2004).

In the specific case of GO, GO nanosheets have proved to be effective fillers as a reinforcement for polymers, but they are electrically insulating, which makes their use as fillers unsuitable for the synthesis of electrically conducting hybrids (Tapas, Sambhu, & others, 2010). (Sayyar, 2014). This is because the functional groups of GO disrupt the conjugated electronic structure of the carbon sheets and make them insulators with irreversible defects and disorders (Sayyar, 2014). Despite this, it is possible to chemically reduce GO *in situ* to obtain reduced graphene oxide, which regains graphite's electrical properties (Tapas, Sambhu, & others, 2010).

However, it is possible to partially restore the electrical conductivity of GO close to the level of graphite by *in situ* chemical or thermal reduction to reduced graphene oxide (Tapas, Sambhu, & others, 2010) (Sayyar, 2014). The beneficial properties of having electrical conductivity is that for some applications of the biomedical field it has been shown that electrically conducting substrates can induce and direct improved cell growth of electro-responsive cells under electrical stimulation (Sayyar, 2014). GO is also thermally unstable due to the presence of oxygen functional groups, as it undergoes pyrolysis at elevated temperatures (Stankovich, y otros, 2007).

There are various methods through which carbonaceous fillers can be inserted into a polymeric matrix to develop GO biocomposites. Solution mixing and *in situ*

polymerization are the most typically used methods of synthesis. Melt mixing is another existing technique which consists on the dispersion of a filler inside a polymer matrix in its molten state, but this method is rarely used due to the poor dispersity of the filler inside the polymer matrix, particularly in polymers with high viscosity, as well as the impracticality of this method for processing polymers with high or unknown melting point (Sayyar, 2014).

In this article we have used the technique of solution blending - or solvent casting - to create our biocomposite material of PCL/GO. This is the most commonly used technique for developing GO biocomposites for biomedical applications. The polymer must be soluble in a suitable solvent which must also have the capability to disperse GO. Therefore, solution blending involves solubilization of the polymer into a homogenous solvent-dispersed GO dispersion that is a suitable solvent for the polymer. The polymer chains cover the GO sheets during the blending, and those sheets become interconnected after removing the solvent through evaporation or other methods. Some problems which can arrive with this method is that some graphene sheets might agglomerate or some bubbles might be created in the dispersion. A solution to this problem is the use of ultrasound power. With the use of an ultrasound bath the agglomerated sheets can be exfoliated, bubbles can be removed, or the polymer/filler dispersion can be homogenized. This method has become an attractive and suitable technique for developing biocomposites because it is a cheap, easy method for the preparation of hybrids. Furthermore, it is possible to disperse nanofillers homogeneously with high efficiency inside the polymer matrix via this method.

#### **1.1.4 PCL/GO Biocomposites**

In this study we are going to study the effects of the addition of GO to the polymer PCL to form PCL/GO biocomposites and how this affects the properties and the degradation rates - and how said degradation affects the structure, properties, etc. - of the original polymer. There have been other studies which have investigated the effects of the addition of this carbonaceous material to this aliphatic polyester, however, the effects of degradation at extreme values have not been extensively studied.

Studies have proven that certain polar organic substances and polymers, including alcohols (Xue, Xin, & others, 2015), poly(ethylene oxide) (Chen, Shi, & others, 2015) (Taghizadeh, Abdollahi, & others, 2015), poly(vinyl alcohol) (Lv, Wu, & others, 2015) (Bian, Tian, & others, 2015), poly(vinyl acetate) (Pawar, Kumar, & others, 2015), poly(furfuryl alcohol) (Lv, Wu, & others, 2015), between others (Bian, Tian, & others, 2015), can be inserted with ease into the GO sheets in order to create intercalated composites. There are strong intermolecular forces such as hydrogen bonds and Coulomb forces between GO and the polymers in their composites. When GO has been incorporated to polymers, it has proved to greatly improve their mechanical properties and their thermal stability (Kai, Hirota, & others, 2008).

Research carried out by Kai et al. (Kai, Hirota, & others, 2008) investigated how the insertion of GO and graphite into PCL as fillers could affect the properties of the original

polymer. The effects on the mechanical properties of the incorporation of these fillers into this molecular weight PCL are shown in Table 3 below.

Table 3: Mechanical properties of PCL and the PCL/GO, PCL/GO-s and PCL/G Composites, as adapted from (Kai, Hirota, & others, 2008).

Sample	Tensile yield stress (N/mm <sup>2</sup> )	Elongation at break (%)	Young's modulus (N/mm <sup>2</sup> )
PCL	15.6 ± 0.2	853.8 ± 144	340.2 ± 18
PCL/GO1	16.9 ± 0.4	735.3 ± 116	411.4 ± 30
PCL/GO5	20.3 ± 0.3	218.7 ± 169	712.4 ± 44
PCL/GO10	19.6 ± 0.6	97.4 ± 74	708.6 ± 46
PCL/GO-s1	17.8 ± 0.1	792.2 ± 17	467.3 ± 16
PCL/GO-s5	21.3 ± 0.7	87.8 ± 79	707.5 ± 7
PCL/GO-s10	26.5 ± 0.5	12.5 ± 6	1037 ± 102
PCL/G1	16.4 ± 0.4	728.0 ± 94	389.5 ± 23
PCL/G5	17.0 ± 0.3	659.7 ± 16	480.9 ± 21
PCL/G10	18.3 ± 0.3	632.5 ± 29	577.8 ± 46

A clear tendency can be seen with the incorporation of GO in the elongation at break, Young Modulus and tensile yield stress of the samples. There is a great decrease in the elongation at break as the content of GO increases - from 853.8 ± 144 (%) of pure PCL to 97.4 ± 74(%) of PCL/GO10 which has 10wt.% GO. There is also a clear tendency in the increase of the Young's modulus and Tensile yield stress with the incorporation of GO up to 5wt.% GO, point at which both mechanical properties seem to reach a plateau. With the incorporation of further GO, both stress properties don't only stop increasing in value, but decrease very slightly. Nevertheless, it can be clearly appreciated that the incorporation of GO significantly increases the Young's modulus and Tensile yield stress and heavily decreases the Elongation at break (%). It can also be appreciated that the incorporation of GO-s (PCL/GO composites treated with ultrasound during mixing) as a filler has a greater impact on the mechanical properties than the incorporation of GO without ultrasound treatment during mixing. The higher mechanical properties which were observed for the GO which had been treated with ultrasound were attributed to a higher intercalation of the GO lamellae. There is evidence of the formation of an intercalation structure for the PCL/GO and PCL/GO-s composites since there is a considerable upgrade in the yield stress and Young's modulus and a decrease in the elongation at break.

In the same article, non-isothermal crystallization and melting behaviour were analyzed for PCL with different wt.% of GO. The resulting DSC images provided data about the thermal properties ( $T_c$ ,  $\Delta H_c$ ,  $T_m$  and  $\Delta H_m$ ) of the analyzed samples, as shown in Table 4.

Table 4: Thermal properties of PCL and PCL composites, as adapted from (Kai, Hirota, & others, 2008)

Sample	T <sub>c</sub> (°C)	ΔH <sub>c</sub> (J/g)	T <sub>m</sub> (°C)	ΔH <sub>m</sub> (J/g)
PCL	25.5	-53.0	56.3	57.4
PCL/GO1	33.2	-56.0	56.4	60.8
PCL/GO5	33.8	-55.2	56.1	59.8
PCL/GO10	33.8	-53.1	56.4	57.8
PCL/GO-s1	31.3	-56.0	56.5	60.3
PCL/GO-s5	33.6	-53.8	57.8	59.3
PCL/GO-s10	33.9	-50.4	58.5	56.0
PCL/G1	33.8	-55.9	56.3	60.9
PCL/G5	33.9	-55.3	56.6	60.4
PCL/G10	34.4	-55.6	56.5	60.3

It can be appreciated that with the incorporation of all the carbonaceous fillers the values of T<sub>c</sub> increased roughly 8°C (from ~25 - 33°C). This can be due to the nucleating effect of GO and graphite on the crystallization of PCL, although different contents of each filler did not appear to affect the crystallization temperature. The crystallization of PCL/G10 appeared to be faster than that of PCL/GO10 and PCL/GO-s10, since the DSC peak appeared at a higher temperature and crystallization takes place at decreasing temperatures. This indicated that graphite had a better nucleating effect on the crystallization of PCL than graphene oxide. The article also concluded that, although T<sub>c</sub> hardly varied, the degree of crystallinity of PCL in PCL/GO, PCL/GO-s, and PCL/G decreased continuously with increasing volume fraction of the fillers. The incorporation of GO and G fillers didn't seem to affect the melting temperatures respect to pure PCL, whilst the melting points of the PCL/GO-s composite augmented with increasing volume fraction of GO, as shown in the following figure 11.

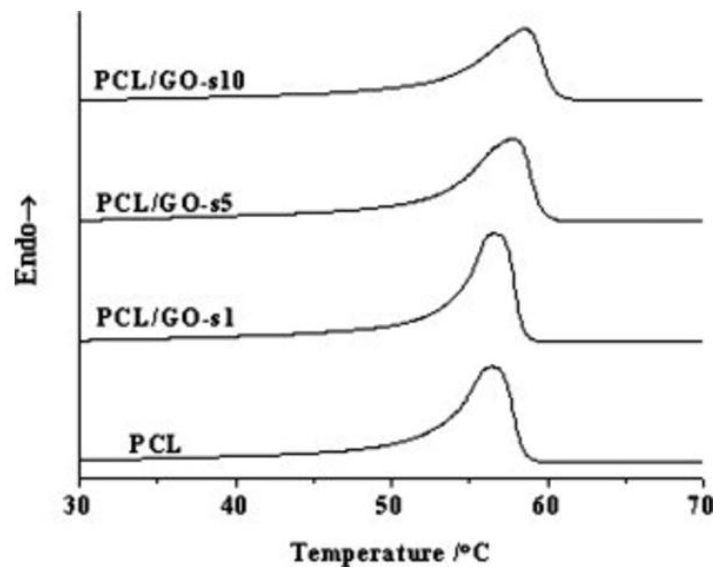


Figure 11: DSC heating curves of the PCL/GO-s composites, as adapted from (Kai, Hirota, & others, 2008)

Finally, Kai et al. concluded that a decrease in  $\Delta H_c$  and  $\Delta H_m$  for the samples of PCL/GO-s5 and PCL/GO-s10 was due to the intercalated structure which the hybrids formed. When the PCL chain intercalated into the layers of GO in the hybrids, their mobility was restricted by the sheets and therefore it was harder for the chain to form crystalline structures, which resulted in a decrease in crystallinity (Kai, Hirota, & others, 2008).

Finally, from the X-ray analysis of the composite films, the researchers came to the conclusion that the distance between the GO layers increased from approximately 0.6 to 1.1 nm in the PCL/GO and PCL/GO-s hybrids, which demonstrated the intercalation of the polymer into the GO lamellae (Kai, Hirota, & others, 2008).

No further information could be learned from this article, since there was a lack of critical material characterization data such as SEMs, FTIR and Raman spectroscopy, which could provide important information about the morphology of the developed materials and the interaction between GO and the matrix, as well as a lack of data about the thermal stability, decomposition temperature, biocompatibility and processability of the composites (Sayyar, 2014).

In another article, Wan and Chen studied the morphology, mechanical properties and bioactivity of electrospun PCL/GO composites. The synthesis method used in this article is similar to the one used in our study, so it can give us an idea of the properties of the composite which we are going to work with. PCL/GO films with different contents in weight (0, 0.3, 0.5, 1 and 2%) were synthesised through solution-casting. A PCL/DMF (10 wt/v%) solution was mixed with a GO/DMF (0.6 wt/v%) dispersion at a temperature of 85°C and were continuously stirred for 2 hours. They were then ultrasonicated for 30 minutes and the casting took place on petri dishes. To ensure that there was no water present in the films they were dried in an oven at 70°C until the weight of the samples remained constant. The final samples were created by compression-moulding at 100°C in order to obtain flat films for further testing (Wan & Chen, 2011).

The results obtained by these researchers back up the information which was obtained from the previous article (Kai, Hirota, & others, 2008), although it is worth noting that the wt.% of GO incorporated to neat PCL in this article is less than in the mentioned previous article, as well as the fact that the samples created had been electrospun. As can be appreciated in Figure 12, which shows the typical tensile stress-strain curves of PCL/GO composite films, the content of GO ranging from 0.3 to 2 wt.% in the PCL/GO hybrids significantly improved the stiffness, strength and energy at break of PCL. However, it did not affect its deformation behaviour. The deformation which all samples underwent are characteristic of semi-crystalline and ductile polymers, since the curve demonstrated yielding, necking propagation and strain hardening (Wan & Chen, 2011).



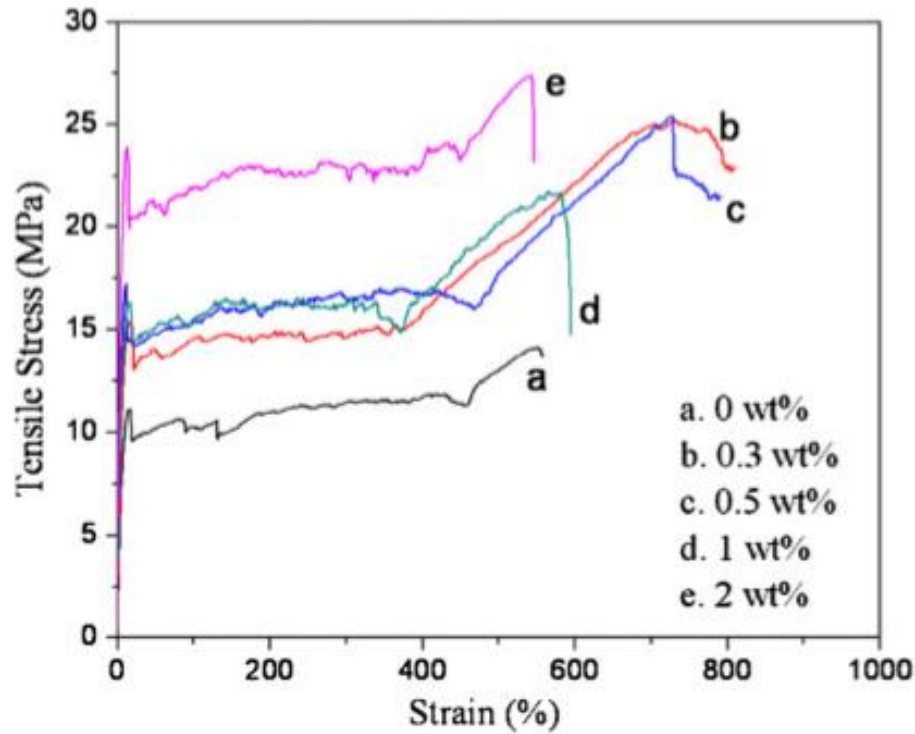


Figure 12: typical tensile stress-strain curves of solid PCL/GO nanocomposite films, as adapted from (Wan & Chen, 2011).

The overall results which summarize the effects on the mechanical properties of incorporating GO to the polymeric PCL matrix is shown in the following table 5.

Table 5: Mechanical properties of solid PCL/GO nanocomposite films, as adapted from (Wan & Chen, 2011)

GO concentration (wt%)	Ultimate tensile strength (MPa)	Young's Modulus (MPa)	Elongation at break (%)	Energy at break (MJ/m <sup>3</sup> )
0	14.2 ± 1.6	209 ± 21	554 ± 72	63.1 ± 4.9
0.3	25.1 ± 4.1	230 ± 30	802 ± 65	101.1 ± 5.1
0.5	25.5 ± 3.2	311 ± 25	732 ± 61	130.7 ± 4.8
1	21.8 ± 5.6	305 ± 35	597 ± 45	101.1 ± 5.2
2	27.5 ± 5.7	442 ± 35	548 ± 81	125.4 ± 3.5

Although different quantities of wt.% are studied in tables 4 and 5 (with the exception of 1 wt.%) the same trends can be observed in the mechanical properties. As Wan et al. states, overall, as the content of GO surpassed 0.5 wt%, the mechanical properties of the hybrids were slightly deteriorated. This is principally due to an improved dispersion when there are lower concentrations of the GO filler. However, the mechanical properties are still much

higher than those of neat PCL, certifying the reinforcing effects which the GO nanoplatelets have on the hybrids. This can be associated with the intrinsic properties of GO nanosheets, dispersion degree of GO in the PCL matrix and interfacial interactions.

The DSC thermograms of this study also corroborated the thermal data obtained from the previous article. The  $T_c$  increased roughly 7°C with the incorporation of the composite - which was attributed to the nucleating effect of GO on PCL,  $T_m$  did not seem to vary, and  $\Delta H_m$  decreased. Wan et al. attributed this reduction in crystallinity to the interfacial interactions which occurred between GO nanolayers and the PCL polymer chains, reducing the flexibility of the chains and therefore limiting the crystallization process. This happened despite the fact that the GO nanoplatelets act as heterogeneous nuclei for the crystallization of PCL.

Finally, the authors of the article concluded that an overall content of 0.3wt.% of GO in the hybrids exhibited the best combination of nanofiller dispersion and the mechanical properties. The improvement of the mechanical properties of the solid hybrids were associated to the good dispersion of the GO lamellae with a high aspect ratio, specific surface area, strength and stiffness, as well as a flexural and wrinkled morphology. The FTIR absorption peaks manifested strong interfacial interactions which were attributed to hydrogen bonding. It was concluded that the combination of a high porosity of 96.9%, an increase in the mechanical properties and an improved bioactivity all give an enormous potential for the PCL/GO fibrous membranes for applications in the field of biomedical engineering.

There are further studies, like Chaoying et al. (Wan & Chen, 2012). They, once again, have studied the incorporation of graphene nanocomposites to different biopolymers to form the biocomposites PCL/GO, PLLA/GO and PS/GO.

### 1.1.5 Degradation Mechanisms

Firstly, in order to properly describe the degradation of PCL and all biopolymers in general, certain definitions need to be clarified, since the incorrect understanding of certain terms can lead to confusion. For example, a material which is biodegradable does not mean it is necessarily bioresorbable, as it may be degraded and moved away from its original position *in vivo* but not completely eliminated from the body. According to Vert. et al. (Vert, Li, & other, 1992), and as adapted from (Woodroof & Hutmacher, 2010), the definitions of biodegradable, bioabsorbable, bioresorbable and bioerodible materials are as follows.

- Biodegradable materials degrade in response to macromolecular degradation with dispersion *in vivo*. However, these materials display no evidence of their complete elimination from the organism (bacterial, fungi and environmental degradation are excluded). These polymers can be broken down by the attack of biological elements leading to the creation of fragments or other degradation by-products. However, although these products of degradation have the ability to move from their original site of action, they are not necessarily expelled from the organism.

- Bioabsorbable substances are compact polymeric devices or materials that have the ability of dissolving in body fluids without the fracture of polymer chains or the decrease of their molecular mass. These materials are considered bioabsorbable if the dispersed macromolecules are eliminated from the body.
- Materials are considered bioresorbable when the complete removal of the original foreign body material and its low molecular weight degradation by-products takes place with no residual effect. Bioresorbables can be considered solid polymeric materials that demonstrate bulk degradation and continue to be resorbed *in vivo*. In other words, they are polymers which are eliminated through naturally occurring pathways as can be by filtration of the degradation by-products or by their metabolization. In conclusion, bioresorbables are ultimately eliminated from the organism.
- Bioerodable materials demonstrate surface degradation on their solid surface and continue to be resorbed *in vivo*. Therefore, similarly to bioresorbable materials, bioerodable materials demonstrate complete elimination of the initial foreign body and their surface erosion by-products with no leftover effects. The difference between bioerodibles and bioresorbables is the type of degradation which they undergo.

Poly( $\epsilon$ -caprolactone) can undergo enzymatic degradation in the environment by outdoor organisms such as fungi and bacteria, but cannot be biodegraded in human and animal organisms due to an absence of the necessary enzymes (Vert, 2009). This was shown by research which, firstly, studied the degradation of PCL *in vitro* (saline) conditions, and secondly, *in vivo* (rabbit) conditions. The results showed that the hydrolytic degradation rates were alike in both mediums and therefore it was concluded that the enzymatic degradation in the first stage of degradation, which lasts 0-12 months, is not a critical factor in the degradation mechanism of PCL (Pitt, Chasalow, & others, 1981) (Sun, Mei, & others, 2006). Although PCL is not initially degraded by enzymatic pathways, it is still considered bioresorbable because the initial phase of degradation takes place via hydrolytic degradation. This phenomenon causes the initial stage of degradation to last longer. The hydrolytic degradation of poly( $\alpha$ -hydroxy) esters can take place by surface or bulk degradation pathways. The extent and the mechanism of hydrolysis is determined by two factors. Firstly, by the presence, abundance and situation of the water molecules, and secondly by the interaction which takes place between the polymer and the molecules of water. Therefore, the interaction which takes place depends on the traits of the medium in which the polymer is immersed, as well as the polymers' chemical composition, hydrophobicity, size and design.

The degradation through which polyester materials, and more specifically, can go through can also vary between three different degradation mechanisms

Another important factor in the degradation of polyester materials, and more specifically poly( $\alpha$ -hydroxy esters), is that they undergo different forms of degradation kinetics and therefore erosion mechanisms, as shown in figure 13 below.

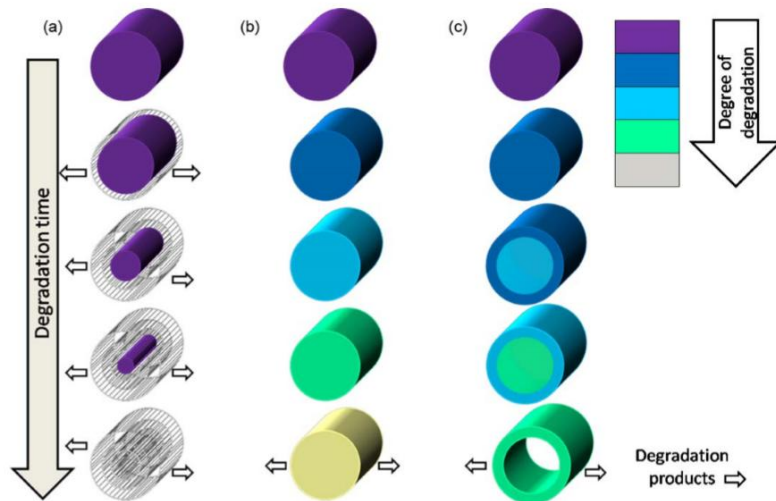


Figure 13: Degradation models for degradable polymers: (a). Surface erosion (b). Bulk degradation and (c). Bulk degradation with autocatalysis, as adapted from (Woodroof & Hutmacher, 2010).

To further understand the degradation process of PCL, surface erosion, bulk degradation and bulk degradation with autocatalysis mechanisms are explained below.

Firstly, it is important to note that the route that is taken in the degradation of a polymeric device is determined by the diffusion-reaction phenomenon, which basically compares the rate of water diffusion into the polymer matrix with the degradation process.

Surface erosion or degradation takes place when the hydrolytic cleavage of the backbone of the polymeric chain takes place specifically at the surface of the material (Ginde & Gupta, 1987). This situation develops when the fracture of the polymer chains is faster than the rate of diffusion of the water molecules into the polymer matrix. The by-products of this erosion rapidly diffuse into the surroundings and the water molecules present in the medium cannot reach the centre of the matrix. As a result, a thinning of the polymer can commonly be seen over time, without the chemical structure of the internal bulk polymer being affected, as seen in figure 13(a). Therefore, the molecular weight of the inner chains is unaffected and remains that way until those inner chains become the outer layer of the material. Surface erosion has the advantage that the degradation times can usually be predicted, enabling the design of suitable drug release vehicles (release rates can be predetermined) (Gopferich, Karydas, & others, 1995).

Bulk degradation takes place when the rate of diffusion of water into the entire polymer matrix is superior to that of the cleavage of the polymer chains, resulting in the penetration of water into the entire polymer bulk, resulting in random hydrolytic chain scission taking place throughout the matrix in a uniform matter giving rise to an overall reduction in the molecular weight. The capacity that the water molecules have to enter the matrix and therefore access the ester bonds present in the PCL chain is dictated by the hydrophobicity, crystallinity, molecular weight, bulk sample dimensions and the glass transition temperature of the polymer (Aharoni, 1998) (Bei, Li, & others, 1997) (Chen, Bei, & others,

2000). The hydrolysis of the chains produces, as with surface erosion, oligomers and monomers which are produced everywhere in the matrix. The by-products of polyester, and therefore PCL's, hydrolysis degradation are frequently the hydroxyl and carboxyl end groups of the polymer chain. When carboxyl end groups are formed from the scission of the ester bonds, carboxylic acid is produced, which acts as a catalyst for the further hydrolysis of the polymer chains. When these low molecular weight by-products are able to diffuse out of the matrix, degradation will steadily take place and an equilibrium for this diffusion-reaction phenomenon is achieved. Therefore, if the carboxylic acid cannot act as a catalyst for the degradation, the chain cleavage will be homogeneous and molecular weight reduction will also be homogeneous, which basically defines bulk degradation.

The third degradation phenomenon which can take place in a polymer is the denominated bulk degradation with autocatalysis, as shown in figure 13(c). When the diffusion-reaction equilibrium is disturbed, in other words, when the by-products of the broken chains are not readily able to diffuse out of the polymer matrix (in the case of surface erosion they can freely diffuse into the surroundings), the degradation mechanism leads to the denominated internal autocatalysis. This autocatalysis takes place via the carboxyl (-R-COOH) and hydroxyl (-R-OH) end group by-products of the degradation process. When the concentration of hydroxyl and carboxyl groups increase inside the matrix, a concentration gradient is formed from the heart of the matrix to the outer surface. As the concentration of acid by-products increases, an exponential rate of degradation occurs in the core of the matrix, breaking down more ester bonds and therefore producing further acid by-products, which in turn accelerate the catalysis which takes place even further. Therefore, the core of the matrix is eventually composed of low molecular weight chains and the outer surface of the polymer is made up of a higher molecular weight skin, causing the degradation mechanism to become defined by a bimodal molecular weight distribution (Woodroof & Hutmacher, 2010). Eventually, a hollowed out structure with a higher average molecular weight skin arises, caused by the rapid diffusion of the small inner oligomers to the surrounding medium. This causes a weight loss and a diminish in the rate of chain cleavage inside the polymer. The two fundamental factors which impose the diffusion-reaction equilibrium, and affect the resistance of the by-products of degradation to diffusion, are the chemical structure of the polymer and its thickness.

As described in by Bergsma (Bergsma, 1995), when the oligomers and acid by-products are rapidly released from the material they can bring about inflammatory responses *in vivo*. Moreover, if the tissue which surrounds the polymer cannot buffer the change in pH values due to a poor vascularization or low metabolic activity, temporary tissue damage may emerge. An example of this disturbance has been observed with the use of fibre-reinforced PGA pins in orthodontic surgery, which brought about an increase in osmotic pressure through local fluid accumulation when rapid degradation took place (Böstman, Hirvensalo, & others, 1990).

In this investigation the degradation of PCL/GO composites is going to be studied at extreme pH values. Due to its significant degree of crystallinity and substantial hydrophobicity, pure PCL has shown to have a slow hydrolytic degradation rate that takes

between 2-3 years, depending on its molecular weight (Sun, Mei, & others, 2006) (Sayyar, 2014). Although a complete consensus has not been reached, since other articles report that PCL with  $M_w$  between 66,000 and 80,000 degrades fully in about 3-4 years (Pitt, Gratzl, & others, 1981) (Grizzli, Garreau, & others, 1995). Furthermore, the molecular weight profile can provide an insight as to which pathway of degradation occurs. Through gravimetric measurements, information about the loss of oligomers and monomers exiting the polymer, polymer degradation, and chain cleavage can be gathered about the degradation pathways which take place.

The chemical reactions which take place in the degradation of polymers always have a preferential law or system of attack, and are defined by different factors such as the functional groups present in the chain, chemical composition, and macromolecular chain arrangements. For example, semi-crystalline polymers like PCL are made up of two regions; a crystalline, highly ordered domain, and an amorphous region, composed of randomly intertwined polymer chains. The crystalline region affects the degradation rate of the polymer since the chains are closely and tightly packed, therefore the access of water to these polymer chains results impeded and the hydrolysis of the amorphous regions generally takes place first. PCL has a semi-crystalline structure with a crystallinity of approximately 60% before degradation, and it seeks to lower its thermodynamic energy balance, permitting its polymer chains to recrystallize. Its amorphous region is governed by a low glass transition temperature ( $T_g = -60^\circ\text{C}$ ) which permits a high chain mobility at  $37^\circ\text{C}$ , which corresponds to the human organism temperature. Due to these properties, the crystallinity of PCL evolves as degradation takes place since the amorphous regions would likely be degraded first and recrystallization can take place, resulting in a dynamic degradation mechanism which is difficult to predict. Additionally, as degradation takes place the size of the polymer chains is reduced, further increasing the mobility of its chains during hydrolysis. The combination of these factors causes PCL to promote its own resistance to degradation as it takes place (Lam, Hutmacher, & other, 2008).

The main causes for the slower degradation rate of PCL compared to other biodegradable polymers is its hydrophobicity and high crystallinity. Its degradation occurs in two distinct phases. Firstly, the amorphous phase is degraded by non-enzymatic random hydrolytic chain scission of ester bonds, giving rise to oligomers and an increase in crystallinity. This theory is backed up by the fact that the degradation rate of PCL is practically identical to the *in vitro* hydrolysis at  $40^\circ\text{C}$  which obeyed first-order kinetics. The results obtained by Sun et al. (Sun, Mei, & others, 2006) backed this theory up. They obtained a linear relationship when representing the logarithm of  $M_w$  against time, which is in conformity with a first-order rate of degradation for ester hydrolysis. 480 days post-implantation, the molecular weight of PCL had been reduced to roughly 24,000, and the polymer capsules remained intact and maintained sufficient strength. However, when the molecular weight had been reduced to 8,000, the capsules had lost their mechanical properties and had broken down into fragments. However, there have been investigations which suggest that PCL degrades by end chain scission rather than random chain scission at higher temperatures, as shown in figure 14 below (Labet & Thielemans, 2009).

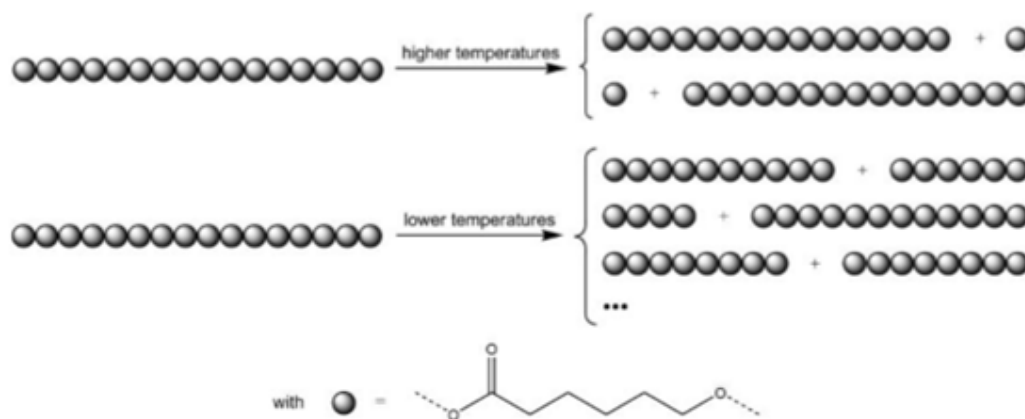


Figure 14. Cleavage of the PCL during the degradation, as adapted from (Sayyar, 2014)

Secondly, when the polymer presents a higher crystallinity and a low molecular weight under 3000 g/mol, it undergoes intracellular degradation. This second stage is manifested when PCL fragments were shown to be present in the phagosomes of macrophages, giant cells and fibroblasts (Woodward, Brewer, & other, 1985), which backs up the theory that PCL can be completely reabsorbed and degraded with intracellular mechanisms when the molecular weight of the polymer drops below 3000 g/mol. Albertsson et al. used low molecular weight PCL ( $M_n = 3000$  g/mol) powder with a size between 53-500 nm in order to study the intracellular degradation of PCL. The results obtained showed that the powder quickly degraded and was absorbed by phagosomes present inside macrophages and giant cells within 13 days. They also reported that the sole metabolite was 6-hydroxyl caproic acid. Hydrolysis intermediates 6-hydroxyl caproic acid and acetyl coenzyme A are formed which in turn enter the citric acid cycle and are eliminated from the body, as shown in figure 15 below (Albertsson & Karlsson, 1997).

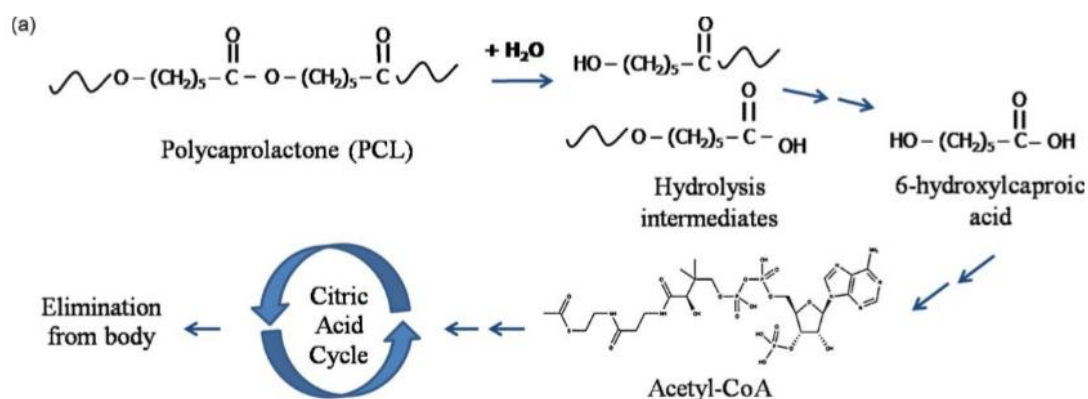


Figure 15: mechanism through which PCL degrades hydrolytically and enters the citric acid cycle, as adapted from (Woodroof & Hutmacher, 2010).

Other studies, like the one proceeded by Woodward et al. reported that the *in vivo* and intracellular degradation in "Dawley" rats initially took place through a non-enzymatic bulk hydrolysis mechanism. They found that during the first two weeks a transient

inflammatory response took place (Woodward, Brewer, & other, 1985). After nine months the molecular weight had decreased to about 5000 g/mol and a loss in mass of the samples were appreciated, indicating the fragmentation of the PCL implants. The interplay between the mass loss and molecular weight loss from typical resorbable-polymer scaffold *in vivo* is shown in figure 16.

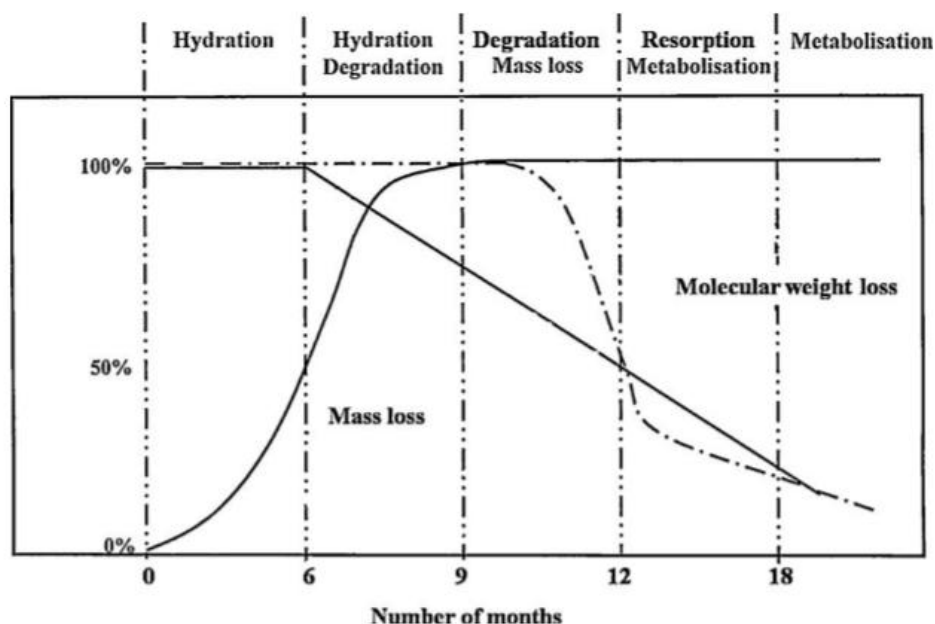


Figure 16: Graphical illustration of the mass and molecular weight loss over time for a resorbable polymer such as PCL. Initial hydration (0-6 months), through degradation and mass loss (6-12 months), resorption (past 12 months) and metabolisation (post 18 months) as adapted from (Hutmacher, 2001).

The *in vitro* PCL degradation mechanism was studied by Ali et al. through different methods - differential scanning calorimetry (DSC), gel permeation chromatography (GPC) and scanning electron microscopy (SEM) - in order to investigate the mechanism of degradation that takes place (Ali, Zhong, & other, 1993). The data they obtained indicated that the HO· (hydroxyl) radical is probably a significant factor in the degradation of PCL in medical systems and devices. In a different study, Chen et al. compared the *in vitro* degradation of PCL microparticles with PCL films at  $37 \pm 1^\circ\text{C}$  in a pH 7.4 PBS medium. The results they obtained suggested that homogeneous degradation takes place in PCL, since the comparison of the degradation rate of both film-like and microparticle-like samples did not differ much from one another, despite the fact that the specific area of the microparticles was much larger than that of the film (about 67 times) (Chen, Bei, & other, 2000).

To fully understand the degradation process of PCL *in vivo*, Sun et al. constructed a long-term 3 year investigation in rats (Sun, Mei, & others, 2006). Through the use of radioactive labelling the distribution, absorption and excretion of the PCL could be tracked. What they observed is that the PCL capsules which had an initial molecular weight of  $M_w =$



66,000g/mol had not changed in shape after 2 years of implantation, and they finally broke down to low  $M_w = 8,000$  g/mol fragments after 30 months. They found a decreasing linear relationship between the  $M_w$  and time. In order to confirm that PCL does not accumulate in body tissue, the scientists subcutaneously implanted a Tritium-labelled PCL with a low molecular weight of 3000 g/mol in rats. Following its absorption and excretion, the radioactive substance present in the PCL was first detected in plasma after 15 days of implantation, and simultaneously radioactive faeces and urine were collected. After 135 days, 92% of the implanted material had been excreted by the rats, and at the same time the plasma radioactivity dropped to background level. This corroborated the results which they expected to obtain.

More recently there have been studies carried out to investigate the accelerated degradation of PCL. Remarkably, in spite of over 1000 articles being published in the past decade in the field of biomedicine, very few of these have investigated the degradation and kinetics of resorption about PCL-based-scaffolds (Woodroof & Hutmacher, 2010). In spite of this, some studies have been carried out which studied the accelerated degradation pattern (mainly by via thermal degradation) of PCL, but a consensus about the degradation of PCL has not been completely reached.

In concordance with the research of this article, Hutmacher et al. (Lam, Hutmacher, & other, 2008), researched an accelerated degradation system using an NaOH solution (5M - extreme basic pH) and compared his results against a medium which simulated physiological conditions. Since PCL takes so long to degrade, the use of accelerated degradation systems is useful in order obtain valuable results in a shorter period of time, since the systems and devices degrade faster. Essentially, the mechanism of degradation should tightly mimic the *in vivo* system in which the implant would be placed. The degradation of the polymer is accelerated due to the high concentration of  $\text{OH}^-$  molecules which accelerate the rate of hydrolysis. Both acidic and alkali mediums are capable of catalyzing the hydrolysis reaction, as reported by (Pitt, Chasalow, & others, 1981) (Cam, Hyon, & others, 1995) (Grizzli, Garreau, & others, 1995). From the molecular weight profiles (figure 17 below) Lam et al. (Lam, Hutmacher, & other, 2008) deduced that, interestingly, the degradation pathways under a heavy basic solution proceeded via the surface degradation mechanism, unlike PCL in normal physiological medium.

This may be because the elevated concentration of  $\text{OH}^-$  molecules increases the rate of hydrolysis above the rate of diffusion of the medium into the centre of the matrix. Figure 17(a) shows that during the six weeks that the experiment took place the molecular weight of the samples remained practically unchanged. This is likely due to surface erosion taking place on the scaffold struts, since the chains which had been broken down on the surface of the sample created chains of a lower molecular weight and dispersed in the solution, leaving the molecular weight of the sample practically unchanged. Another interesting feature they found is that the crystallinity of the sample generally increased with time, as shown in figure 17(b). As the amorphous region undergoes the first step of degradation before the crystalline phase, and since the degradation was superficial, the regions with a low molecular weight were probably the remainders of areas attacked by erosion, and

likely consisted of crystalline regions still attached to the scaffold bulk. Furthermore, an increase in the standard deviation of the molecular weight could only start to be appreciated after five weeks.

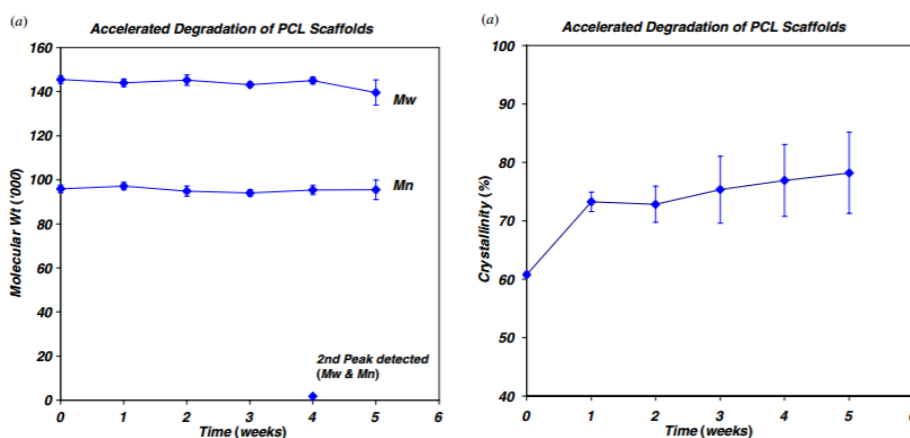


Figure 17. (a) Average molecular weights profile of PCL scaffolds over 5 weeks. A second peak appeared at 4 weeks and was approximately  $M_w = 1720$  and  $M_n = 1660$ . (b) Crystallinity profile of PCL scaffolds degraded over 5 weeks. Polydispersity was consistent at about 1.5 and 1.6 respectively.

In theory, the initial mass loss which takes place when submitted to degradation corresponds to the random hydrolytic chain scission of the amorphous region of the polymer which is more susceptible to the interaction with water molecules than the crystalline region (Li & Vert, 1995). In the same article it is stated that the degradation of the crystalline regions took place simultaneously, but at a slower rate than the amorphous region, despite the fact that the crystalline regions are typically attacked secondarily. Single-crystal areas were also selectively attacked and degraded which explains why the degradation was able to proceed in a rapid manner, even for regions with a high crystallinity. The authors of the article hypothesized that since the degradation of the amorphous regions proceeded at a very fast rate, the remaining crystalline regions held together by these amorphous segments would also be dislocated from the main polymer bulk. As the amorphous polymer regions were being eroded away, it could cause the fragmentation and erosion of the packed crystalline regions at the surface as well, thus contributing to a faster initial mass loss (Lam, Hutmacher, & other, 2008), as shown in figure 18 below.

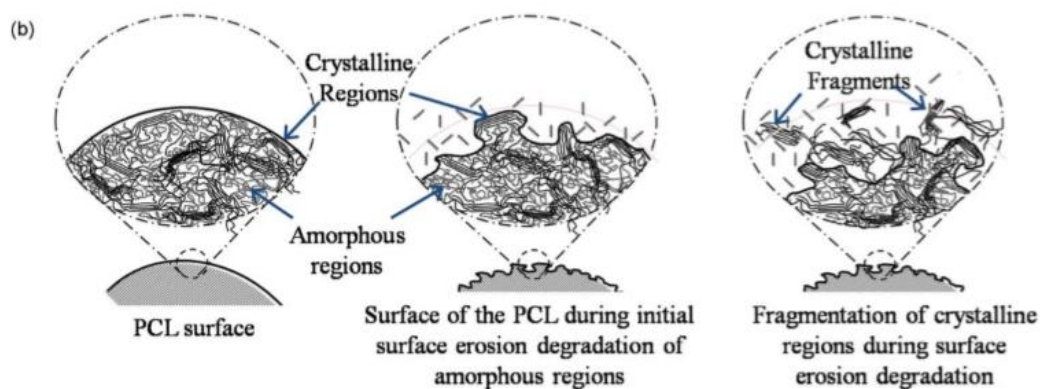


Figure 18. Accelerated degradation of PCL over 5 weeks in NaOH 5M, as adapted from (Woodroof & Hutmacher, 2010).

As previously described, PCL is an excellent candidate for copolymerization or blending to engineer desired mechanical properties and degradation kinetics of a medical device or scaffold. The rate at which the hydrolysis of the polymer chains takes place can be modified by copolymerization of PCL with other lactones or glycolides/lactides, as the presence of one polymer influences the degradation of the other polymer (Pitt C. , 1990). Hutmacher et al. accomplished extensive studies of the degradation *in vivo* and *in vitro* of PCL scaffolds, and examined the cross-section of the scaffold struts over a month as well as the molecular weight distribution over time, and found that there was a uniform distribution of molecular weight over time, so concluded that there was no evidence of internal autocatalysis (Lam, Hutmacher, & others, 2009). In another study, Sivalingam et al. investigated the presence of poly(vinyl acetate) in a PCL matrix and found that the enzymatic degradability is reduced (Sivalingam, Karthik, & others, 2004). However, the copolymers of lactones have been reported to enhance the biodegradability of the copolymers, and because the copolymer degrades faster than the homopolymers, some kind of interaction is expected. Pitt et al. demonstrated that the *in vivo* degradation mechanism of PCL, PLA and their random copolymers was qualitatively equal. The degradation rate of random copolymers was much higher than those of the homopolymers under the same physiological conditions (Pitt, Gratzl, & others, 1981). Interestingly, the rate of degradation of a copolymer PLA/PCL block was found to be intermediate between that of the PLA and PCL pure polymers, and increased with PLA content in the 0-40% range (Ye, Du, & others, 1997). However, when the content of PLA in the copolymer increased above 40%, the degradation exceeded the degradation of the homopolymers (Huang, Li, & others, 2006). Therefore, it can be concluded that depending on the composition and synthesis methods of the copolymers, different degradation mechanisms and rates can be expected.

In conclusion, the degradation of PCL is slow compared to other popular biopolymers, making it much more suitable for long-term degradation applications such as delivery of encapsulated molecules extending over a period of more than 1 year. It is also a very useful material to form composites or co-polymers to earn other desirable properties, and has proven to be very promising in the field of tissue engineering.

## 1.2 Motivation

Due to the exponential growth that the biomedical field is experiencing in the past decades, giving rise to a broad amount of new synthesis techniques and therefore applications, there is a necessity for new materials to arise. This requirement is the primary motivation in the development of biocomposites. PCL is a widely used polymer in the field of biomedicine, but it lacks certain properties which can be very useful for implants or devices which require good mechanical properties.

The present end of degree project emerges from the need of creating a composite hybrid polymer which enhances the mechanical properties of PCL making it suitable for applications in devices with a high-bearing mechanical charge, such as bone implants or fixation devices. It is part of an investigation which is taking place at the "Centro de Biomateriales e Ingeniería Tisular" (CBIT) of the Universitat Politècnica de Valencia (UPV). Furthermore, there is a large interest in developing materials which dispose of highly reactive functional groups to which molecules of interest can be incorporated, increasing the bioactivity of the original polymer.

But, although it is crucial to find a material which can fulfil the necessities mentioned previously, it must also follow a valid economical and technological synthesis technique. The method of synthesis must not contain raw materials which are excessively expensive, and the synthesis technique should be rather simple, so that it can be emulated in a relatively simple manner.

## 1.3 Justification

PCL has been used as the base of the polymeric matrix because it has been widely studied as a biomedical material and has a high availability. It has plenty of useful properties, as described in section 1.1.2, and the objective of this article is to find a suitable hybrid which can compensate for the properties which limit the use of the polymer in certain fields of biomedicine. Therefore, GO was thought of because it has been reported that it can improve the mechanical properties of biopolymers, as well as increasing its bioactivity.

The specific use of GO as a filler comes from the reported properties which arise from the carbon sheets which contain hydrophilic hydroxyl and epoxy groups on the basal plane of GO and carboxyl groups situated at the sheet edges. These functional groups can act as reactive sites that can potentially provide an anchor point for bioactive substances due to GO's relative ease to react with them. Furthermore, it can greatly increase the mechanical properties of the original polymer due to the strong intermolecular forces such as hydrogen bonds and Coulomb forces which have been reported between GO and the polymers in their composites.

## 2 OBJECTIVES

The overall objective of this end of degree project was to understand the kinetics of degradation of a series of polycaprolactone/graphene oxide hybrid biocomposites which could enhance the properties of neat PCL so that new biomedical devices with new possible applications could be created. The reinforcement of PCL with GO searched to provide the hybrid with functional groups which could act as reactive sites for molecules of interest to increase the bioactivity of the polymer inside the human organism as well as to improve the mechanical properties of PCL.

Another objective was to find an appropriate synthesis technique for the creation of the hybrids in order to create four samples, each containing different percentages of GO in weight in proportion to PCL (0%, 0.1%, 0.2% and 0.5%). To do so, a suitable solvent which could dissolve PCL and disperse GO needed to be found, and secondly a synthesis technique through which the samples could be obtained needed to be designed. It is of interest that this technique could be easily reproduced in the laboratory at a reasonable cost.

The degradation of the synthesized polymer was studied at extreme pH values in order to study the degradation kinetics and pathways in both mediums. By doing so, the properties of the hybrids were obtained at different phases of its degradation as well as before being inserted into the degradation mediums. Through this method, it was possible to study how three different variables (the composition of GO in the hybrids, the degradation times to which the samples are submitted, and the mediums in which they degrade) affected the properties of the samples.

The final objective was to take conclusions about the mechanical, thermal, and structural properties of the hybrid through various synthesis techniques, namely equilibrium water content and weight loss (EWC-WL), scanning electron microscopy (SEM), differential scanning calorimetry (DSC) and X-ray diffraction(XRD).

### 3 POLICIES

Since the present end of degree project was performed in the laboratory of the "Centro de Biomateriales e Ingeniería Tisular" (CBIT), there are certain laws and policies which must to be known and strictly followed in order to maintain the safety, hygienic and environmental measures in the lab, taking into account the storage of chemical products, as well as the treatment of waste products. The current policies which need to be complied with are as follows.

In terms of the management of chemical substances:

- Royal Decree 374/2001 of the 6 of April, on the protection of the health and safety of the workers against the risks related to chemical agents at work. This Royal Decree aims, within the framework of Act 31/1995, of the 8<sup>th</sup> of November, on the Prevention of Occupational Risks, to establish the minimum provisions for the protection of workers against risks arising or which can arise from the presence chemical agents in the workspace or any activity using chemical agents.
- Law 54/2003, of the 12 of December, on the improvement of the policy framework of the prevention of labour risks. BOE n° 298 12/13/2003. This law aims to promote the improvement of the working conditions in a way that the protection of the health and safety of workers is increased. To do so, general principles are established that organize the obligations and responsibilities of the employers and workers regarding the preventive measures of professional risks.
- Royal Decree 822/1993 of the 28 of May 1993, which lays down the principles of good laboratory practice and its application in the accomplishment of non-clinical studies of chemical substances and products. The principles of « good laboratory practice» shall apply to investigations in order to obtain data on the properties of the substances and chemicals and their safety with regard to human health and the environment. Good laboratory practice shall also apply to field studies.
- -ROYAL DECREE 840/2015 of 21 September, which approves measures to control the risks inherent in major accidents involving dangerous substances. This Royal Decree aims at the prevention of serious accidents involving dangerous substances, as well as the limitation of their consequences on human health, property and the environment.
- ROYAL DECREE 773/1997, 30 May, on minimum safety and health requirements concerning the use by workers of personal protective equipment. BOE n° 14012/06/1997. The present Royal Decree establishes, in the framework of Act 31/1995, of November 8, on Prevention of Occupational Risks, the minimum safety and health provisions for the election, use by workers at work and maintenance of the Individual Protection Equipment.

- ROYAL DECREE 379/2001 of 6 April approving the Chemical Storage Regulation and its accompanying technical instructions MIE APQ-1, MIE APQ-2, MIE APQ-3, MIE APQ-4, MIE APQ5, MIE APQ-6 and MIE APQ-7. The purpose of this Regulation is to establish the safety conditions for storage, loading, unloading and transfer of dangerous goods.
- LAW 22/2011, of July 28, on contaminated waste and soils. This Law aims to regulate waste management by promoting measures to prevent their generation and mitigate adverse impacts on human health and the environment associated with its generation and management, improving the efficiency of resource use. It also aims to regulate the legal regime of contaminated soils.
- ROYAL DECREE 833/1988, of 20 July, which approves the Regulation for the execution of Law 20/1986, Basic of Toxic and Hazardous Waste. The purpose of this Regulation is the development of Law 20/1986, of May 14, Basic of Toxic and Hazardous Waste, so that the activities producing such waste and the management thereof are carried out guaranteeing the protection of human health, The defense of the environment and the preservation of natural resources.

## **4 Extension of Applications and Range of Solutions**

### **4.1 Experiment Design**

In order to achieve the objectives mentioned previously, an experiment was designed based on the synthesis of a series of PCL/GO hybrids with different GO contents, submitted to degradation in two different media, one alkaline and the other acidic. In order to study the kinetics of degradation, the characterization of the materials was carried out at different times of the degradation.

The initial step of the project was to find a suitable solvent which could dissolve PCL and disperse GO effectively. To do so, various polar solvents were thought of and analyzed.

Once a suitable solvent had been identified the objective was to obtain the polymeric matrix by mixing both the GO dispersion (dispersed in an ultrasound bath) and PCL solution to create a polymeric matrix with GO sheets dispersed inside it forming chains of GO inside the three-dimensional structure once the solvent had been evaporated. The intention was to create four samples: one of pure PCL, and three containing different percentages in weight of GO in proportion to PCL.

Once a suitable and efficient method of synthesis had been designed, the next objective of the project was to punch the samples into small discs and place them under degradation solutions at extreme pH values for different degradation times in order to observe how this affected the properties of the hybrids. To analyze the properties of the samples different characterization techniques were thought of, such as weight loss and equilibrium water content, scanning electron microscopy, differential scanning calorimetry, gel permeation chromatography and X-ray analysis.

### **4.2 Materials**

#### **4.2.1 Poly( $\epsilon$ -caprolactone)/GO hybrids**

PCL pellets with a molecular weight of  $M_n = 70,000 - 90,000$  from the company ALDRICH were used without further purification.

Graphene oxide powder from the company Graphenea was used as received.

Dioxane, from the company FISHER was used as received

#### **4.2.2 Degradation solutions**

Sodium hydroxide, NaOH, and hydrochloric acid, HCl, from Sharlab were used as received. Distilled water with 10 mS conductivity was used as a solvent. 2.5 M degradation solutions were prepared from HCl (pH 1), and NaOH (pH 13).

The pH measurements in the degradation medium were carried out using a pH meter equipped with an Ag/AgCl electrode with an accuracy of  $\pm 0.01$  (XS instruments 510). The instrument was calibrated using solutions at pH 4, pH 7, and pH 10.



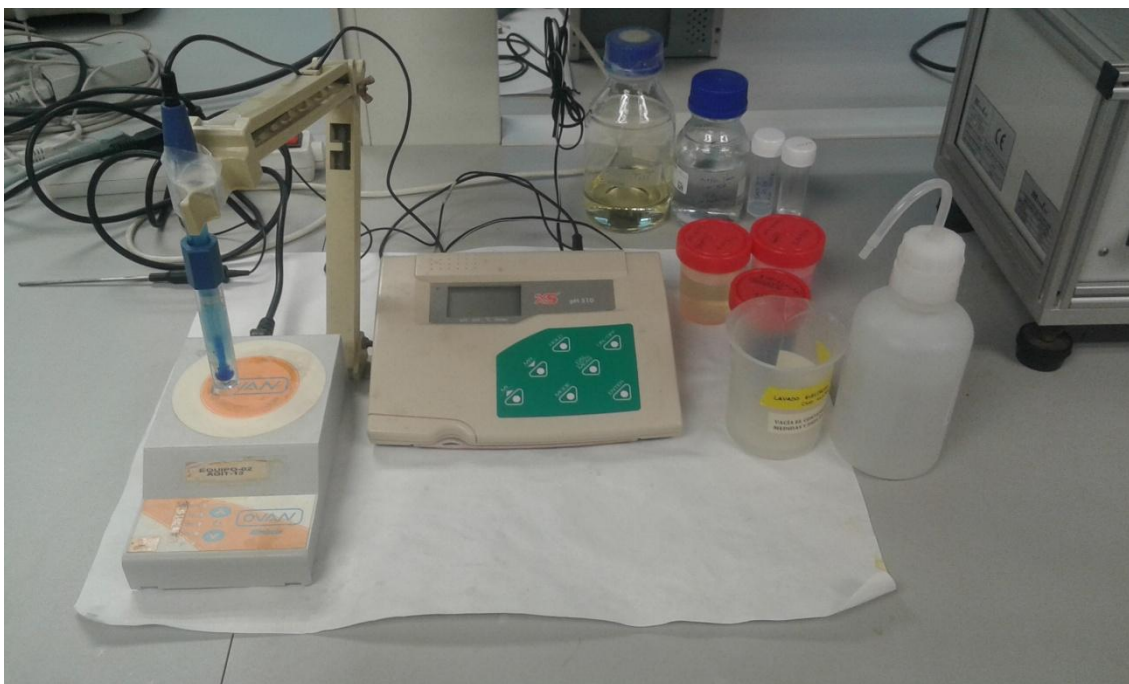


Figure 19. pH-metre used to measure the pH of the degradation solutions.

### 4.3 Synthesis

The first trial and error experiments which took place in the project are described in the section 'attachments'. In these first steps of the project the initial experiment design was followed, and various problems arose which were fixed. The final satisfactory synthesis method is described below. All the laboratory materials used in the following synthesis technique were previously cleaned with ethanol and acetone to eliminate any possible unwanted products present on the laboratory apparatus.

The objective was to create four samples with the following proportions of GO in wt.% respect to PCL.

1. Pure PCL (0% GO)
2. PCL + 0.1% GO
3. PCL + 0.2% GO
4. PCL + 0.5% GO

The theoretical amount of PCL, dioxane and GO to be used were calculated in relation with the size of four geometrically identical Teflon crystallizers. Their diameters were measured to calculate an average diameter, and the mass of PCL needed was obtained from the volume occupied by the sample in the crystallizer cup (the objective was to create a sample with a thickness of ~2mm) and from the properties of the material given by the supplier. It was obtained that a theoretical mass of 6.09g of PCL was needed. Four times the amount of solvent was used (24.35g) to assure that all the PCL dissolved without saturating, and the respective percentages in weight (wt.%) of GO in proportion to PCL were prepared.

The solutions of PCL/dioxane (A) and GO/dioxane (B) were prepared, using the quantities specified in tables 6-9.

Table 6. PCL + 0% GO.

A	Theoretical amount	Experimental amount
Dioxane	24.35 g.	24.16 g.
PCL	6.1 g.	6.17 g.

Table 7. PCL + 0.1% GO.

A	Theoretical amount	Experimental amount	B	Theoretical amount	Experimental amount
Dioxane	12.2 g.	12.35 g.	Dioxane	12.2 g.	12.47
PCL	6.1 g.	6.11 g.	GO	6.087 mg.	6.47 mg.

Table 8. PCL + 0.2% GO.

A	Theoretical amount	Experimental amount	B	Theoretical amount	Experimental amount
Dioxane	12.2 g.	12.13 g.	Dioxane	12.2 g.	12.69 g.
PCL	6.1 g.	6.18 g.	GO	12.174	12.38 mg.

Table 9. PCL + 0.5% GO.

A	Theoretical amount	Experimental amount	B	Theoretical amount	Experimental amount
Dioxane	12.2g.	12.37 g.	Dioxane	12.2 g.	12.85 g.
PCL	6.1 g.	6.1 g.	GO	30.435 mg.	31.07 mg.

For the creation of the samples two separate methods were followed.

Firstly, four solutions which we labelled as 'A' were created. These solutions contained PCL and were dissolved in dioxane in an oven at 37°C inside four Teflon crystallizers for 20 hours.

Secondly, once the PCL had dissolved in the dioxane, three solutions which we labelled as 'B' were created. These solutions contained different amounts of GO mixed with dioxane and were inserted in an ultrasound bath for 22 minutes in order to let the GO disperse in the organic polar solvent, as shown in figure 20 below.



Figure 20. Arrangement of the ultra-sound bath and the containers containing GO and dioxane prior to sounding.

Once the GO had dispersed in the solvent, the different solutions were mixed by pouring 'B' into 'A' (the solutions which contained dissolved PCL were of a viscous nature, so as to lose the minimum amount of material we concluded that the best option was to pour 'B' - which maintained its liquid nature - into 'A'), and were agitated with a mixing rod to help both phases mix. The resulting mixtures were placed in an ultrasound bath and were sounded for 1 hour 30 minutes (as shown in figure 21) - the plan was to sound for four hours, but in this time the phases had mixed properly and it was observed that more bubbles were created with more sounding time. The creation of bubbles was attributed to two reasons which affected each other. Due to the vibration energy of the ultrasound bath bubbles became trapped in the samples, which in turn found it harder to escape to the surface when the sample became more viscous due to the evaporation of the solvent.



Figure 21. Ultra-sound bath containing four Teflon crystallizers which contained the PCL/GO/dioxane mixture to be sounded.

After the sounding, the samples were taken to a vacuum pump left in continuous extraction for 30 minutes at a temperature of  $40^{\circ}$  in order to eliminate all the bubbles from the PCL/GO/dioxane mixture. Whilst doing so there were bubbles which rose to the surface and popped due to the vacuum. The samples were then placed inside a vacuum. Two days later the system which maintained the vacuum was cleaned to eliminate the excess dioxane which had evaporated from the sample and was trapped in the sealed environment of the vacuum in order to enable the dioxane to keep evaporating (liquid droplets of dioxane could be seen on the inner surface of the glass which assisted in creating the vacuum, as seen in Figure 22), and another two hours of continuous extraction were performed on the samples to eliminate any remaining bubbles. In Figure 23 it is possible to observe how the bubbles get forced to the surface of the sample. Once again, the vacuum was performed for a day, cleaning the water droplets and atmosphere of dioxane daily and producing one more continuous extraction for 10 minutes.

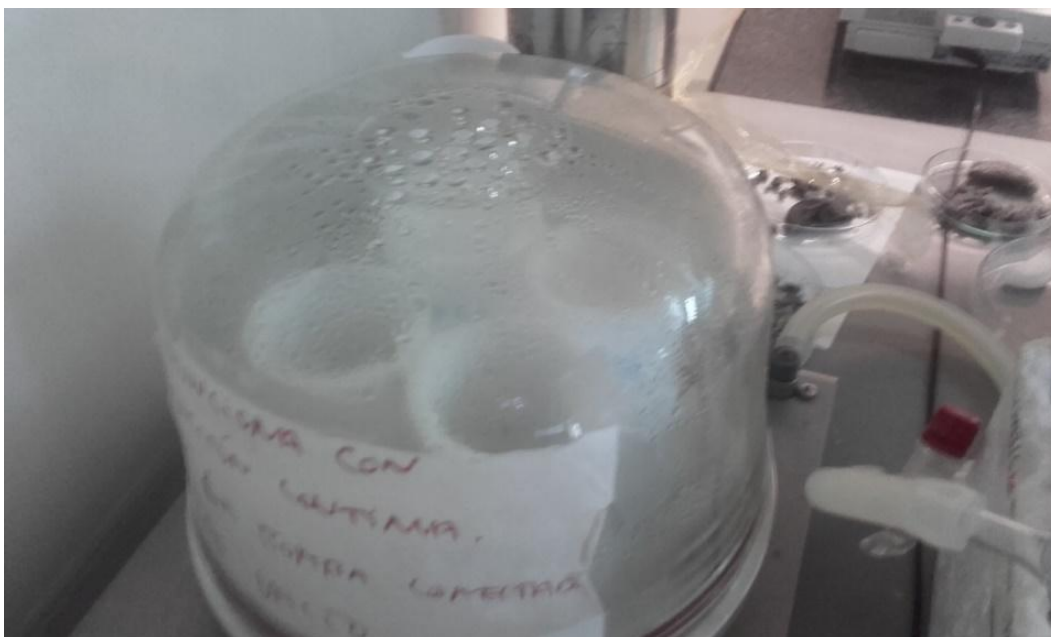


Figure 22. System through which the vacuum was created. Liquid droplets can be observed on the glass, which showed that there was an equilibrium of dioxane in the closed atmosphere.

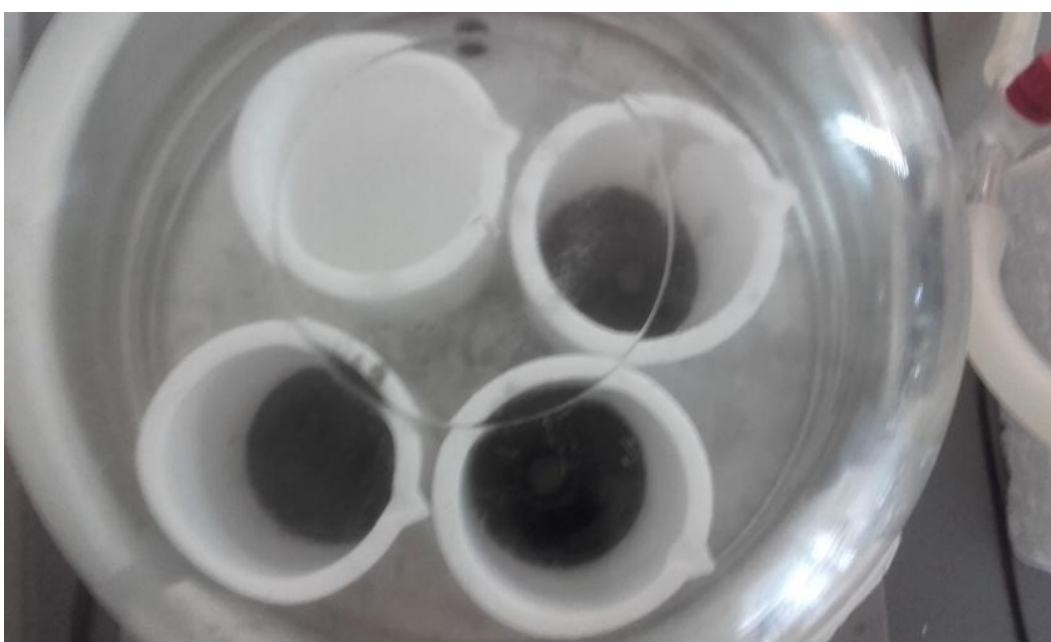


Figure 23. Bubbles can be observed on the surface of the sample. These bubbles were forced to the upper interphase of the sample due to the vacuum produced, and ended up being eliminated.

After six days from the beginning of the assisted evaporation the samples were placed in continuous extraction for another two hours to eliminate any remaining dioxane. After this time the samples were placed in a refrigerator at 4°C, since at room temperature the samples were not completely solid (PCL is quite malleable at relatively low temperatures) and they could not be removed from the Teflon crystallizers. After spending a day at 4°C the samples had hardened and they were removed from the crystallizers with ease. To

ensure that all the dioxane had been eliminated from the samples they were placed on four clean Petri dishes and left under a vacuum for another four days, and weighed. They were then left under atmospheric pressure for another 2-3 weeks, weighing every few days until the weight was constant, moment at which all the solvent had evaporated. The resulting samples proved to be suitable, since they seemed to have a homogeneous PCL/GO distribution with no hollow parts inside them. As in the previous trial and error experiments, the sample containing 0.5 wt.% in GO seemed to be brittle and seemed to form areas separated by GO sheets.

#### 4.4 Degradation study

The final samples obtained after the evaporation of the solvent are shown in figure 24. They were punched into discs with a diameter of 5mm and a thickness of approximately 2mm, and used for the degradation experiments, as shown in figure 25. The sample with a content of 0.5% wt. GO couldn't be punched to produce the mentioned discs due to its brittle nature, as shown in figure 26 below. Instead, it was carefully cut with a sharp cutter to obtain a volume which was proximate to the cylindrical samples, although obtaining samples of equal mass and shape resulted hard since the edges broke off while cutting and as a result different sizes and geometries were obtained. It is also worth noting that the samples cut into discs also varied slightly in weight because the original samples created in the previous chapter didn't have a homogeneous thickness of 2mm. due to the shape of the crystallizer, and therefore those which were punched in the centre were a little thicker than those punched at the edges.



Figure 24. The four samples created (from left to right- 0%, 0.1%, 0.2% and 0.5% wt. GO in proportion to PCL) and the apparatus used to punch the discs from the samples.

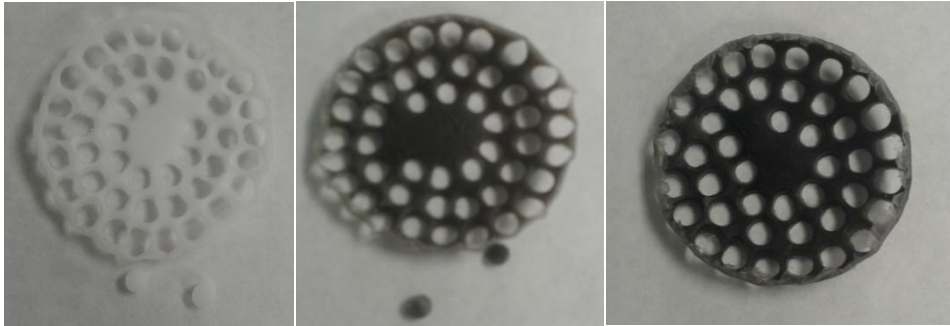


Figure 25. From left to right the content of GO is 0%, 0.1%, 0.2%.



Figure 26. Sample PCL/GO containing 0.5% wt. GO respect to PCL and the smaller samples used for posterior characterization techniques.

The discs were inserted into different 10mL vials, and two different degradation solutions were added ( $\text{pH} = 1$  to one half and  $\text{pH} = 13$  to the other). The amount of solution to be added was obtained by following a 1:50 relation in weight between the samples and the solutions. Therefore, having weighed various random samples and taking the heaviest, it was obtained that  $2,84 \approx 3\text{mL}$  of solution needed to be added to each vial. The samples contained in both pH's were then left to degrade for different times. Figures 27 and 28 below show how the distribution of the samples was arranged. As can be observed, there were three controlled variables which would later be studied: composition of GO, degradation time, and the type of degradation solution used. In the case of the degradation times,  $t_0$  represents the samples as they were obtained, without having submitted them to any degradation solution. The rest of the degradation times are described in table   . In order to minimize the effects of random errors, triplicates were prepared for both pH settings in each period of degradation and composition of the sample. Additionally, in order to further minimize the chance of random errors occurring, the punched discs were randomly placed into the vials, so that if in a certain area of the original sample there was a little more GO than in another, this would not bias the future results. The ratio of sample/degradation medium was 1:50 in mass, so it was easy to calculate the amount of degradation solution needed. The properties specified in the respective bottles were used to create the 2.5M solutions. Once the experiment had been prepared it was inserted into an oven at  $37^\circ\text{C}$  and the samples were left to degrade until at predetermined time intervals each row ( $t_1, t_2$ , etc.) were taken out of their respective solution, washed with distilled

water, wiped, weighed, and subsequently vacuum dried prior to posterior analyses. In total there were 168 samples, 84 for each pH, and each were weighed and placed in their respective vial.

	pH = 1 (HCl)				pH = 13 (NaOH)			
	0%	0.1%	0.2%	0.5%	0%	0.1%	0.2%	0.5%
t0								
t1								
t2								
t3								
t4								
t5								
t6								

Figure 27. Scheme of the distribution of the samples.

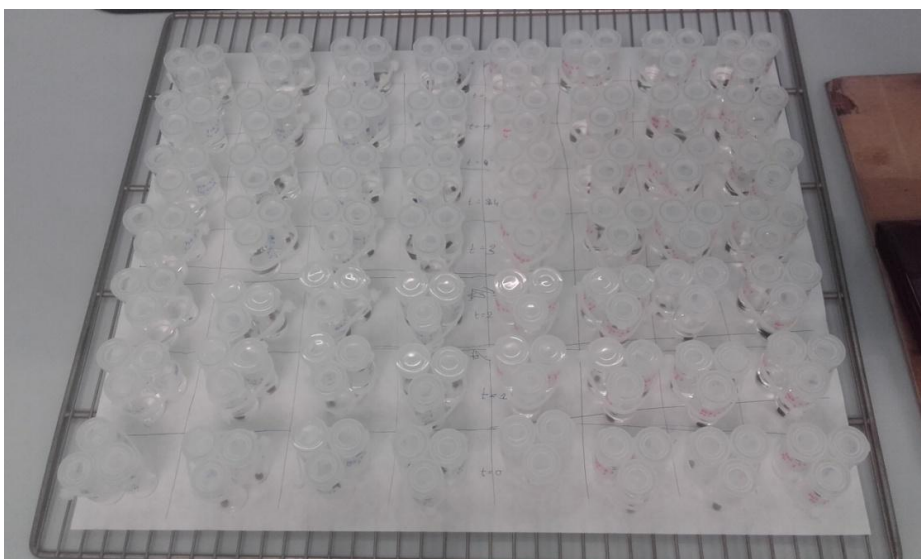


Figure 28. Distribution of the samples which were placed on top of a support which was introduced into the oven at 37°C.

Table 10. Different degradation times which the samples were submitted to.

	HOURS	DAYS	REAL TIME	REAL TOTAL HOURS	REAL TOTAL DAYS
t=0	0	0.0	12/04/2017 17:20	0	0
t=1	150	6.3	18/04/2017 16:40	143	6.0
t=2	300	12.5	24/04/2017 13:00	284	11.8
t=3	600	25.0	08/05/2017 11:00	618	25.7
t=4	900	37.5	19/05/2017 18:30	889	37.0
t=5	1300	54.2	05/06/2017 19:00	1298	54.1
t=6	1700	70.8	22/06/2017 12:30	1699	70.8



## 4.5 Characterization

### 4.5.1 Weight Loss and Equilibrium Water Content

The process of degradation was followed by determining the amount of water absorbed by the samples and the mass loss of the materials. The samples were taken out of their respective solutions, washed with distilled water and carefully wiped with paper to eliminate any water present on the surface of the sample. The wet weight was determined to evaluate the evolution of the samples' hydrophilicity. The degree of swelling was determined by comparing the wet weight ( $w_w$ ) at a specific degradation time with the dry weight ( $w_d$ ) of the same sample after being submitted to a vacuum (figure 29, left) to eliminate all water particles, according to Eq. 1.

$$\text{degree of swelling (\%)} = \frac{w_w - w_d}{w_d} \times 100 \quad (1)$$

The percentage of weight loss of the samples was determined by comparing the dry weight ( $w_d$ ) at a specific time with the initial weight ( $w_0$ ) according to Eq. 2

$$\text{weight loss (\%)} = \frac{w_0 - w_d}{w_0} \times 100 \quad (2)$$

The triplicates of the dry samples were stored for further analyses.

A balance (Mettler Toledo XS105 DualRange) with a sensitivity of 0.01mg was used when doing all weighing measurements (Figure 29, right).

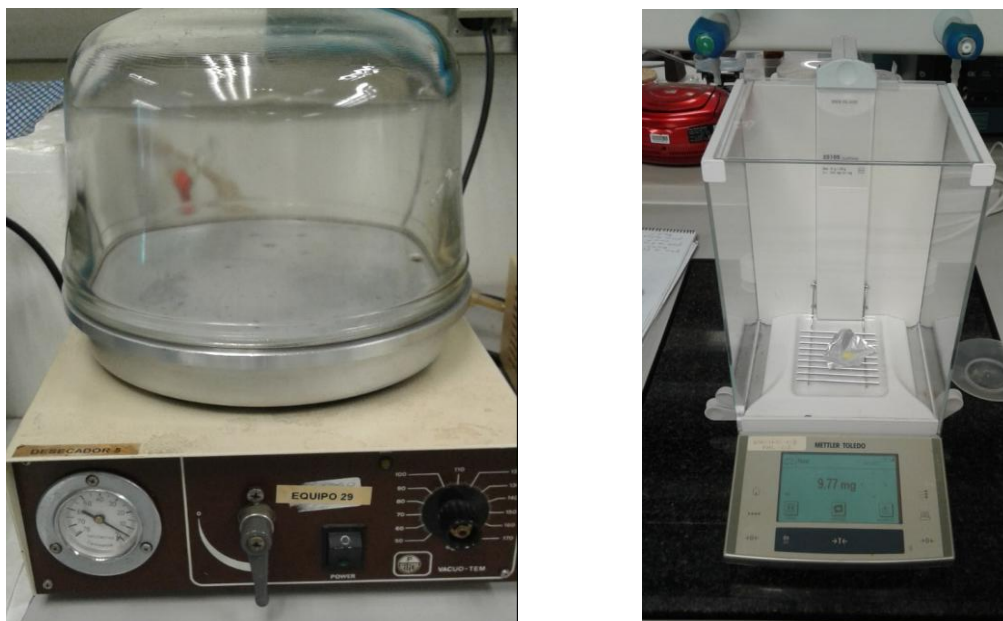


Figure 29. Left: vacuum. Left: Mettler Toledo XS105DU balance.

#### 4.5.2 Scanning Electron Microscopy (SEM)

In order to investigate the surface and cross section morphology of the dried samples, SEM pictures of degraded and non-degraded samples were taken using a JEOL JSM 6300 scanning electron microscope (shown in figure 31) at different focuses. The pictures of the samples were taken at focuses  $\times 20$ ,  $\times 100$ ,  $\times 500$ ,  $\times 2000$  and  $\times 4000$ . The discs were cut in half so that a photo of the surface and the cross-section of the discs could be taken. They were stuck onto an aluminium platform and the top of the surface of the discs were electrically connected to the bottom platform with carbon since the samples are not electrically conducting. They were finally sputtered with a gold layer (as shown in figure 30) and the micrographs were taken at an accelerating voltage of 10 kV in order to ensure a suitable image resolution.



Figure 30. Arrangement of the samples which were to be placed in the scanning electron microscope.



Figure 31. JEOL JSM 6300 Scanning electron microscope.

### 4.5.3 Differential Scanning Calorimetry (DSC)

The thermal properties of the samples were measured by using a Mettler differential scanning calorimeter (DSC) calibrated with indium. In order to perform the DSC tests, the samples, which required a minimum weight of 5mg, needed to be encapsulated in 40 $\mu$ L capsules, using the equipment shown in figure 32. In order to not cause any damage to the equipment, the capsules were perforated to allow any possible gas or solvent which may be present in the sample to escape.



Figure 32. Preparation of the samples for DSC measurements

The measurements were carried out at a scan rate of 10 °C/min between a temperature range of -10°C and 100°C. To keep the same thermal history, each sample was first heated from -10°C up to 100 °C, cooled once more to -10 °C, and finally heated again to 100°C. Crystallinity was calculated assuming proportionality to the experimental heat of fusion of neat PCL, using the reported heat of fusion of 139.5J/g for the 100% crystalline PCL (Crescenzi, Manzini, Calzolari, & Borri, 1972). The first scan analyses the effect of the degradation process on the sample; the second heating scan measures the melting of the crystals once the first heating scan has erased the previous history of the material (Vidaurre, Crescenzi, & others, 1972). As all the samples have crystallized under the same conditions, the melting peak corresponding to the second heating scan depends on the material properties, not on their history. In this section only the first heating scan is going to be analyzed since the thermal history of the material is going to be studied.



Figure 33. Mettler Toledo 823e differential scanning calorimeter (DSC) equipped with a TSO 801 RO sample robot and cooled with liquid nitrogen.

#### 4.5.4 X-Ray Diffraction (XRD)

X-ray diffraction spectra of degraded samples were obtained on an X-ray diffractometer, Rigaku Ultima IV (shown in figure 34), in the Bragg-Bentano configuration using the  $K\alpha$  radiation of a Cu anode. The samples were scanned from  $2\theta=10-35^\circ$  at a speed of  $2^\circ/\text{min}$ . The determination of the size of the crystals was carried out using the Debye-Scherrer equation (Klug, 1967), according to equation 3.

$$D = 0.9 \frac{\lambda}{\beta \cos \theta} \quad (3)$$

where  $D$  is the apparent particle size,  $\beta$  is the full-width at half-maximum (FWHM) of the X-ray diffraction line (additional peak broadening) in radians,  $\lambda$  is the wavelength used, and  $\theta$  is the angle between the incident ray and the scattering planes. The constant 0.9 in Eq. (3) depends to an extent on the symmetry of the crystal and has been discussed by several authors (Guinier, 1963) (Luo, Meng, & other, 2010).

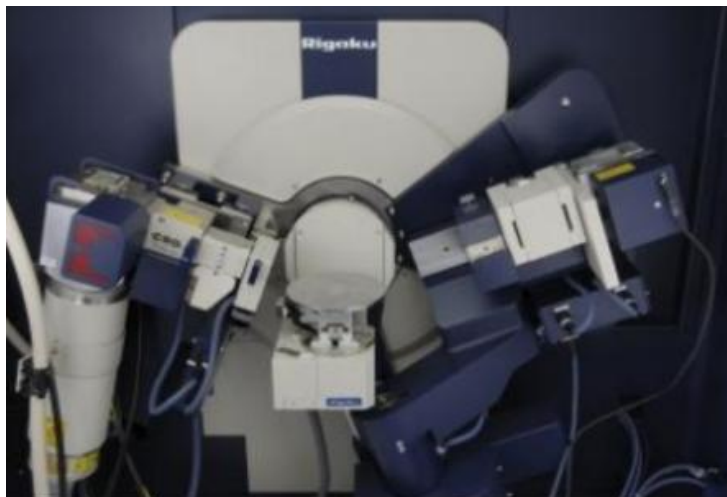


Figure 34. X-ray diffractometer Rigaku Ultima IV.

## 5 PRESENTATION AND ANALYSIS OF THE RESULTS

Materials were synthesized and characterized according to the following techniques: equilibrium water content - weight loss (EWC-WL), scanning electron microscopy (SEM), differential scanning calorimetry (DSC) and X-ray analysis.

### 5.1 Synthesized Materials

The resulting samples which would later be punched into discs and analyzed are shown in figure 35.

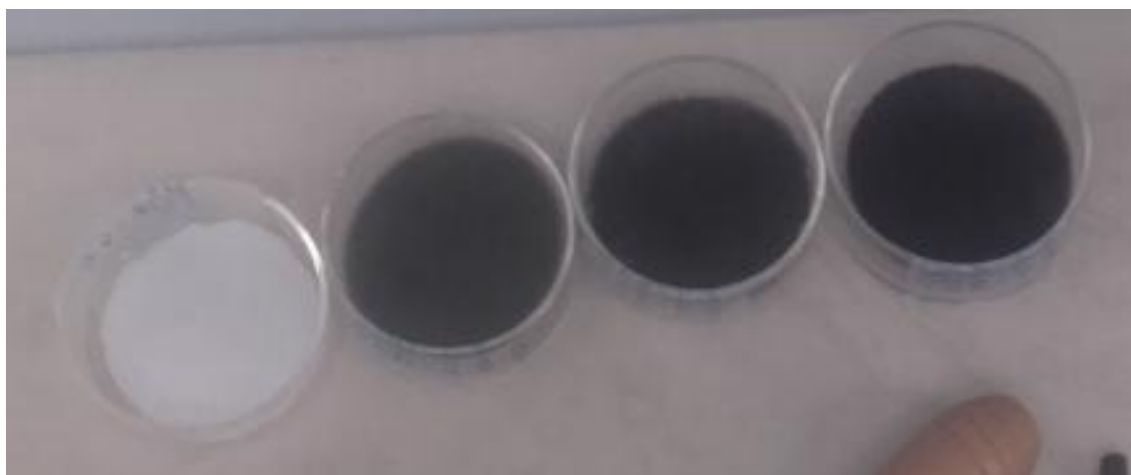


Figure 35. From left to right - 0%, 0.1%, 0.2% and 0.5% wt. of GO in proportion to PCL.

### 5.2 Characterization Study

#### 5.2.1 Weight Loss - Equilibrium Water Content

##### 5.2.1.1 Weight loss

Weight loss profiles as a function of time of neat PCL and PCL/GO hybrids were measured at 37°C. In figure 36 it is observed that the specimens of neat PCL submitted to a basic medium showed a much faster rate of degradation (caused by the severe attack of the -OH groups present in the solution) than those which degraded at pH 1, which barely degraded. At pH 13 it is noticeable that there were two distinguishable weight loss rates. The first occurred from 0 to 500 hours, point in which the degradation was approximately 67%, and the latter from 500 hours to its complete degradation at 1300 hours. In the case of the first, there seemed to be an exponential rate of weight loss which is caused by bulk degradation with autocatalysis due to the acidification of the core of the sample when degradation by-products are produced. After this period the degradation slowed down and there seems to be a close to linear degradation profile. This is probably because the sample has degraded sufficiently for the by-products of degradation to be released into the media and therefore there is no acidic concentration gradient which fuels the degradation. In the case of the degradation at pH 1, there seems to be an induction period which continues to last by the time the project experiment finished.

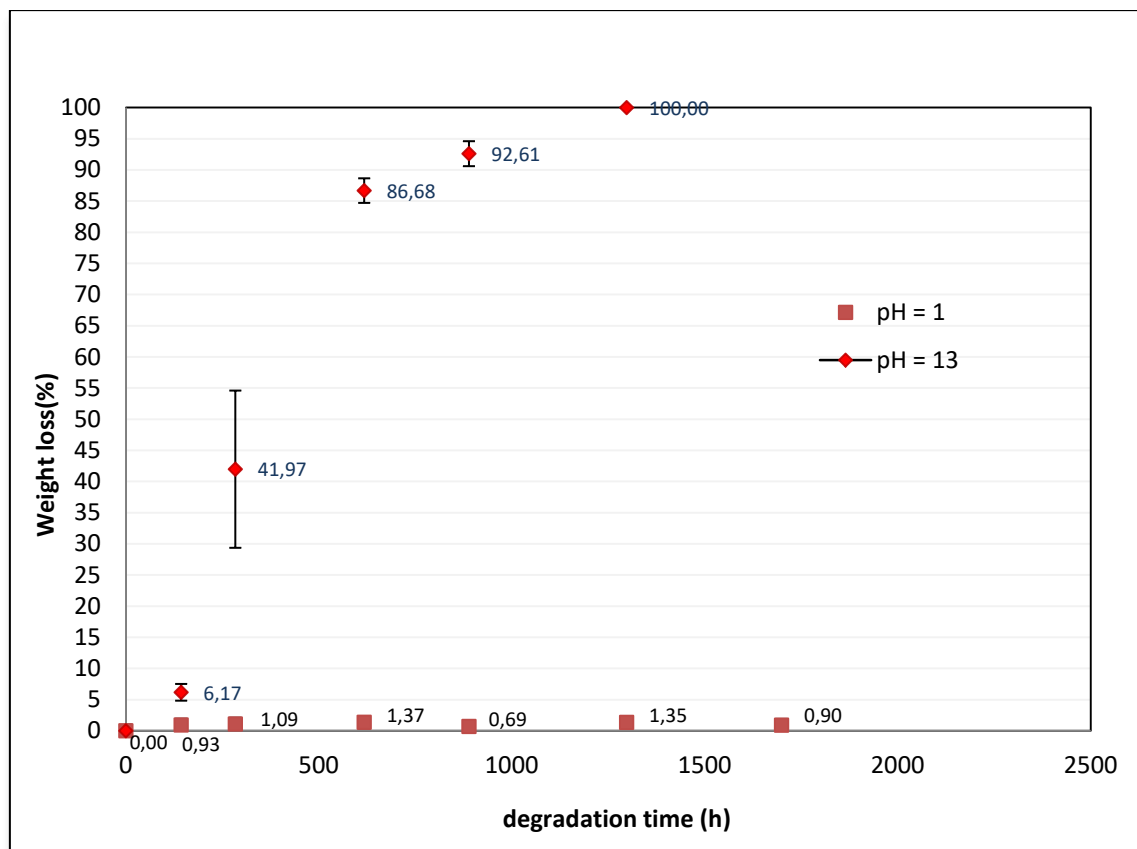


Figure 36. Weight loss profile as a function of degradation time for neat PCL.

In figure 37, which studies the degradation of PCL/GO-0.1% hybrid samples, the trend observed in the degradation of neat PCL is also followed. The specimens which were immersed in the pH 13 solution degraded much faster than those immersed in pH 1, which hardly degraded at all. There are also two distinguishable weight loss rates, which behave in a similar way to those described in figure 36. There is a noticeable difference between both, which lies in the fact that the first exponential growth rate occurs at a higher rate, lasting up to approximately 400 hours, point at which the degradation had reached approximately 70%. In the case of neat PCL the weight loss at this point was roughly 50%. After this first region, the linear tendency of weight loss was also coincident, although the samples which contained GO took more time to be fully degraded.

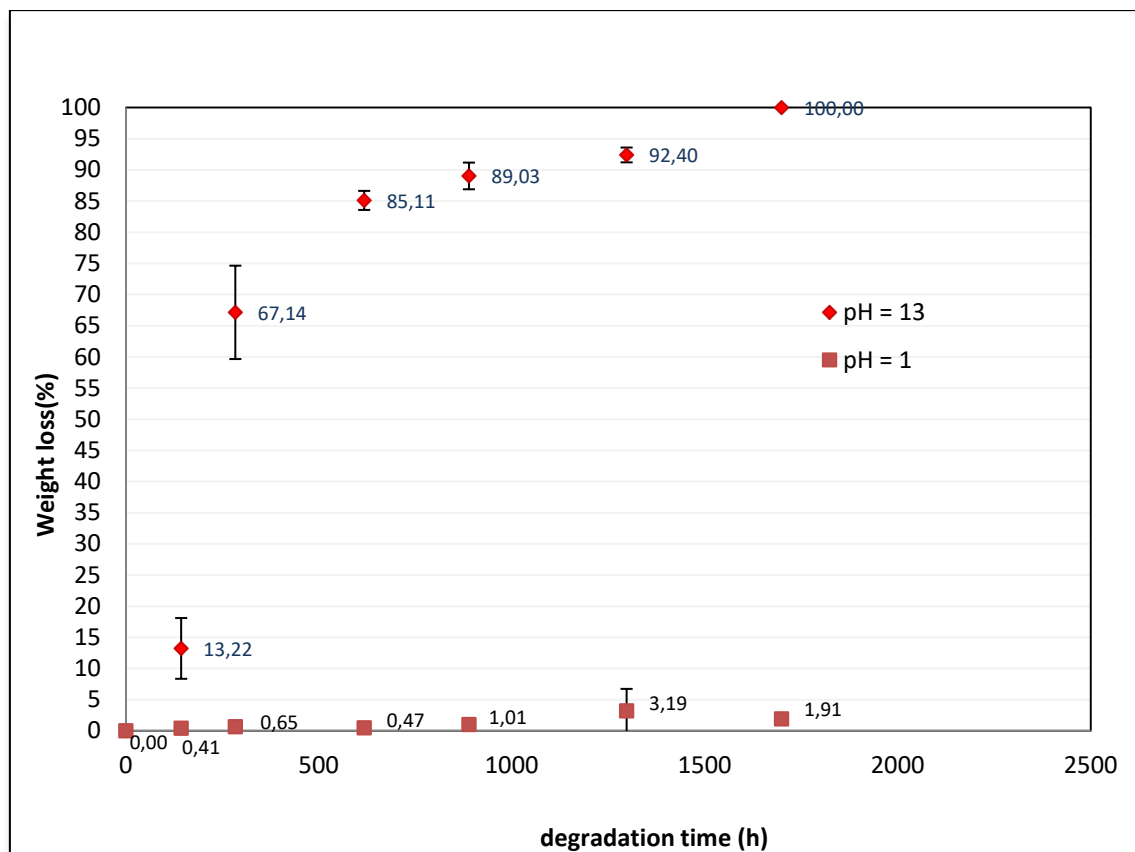


Figure 37. Weight loss profile as a function of degradation time for PCL/GO hybrids with 0.1% wt. content of GO.

The trend observed in the first two analyzed compositions is also followed in the samples which contained 0.2% wt. of GO in the PCL matrix, as the samples degraded much faster in pH 13, whilst those submitted to pH 1 hardly degraded. Once again there are two distinguishable weight loss rates, which can be appreciated in figure 38. In this case, the first weight loss profile seems to follow a linear tendency rather than an exponential one. Despite this fact, the degradation of this hybrid is much faster initially than the hybrid containing half the amount of GO, having a weight loss of 29.93% after 143 hours against a weight loss of 13.22% for the same time for the hybrid containing 0.1% GO and 6.17% for neat PCL. This may be because the GO acts as a reactive site due to its functional groups through which the -OH groups of the NaOH solution can attack the matrix.

As has happened with the previously analyzed samples, those submerged in pH1 solution barely degraded, and there seems to be an induction period which has not yet passed. Therefore, the degradation mechanism in this medium cannot be commented.

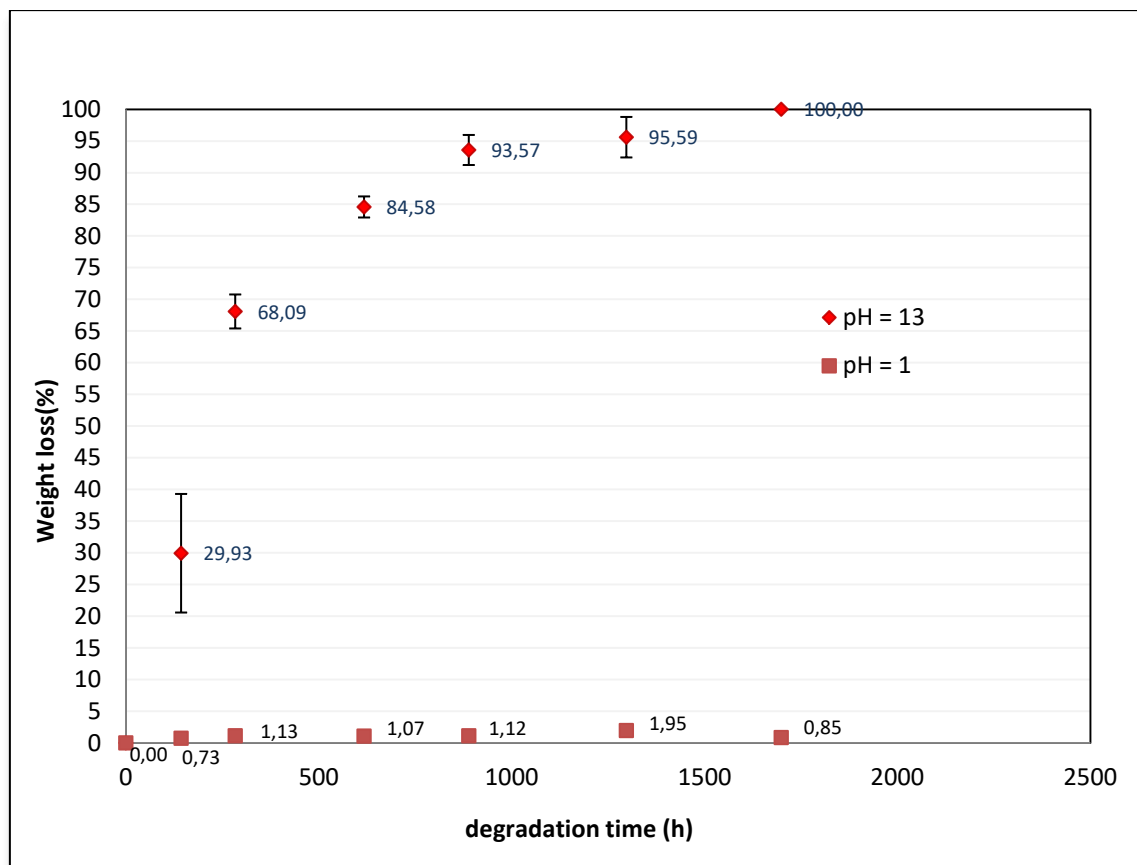


Figure 38. Weight loss profile as a function of degradation time for PCL/GO hybrids with 0.2% wt. content of GO.

The hybrids containing 0.5% wt. of GO which were immersed in a pH 13 solution degraded completely before the first analysis of weight loss which occurred after 143 hours. The samples submitted to an acid medium followed the same trend as the previously analyzed samples, in which there seems to be an induction period before the samples start degrading.



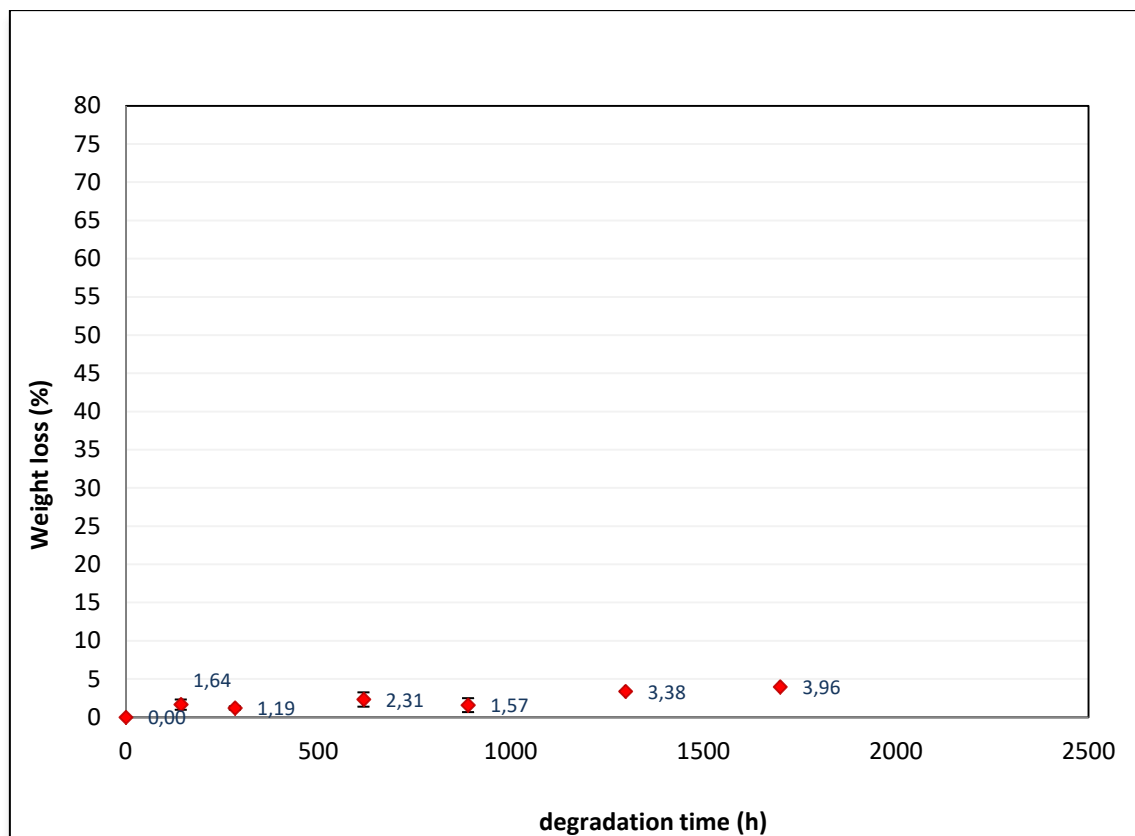


Figure 39. Weight loss profile as a function of degradation time for PCL/GO hybrids with 0.5% wt. content of GO.

pH 13	Degradation rate at t=284 h	Time at 100% degradation
PCL	41,97 %	1298h
PCL/GO 0.1%	67,14 %	1699h
PCL/GO 0.2%	68,09 %	1699h
PCL/GO 0.5%	100 %	143h

### 5.2.1.2 Degree of swelling

The degree of swelling follows a different trend depending on the pH values at which the samples were immersed. The samples of neat PCL submitted to pH 13 showed an increase in the degree of swelling with time until reaching a maximum of 21% for a period of 284 hours, as shown in figure 40. After this point, the amount of water contained inside the samples was gradually reduced up to 15% for a period of 889 hours.

The samples submitted to an acid medium showed a small initial increase in the degree of swelling up to approximately 1% at 143 hours, and maintained constant for the rest of the experiment. Since the samples barely degraded, the water uptake was going to be predictably constant.

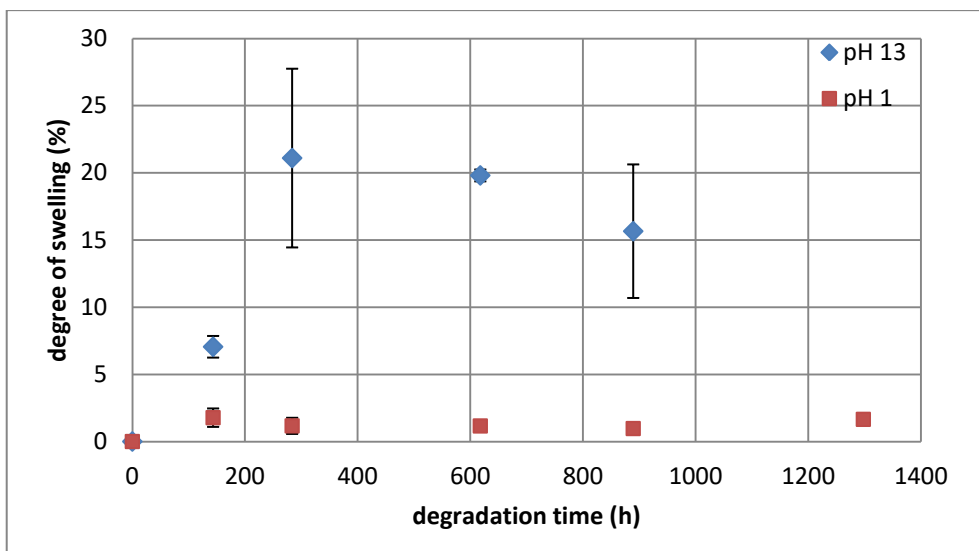


Figure 40. Degree of swelling as a function of degradation time for neat PCL.

The hybrid samples containing 0.1% wt. of GO which were submitted to pH 13 showed an initial increase in the degree of swelling with time until reaching a maximum of 14.5% for a period of 284 hours, moment at which the water uptake was gradually reduced up to 8% for a period of 889 hours. After this point, the degree of swelling was newly increased up to nearly 14% for a period of 1298 hours. When the polymer is immersed in an alkaline solution it maintains its apolar (hydrophobic) character, probably due to the hydroxyl ions entrapped by the ester groups on the film surface, which theoretically lowers its absorption capacity. Since PCL is a hydrophobic polymer, the degree of swelling was expected to increase with an increasing content of GO due to the polar (hydrophilic) functional groups present in the GO lattice, but the results do not match this hypothesis, as the water absorption of neat PCL is higher than that of PCL/GO-0.1%.

In the case of the samples submitted to an acid (pH 1) medium, the absorption increased slightly from a constant 1% in neat PCL to a consistent 2% in the studied composition.

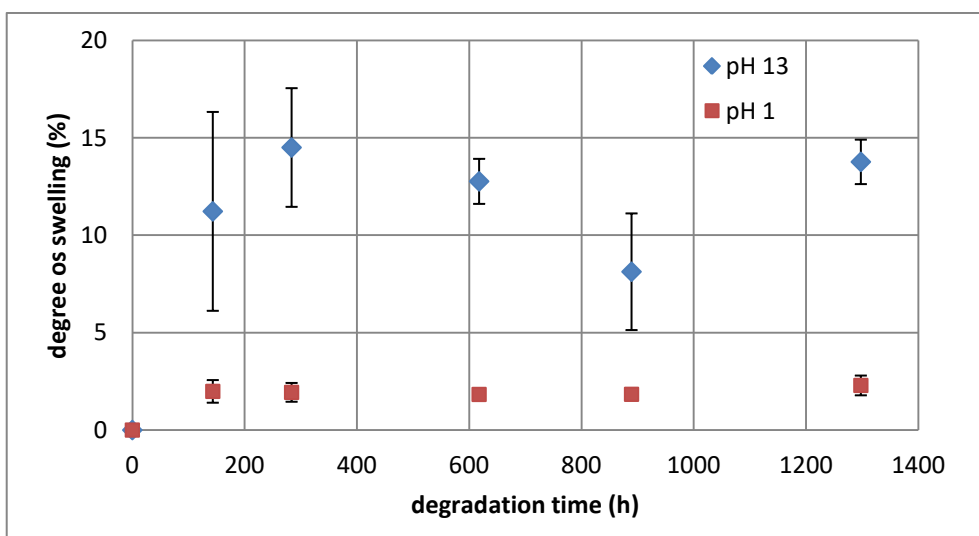


Figure 41. Degree of swelling as a function of degradation time for PCL/GO hybrids with 0.1% wt. content of GO.

The degree of swelling at pH 13 for PCL/GO-0.2% hybrids followed the same trend as the previous two samples studied. The initial water uptake reached a maximum, in this case of nearly 25%, for a period of 143 hours, and saw its capacity to absorb water reduced with time until it reached 889 hours, point at which the equilibrium water content was newly increased up to 18% at 1298 hours, as shown in figure 42.

The behaviour of these samples in an acid medium was practically identical to the PCL/GO-0.1% hybrids, since the degree of swelling initially reached 2% and maintained constant throughout the experiment.

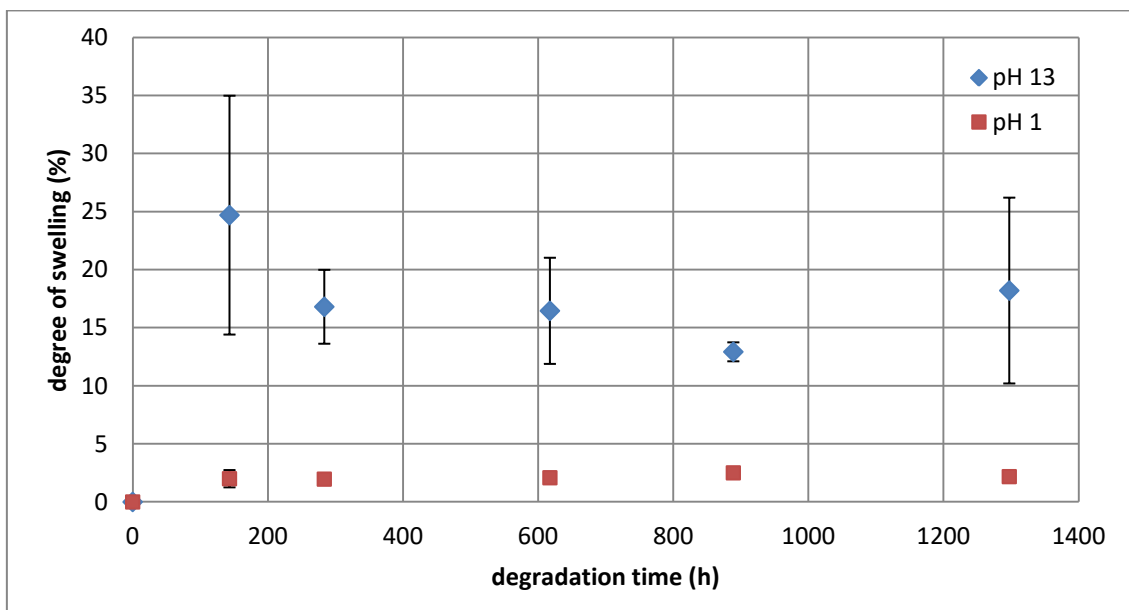


Figure 42. Degree of swelling as a function of degradation time for PCL/GO hybrids with 0.2% wt. content of GO.

The study of the water uptake for the PCL/GO-0.5% hybrids in an alkaline medium could not be studied since the samples had degraded completely. It is thought that this quick degradation is due to the porous structure which results from the higher content in GO. This porous structure allows the -OH groups to freely attack the inner matrix of the hybrid and therefore the ester bonds are quickly cleaved and the polymer chains degraded. When the PCL/GO-0.5% samples are immersed in the pH 1 solution, the water uptake is much higher than the previously analyzed samples, as it reaches an initial amount of approximately 8%, and maintains this value between 7 and 8% throughout the experiment. This, once again, is due to the porous structure which results from the higher content of GO. The pores permit the water to enter the matrix much easier than in the previous cases and therefore the water content increases.

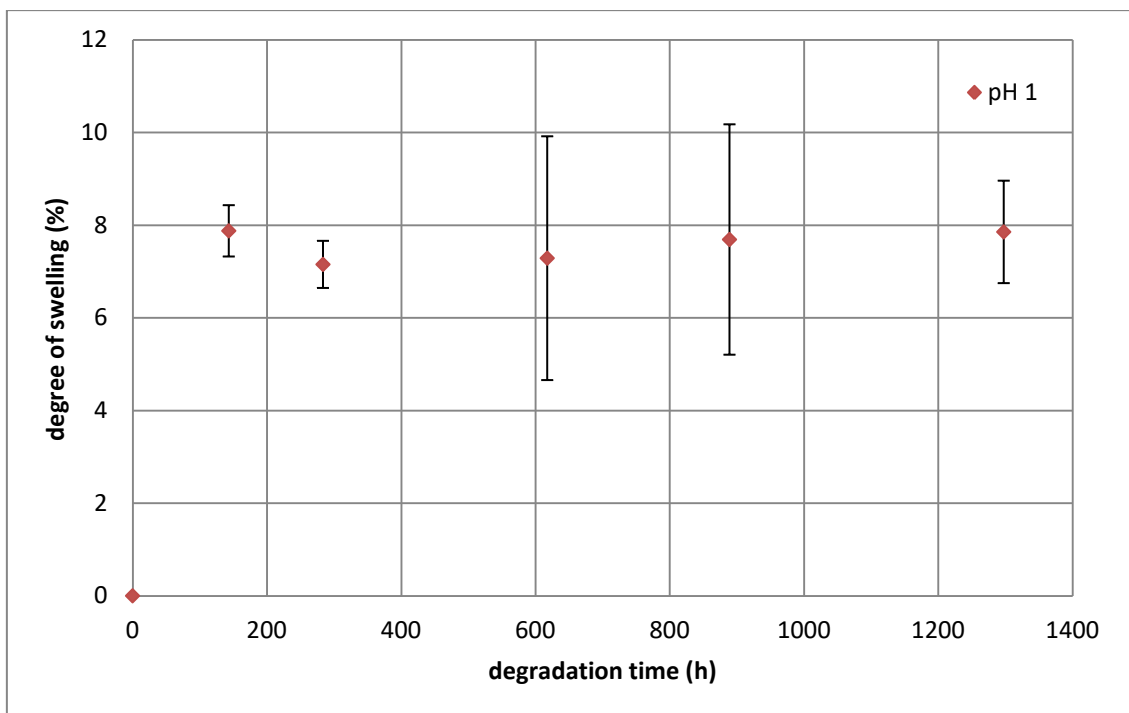


Figure 43. Degree of swelling as a function of degradation time for PCL/GO hybrids with 0.5% wt. content of GO.

In general, a larger water uptake was expected in alkaline pH's, since the degradation of the solutions in this medium was much larger than that of pH 1, despite the fact that the samples maintained their hydrophobic character when in contact with the basic medium. When the degradation starts at pH 13, large hollow and porous areas with an increased surface roughness appear, which in turn favour the absorption of water into the matrix.

The content of GO in the PCL/GO matrices did not seem to affect the water uptake of the samples, since there is a high variability between the obtained results.

### 5.2.2 Visual examination and scanning electron microscopy (SEM)

Through visual examination it could be observed that the higher the presence of GO in the hybrid, the darker the sample. Before submitting the samples to degradation, the samples were homogeneous and their surface was practically smooth and even, as shown in figure 44 below. The exception were the samples which contained 0.5% GO, which had a different structure than the others since it didn't have a homogeneous uniform distribution. These samples had a flat, smooth upper surface, but possessed a inconsistent porous distribution in the matrix, as shown in figure 45. The structure of the PCL/GO-0.5 samples is thought to be due to the higher concentration of GO sheets in the matrix. The higher presence of the GO sheets probably causes the PCL chains to lose their continuity, and therefore areas where the PCL chains are trapped between the GO sheets become abundant. This causes the hybrid to crumble very easily, and endows it with a porous structure in the matrix. However, on the surface of the sample there are no visible pores. It is unknown why the upper surface becomes a uniform smooth structure, whereas the inner matrix becomes brittle and porous.

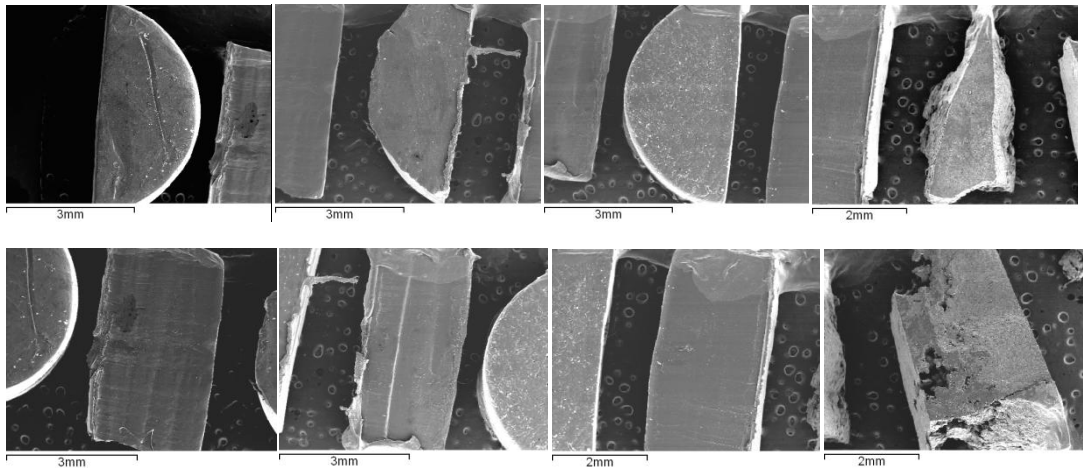


Figure 44. Superficial (top) and transversal section (bottom) SEM photos (x20) of PCL/GO samples containing different quantities of GO (0, 0.1, 0.2 & 0.5%) before being submitted to degradation (t0).

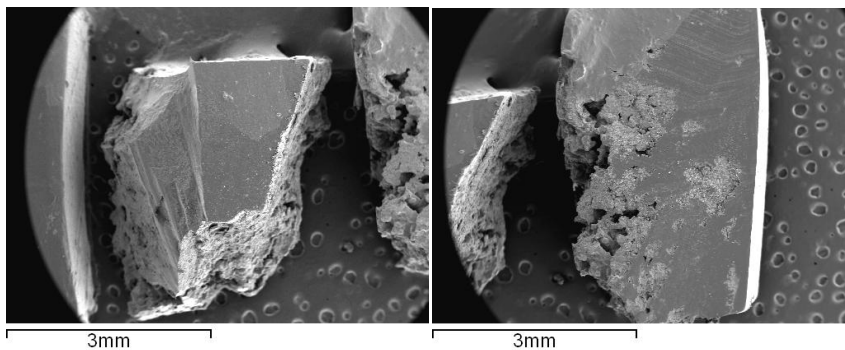


Figure 45. Superficial (left) and transversal section (right) SEM photos (x20) of PCL/GO-0.5.

When the samples are submitted to degradation, their morphologies notably vary with time depending on the medium of degradation (acid and basic).

### 5.2.2.1 Basic medium

In the basic medium (pH 13), the samples of neat PCL were completely broken down after 1300 hours through a mechanism which seemed to be by bulk degradation with autocatalysis, as shown in figure 46 and 47. This conclusion has been reached due to the shape of the sample which arises as the degradation takes place and through the visual examination of the photographs taken at a higher magnification. The degradation seems to occur faster in the centre of the matrix, leaving a 'skin' which is the last part of the polymer which is degraded.

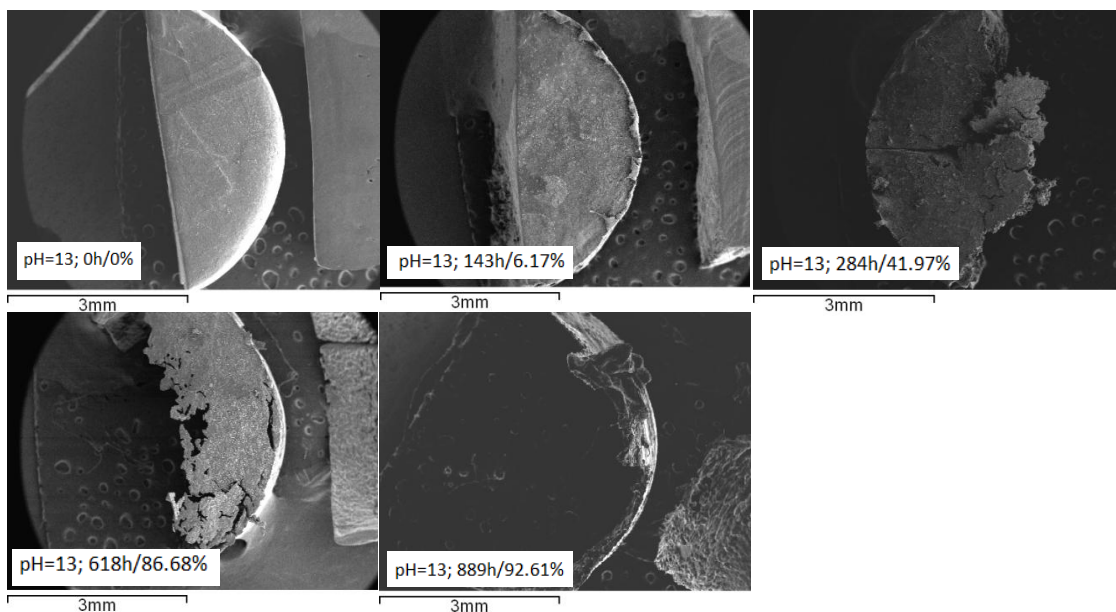


Figure 46. SEM photos (x20) of the upper surface of neat PCL samples immersed in basic pH 13 medium. Starting from top-left and finishing in bottom right, the degradation times are 0h, 143h, 284h, 618h and 889h.

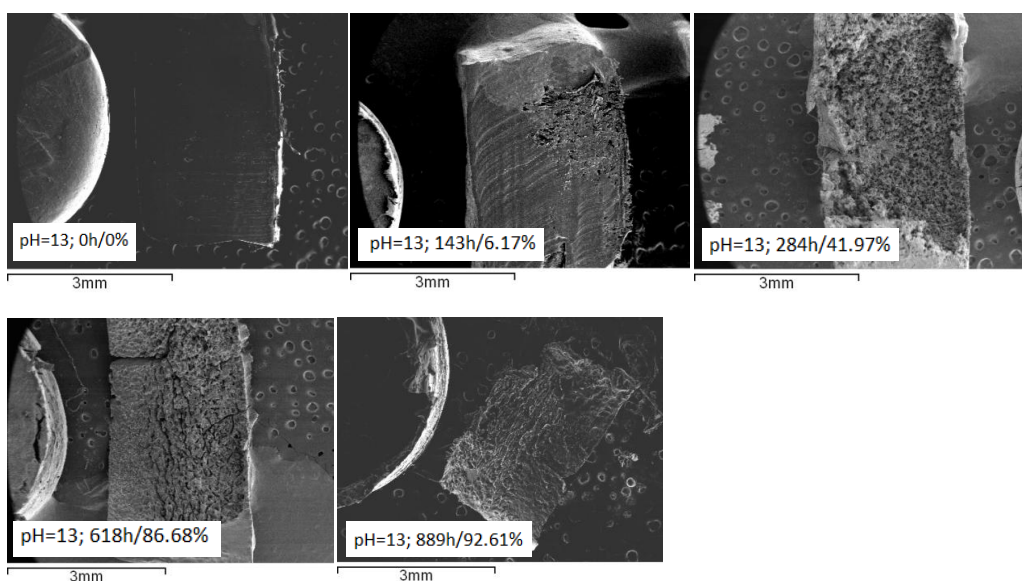


Figure 47. SEM photos (x20 magnification) of the cross section of neat PCL samples immersed in basic pH 13 medium. Starting from top-left and finishing in bottom right, the degradation times are 0h, 143h, 284h, 618h and 889h.

This contradicts the results obtained by Sailema-Palate et al. (Sailema-Palate, Vidaurre, & others, 2016), which obtained that neat PCL was degraded through a non-uniform surface erosion at pH 13. This may be due to the difference in molecular weight of the samples studied in this article ( $M_n = 70,000-90,000$ ) and those studied in the mentioned article ( $M_w = 43000-50000$ ). Since the samples analyzed in this article are much smaller, the diffusion of -OH groups into the polymer through all its surfaces is easier and these groups can reach the centre of the polymer matrix faster. This in turn hydrolyzes the PCL chains forming by-products which cannot diffuse out of the matrix, and therefore internal autocatalysis takes

place via the carboxyl (-R-COOH) and hydroxyl (-R-OH) end group by-products of the degradation process. This causes an acidification in the centre of the matrix which causes an exponential rate of degradation, fuelling itself as more by-products are formed.

The same phenomenon was observed in the degradation process of the PCL/GO hybrids. In the case of these - with the exception of PCL/GO with 0.5% wt. content, which will be explained further on - a few more weeks were needed to fully degrade the sample. However, the same degradation mechanism seemed to take place, since the samples seemed to be hollowed out before they got completely degraded. It is also observed that through the comparison of figures \_ and \_ with figures \_ and \_, the hybrids start degrading faster than neat PCL, but took longer to be completely degraded. This is confirmed by the weight loss profiles of the samples after the same given degradation times.

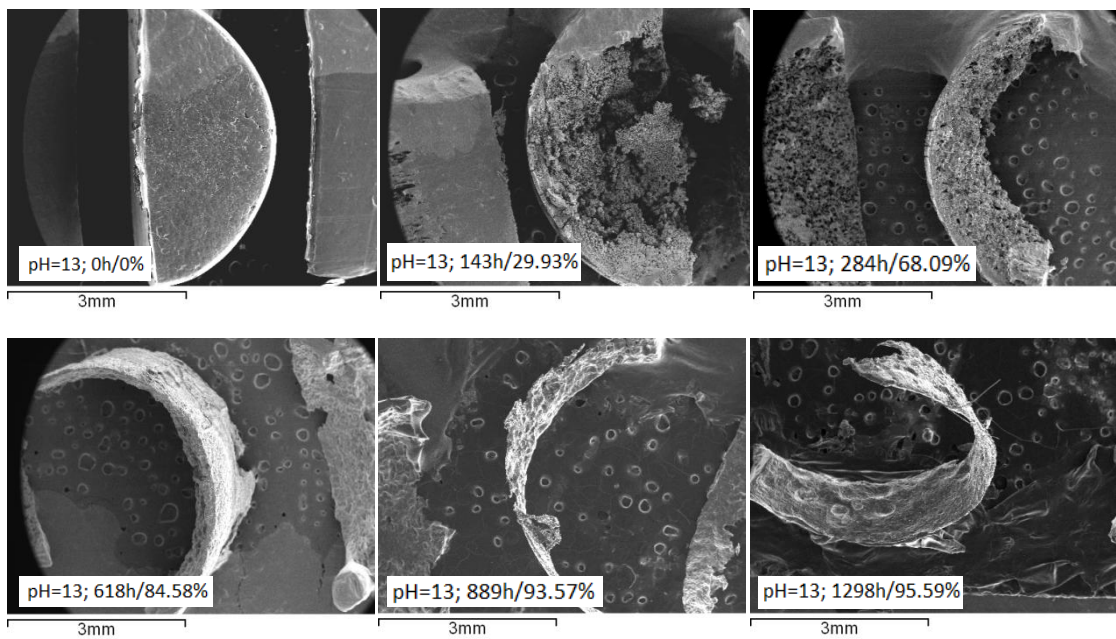
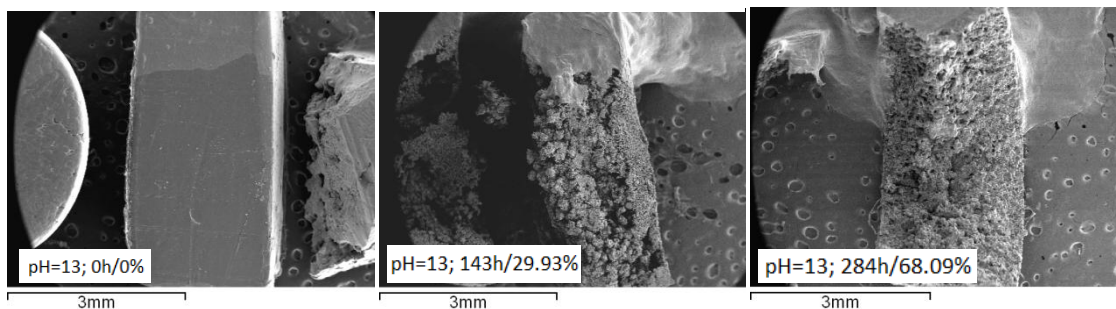


Figure 48. SEM photos (x20) of the upper surface of PCL/GO hybrids with 0.2% wt. GO immersed in basic pH 13 medium. Starting from top-left and finishing in bottom-right, the degradation times are 0h, 143h, 284h, 618h, 889h and 1298h.



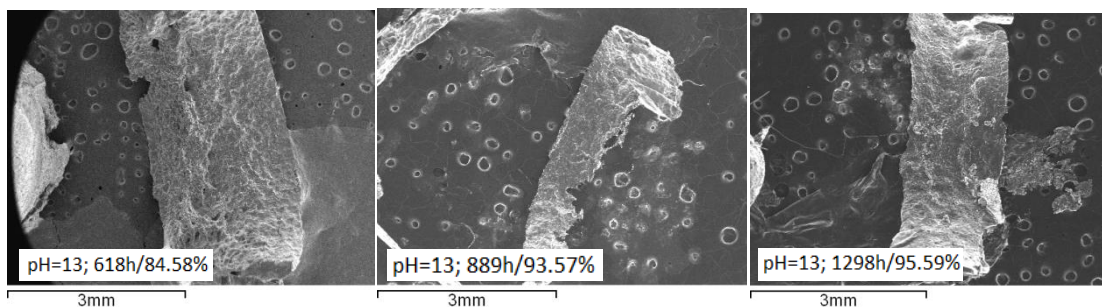


Figure 49. SEM photos (x20) of the cross section of PCL/GO hybrids with 0.2% wt. GO immersed in basic pH 13 medium. Starting from top-left and finishing in bottom-right, the degradation times are 0h, 143h, 284h, 618h, 889h and 1298h.

The rate of degradation of the samples seemed to increase as the quantity of GO in the matrix increased, as shown in figure 50. It can be clearly seen how the surface of the samples is increasingly degraded as the content of GO increases. The amount of porous indents and hollowed out regions where the polymer has been degraded increases with the composition. In the case of neat PCL, small cavities can be seen where the degradation has begun. The hybrid containing 0.1% wt. of GO presented larger hollow regions, pores and insets containing enlargements, which were created by the attack of OH groups to the polymeric chains. The trend is confirmed by observing the degradation which occurred in the hybrid containing 0.2% wt. of GO. The presence of GO sheets in the polymer matrix seem to accelerate the degradation of the hybrids by either acting as an anchor point through which the -OH groups can attack the matrix, or by altering the structure of the matrix making it more porous, separating the polymer chains, creating 'tunnels' through which the -OH groups can access the matrix and freely attack the polymer chains. Another reason which could explain the fast acceleration is that GO sheets intercalate between chains, acting as a separation point through which hydrolysis can occur. This may explain the fact that the hybrid samples which contained 0.5% wt. of GO were completely degraded before being taken out of the degradation medium after 143 hours. It is worth noting that when observing the degradation solution in which the PCL/GO-0.5 hybrid had been degraded, there were GO sheets left behind and the solution obtained a greyish colour, due to smaller GO sheets present in the solution.



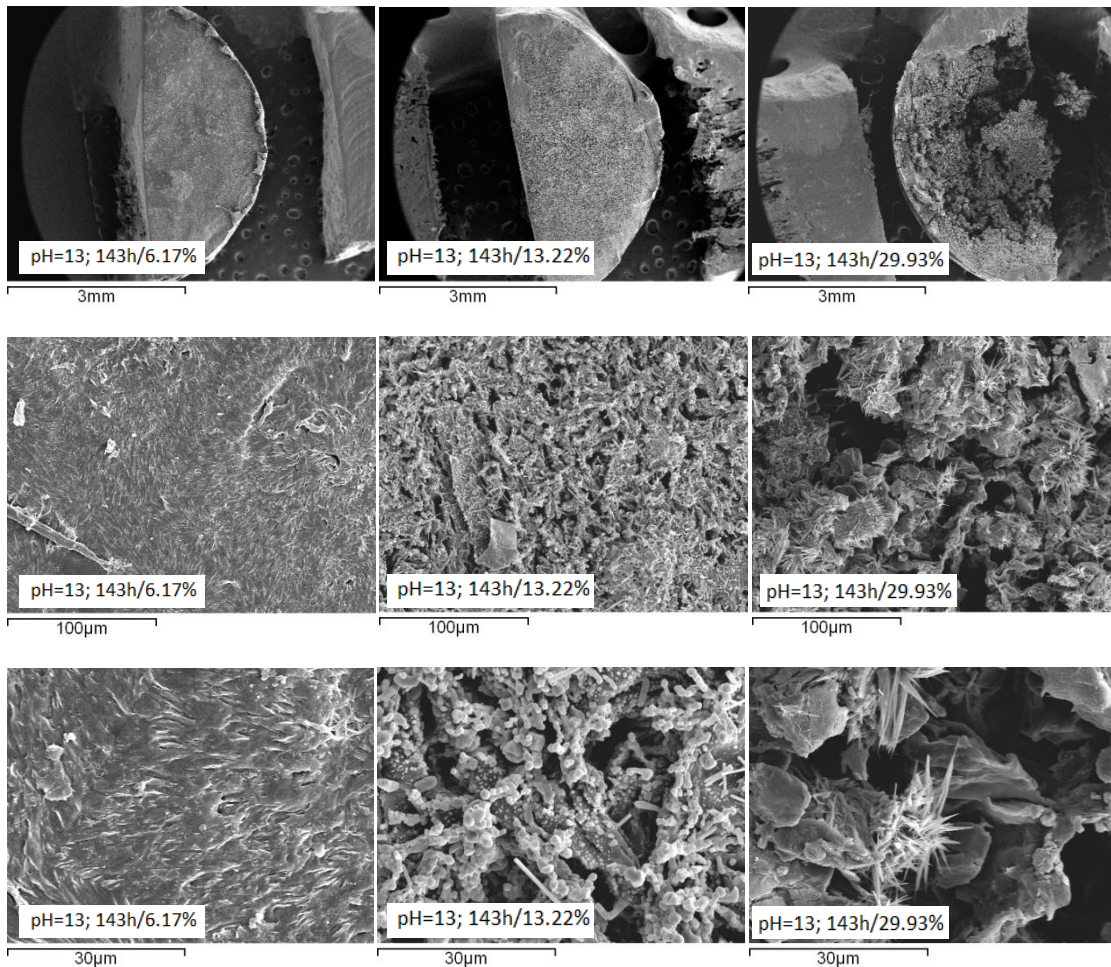


Figure 50. SEM photographs of the upper surface of the samples after being submitted to the same degradation time ( $t_1 = 143\text{h}$ ). From left to right - neat PCL, PCL/GO-0.1, PCL/GO-0.2. Top row - x20 magnification. Middle row - x500 magnification. Bottom row - x2000 magnification.

In figure 51 (a) below neat PCL is observed after 283 hours of degradation. The degradation has continued, creating further cavities and unearthing new polymer chains where hydrolysis can take place. At this point the NaOH solution had reached the centre of the matrix. In figure (b) the sample has continued to degrade for 618 hours. The polymer chains which were observed in figure (a) have fully degraded and the abundance of these is much scarcer. This is probably due to the fact that there was barely inner matrix left, and the remaining polymer was the outer 'skin' of the original sample. Therefore, autocatalysis of the carboxylic acids cannot take place because the by-products of the degradation process are able to escape into the surrounding media.

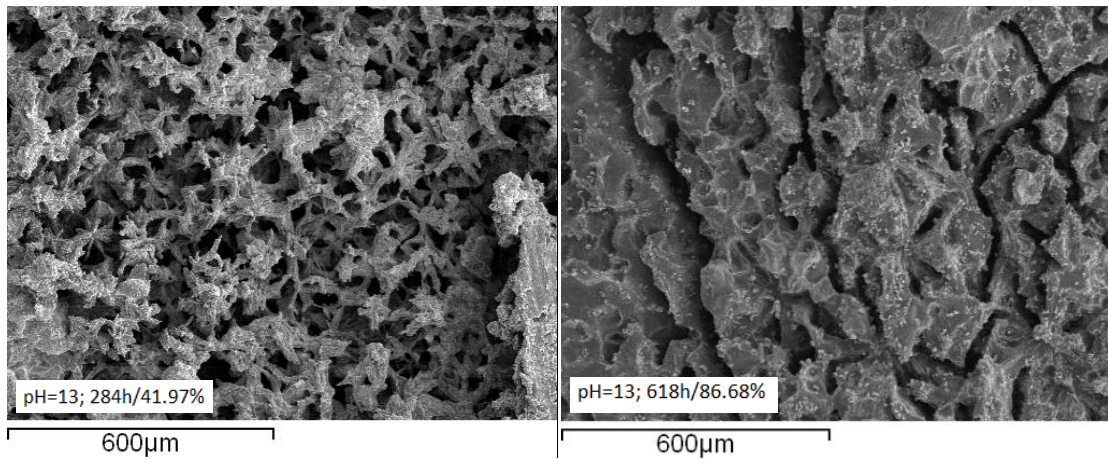


Figure 51. SEM photographs of the cross-section of the neat PCL sample after being immersed (a)  $t_2 = 284$  hours (left) and (b)  $t_3 = 618$  hours in pH 13.

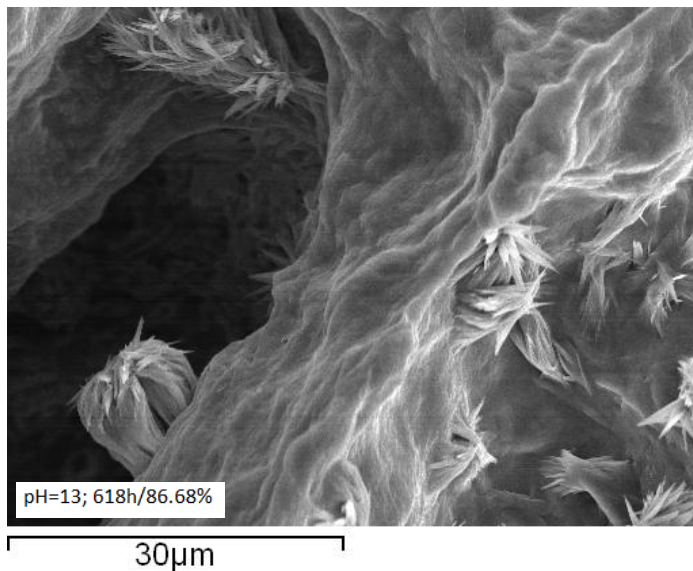


Figure 52. SEM photograph of the cross-section of the neat PCL sample after being immersed 618 hours in pH 13.

After 284 hours of immersion in the medium, the degradation mechanism followed by the hybrids containing 0.1% wt. of GO is very similar to that of PCL, since large cavities and hollow areas can be observed in figure \_ (a) below. When observing the photograph with a larger magnification, it is possible to observe sheet-like structures which are corresponding to GO integrated into the polymer matrix. These are very similar in structure and shape to the upper surface observed in the hybrids containing 0.5% wt. of GO before these were submitted to degradation. A similar behaviour is observed in the sample containing 0.2% wt. of GO.

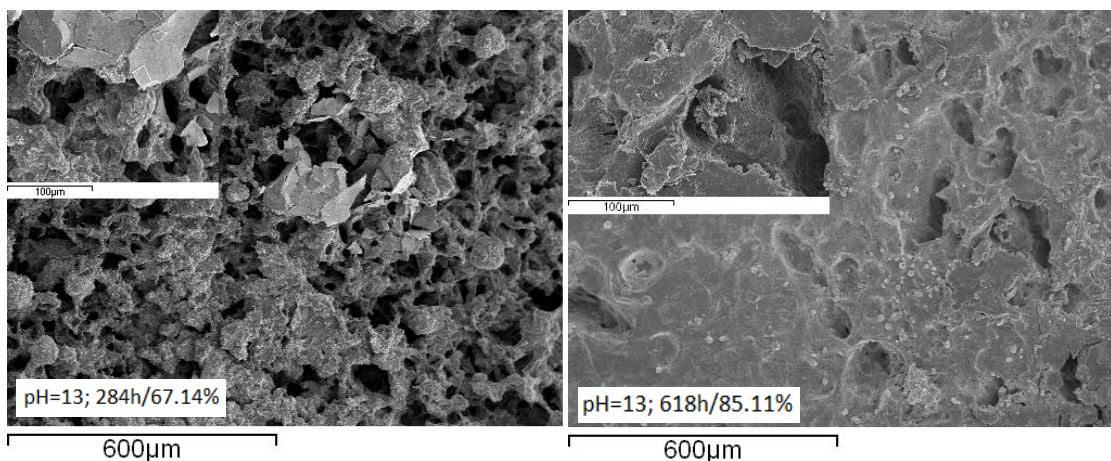


Figure 53. SEM photographs of the cross-section of a PCL/GO-0.1 sample after being immersed (a)  $t_2 = 284$  hours (left) and (b)  $t_3 = 618$  hours (right) in pH 13. The insets show a higher magnification (bar =  $100\mu\text{m}$ ).

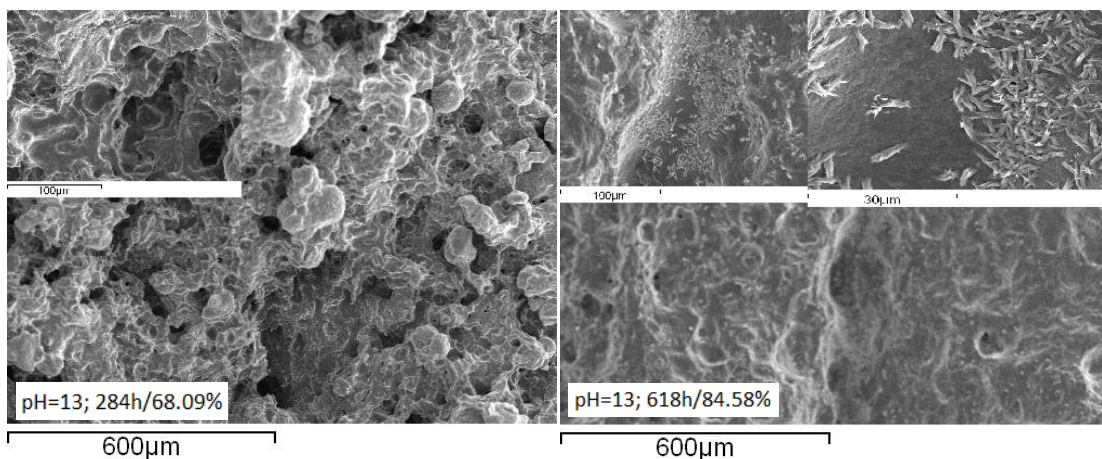


Figure 54. SEM photographs of the cross-section of a PCL/GO-0.2 sample after being immersed (a)  $t_2 = 284$  hours (left) and (b)  $t_3 = 618$  hours (right) in pH 13. The insets show a higher magnification (bar =  $100\mu\text{m}$  (left) and  $30\mu\text{m}$  (right)).

In conclusion, the samples which were immersed in a basic medium are thought to degrade through a bulk degradation with autocatalysis mechanism initially, and once the centre of the matrix has broken down, through bulk degradation to fully degrade the rest of the sample. In addition, it has been observed that the degradation increases with an increasing amount of GO present in the matrix, reaching a very fast complete degradation when the content of GO rises up to 0.5% wt. respect to PCL. Furthermore, although these samples start degrading faster, they take longer to be fully degraded, since the neat PCL samples disappeared before the hybrids did. This is backed up by the weight loss profiles of the samples.

### 5.2.2.2 Acid medium

The samples which were immersed in the acid medium (pH 1) degrade at a much slower rate than those immersed in a basic medium. At the final degradation time which was studied in this project ( $t_6 = 1699$  hours) all the samples submitted to the acid solution had barely started to degrade, as can be clearly appreciated in figures \_ and \_ below for neat PCL and PCL/GO hybrids with 0.2% wt. content of GO.

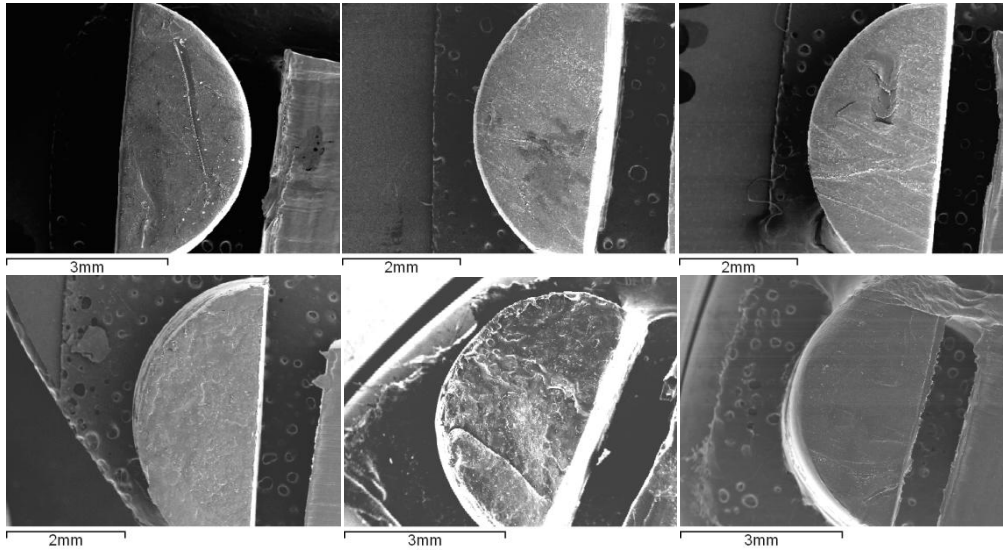


Figure 55. SEM photos (x20) of the upper surface of neat PCL samples immersed in acid pH 1 medium. Starting from top-left and finishing in bottom right, the degradation times are 0h, 143h, 284h, 618h, 889h and 1298h.

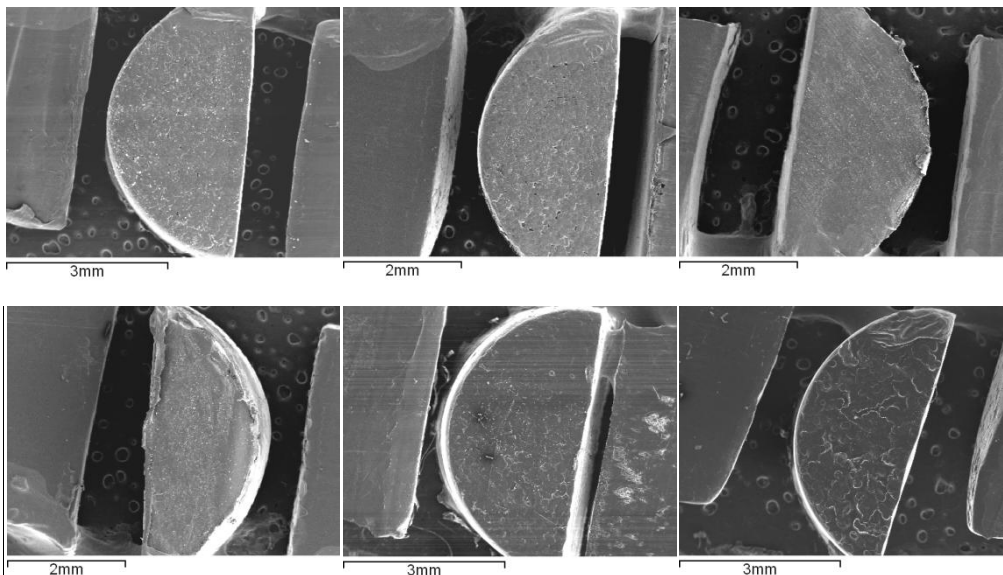


Figure 56. SEM photos (x20) of the upper surface of PCL/GO hybrids with 0.2% wt. GO immersed in an acid pH 1 medium. Starting from top-left and finishing in bottom-right, the degradation times are 0h, 143h, 284h, 618h, 889h and 1298h.

When observing the cross-section photographs of the same samples, there is practically no degradation seen in the core of the matrix. In figure 57 the cross-section photographs of samples containing 0.1% in wt. of GO which were immersed in the acid are studied.

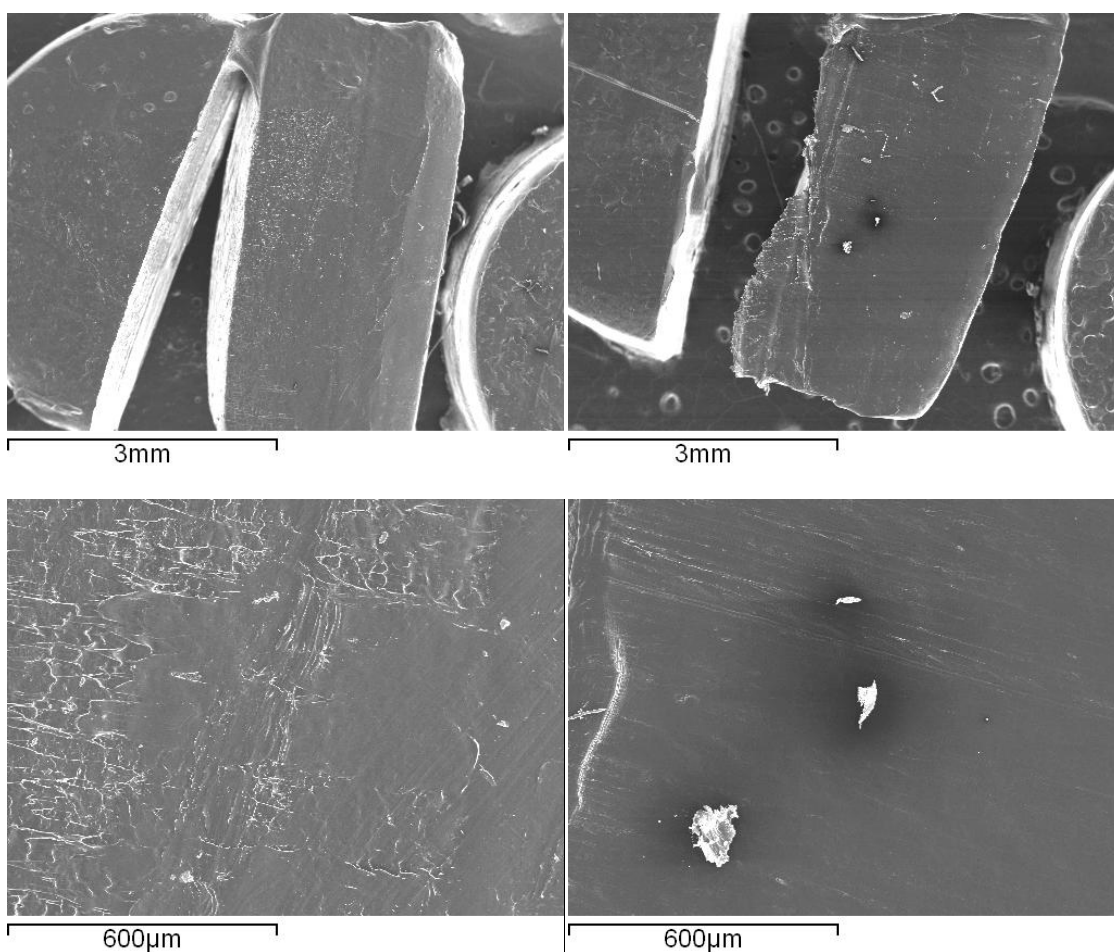


Figure 57. SEM photos (x20) of the cross-section of PCL/GO hybrids with 0.1% wt. GO immersed in an acid pH 1 medium. The sample on the left side had been immersed in the medium for 889 hours, and the sample on the right had been immersed for 1298 hours. Top row - x20 magnification. Bottom row - x100 magnification.

It is evident that there has been no degradation involved in the core of the substances. The strange shapes seen in the sample which had been immersed for 889 hours are not formed due to the action of the degradation, but rather by the blade used to cut the samples in half.

In the article published by Sailema-Palate et al. (Sailema-Palate, Vidaurre, & others, 2016) they found that the films which were degraded at pH 1 were degraded through a bulk degradation mechanism. These samples had an induction period of approximately 600 hours before cavities, cracks and fissures appeared, which are consistent with bulk degradation. At this time the degradation of the samples seemed to begin accelerating. The PCL samples studied in their article had a molecular weight between 43000-50000g/mol, nearly half the molecular weight of the PCL used in this article. It is thought that the reason why the samples in this article are taking so long to degrade is likely due to the higher molecular weight of the samples. Since the polymer chains are much longer, it is much harder for the  $H^+$  groups to attack the ester linkages, and therefore the time at which the

chains start degrading is much larger. It is thought that the samples studied are experiencing the same induction period observed in the mentioned article, but said induction period is taking much longer due to the higher molecular weight of the chains. Therefore, if the study of this article was on-going, there would probably be a trend in which the samples started degrading through a bulk mechanism, and cavities, cracks and fissures would start to be seen.

Since the degradation of the samples cannot be observed, the effect of the composition of the samples on the degradation of the hybrids cannot be studied.

### 5.2.3 DSC

For the sake of clarity in the interpretation of the results, the heat scan corresponding to each sample have been separated.

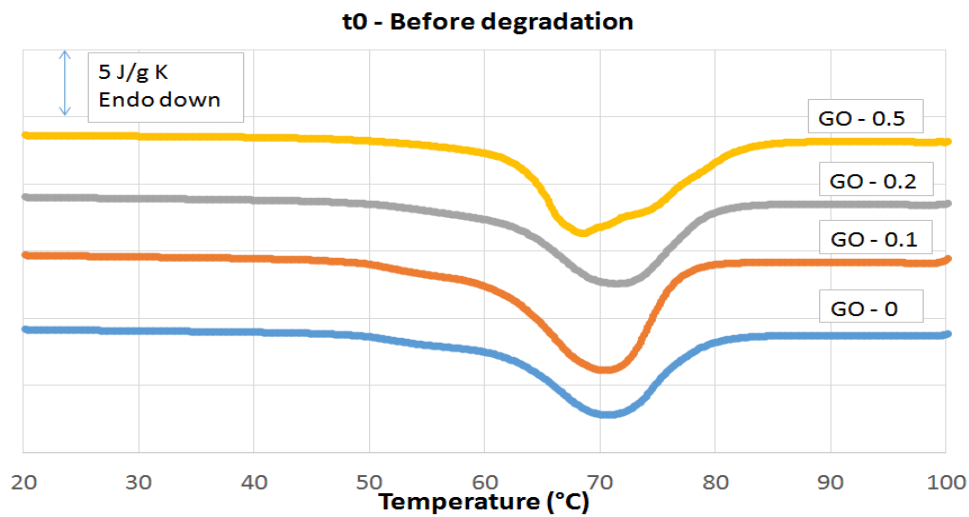


Figure 58. Endothermic DSC curves for the first scan before degradation.

Table 11. Crystallinity,  $\chi$ , and melting temperature,  $T_m$ , determined during the first scan for the samples before degradation.

$t_0$	$\chi$ (%)	$T_m$ (°C)
PCL/GO - 0	52.39	70.34
PCL/GO - 0.1	51.90	70.13
PCL/GO - 0.2	57.97	70.92
PCL/GO - 0.5	67.17	69.01

From the information obtained in figure 58 and table 11, the content of GO filler doesn't affect the melting temperature of the hybrids respect to neat PCL. However, the crystallinity of the samples increased continuously with an increasing weight fraction of GO, which contradicts the results obtained by Kai et al. (Kai, Hirota, & others, 2008), in which they found that the crystallinity decreased continuously with increasing volume fraction of the fillers. They attribute this decrease in crystallinity to the interfacial interactions between GO nanoplatelets and PCL molecular chains which reduce the chain

flexibility and retard the crystallization process. However, the GO nanosheets can serve as heterogeneous nuclei for PCL crystallization, which can be the cause in an increase of crystallinity in our samples with an increase in GO content. As is the case before degradation, the melting temperature of PCL/GO hybrids hardly varies from neat PCL. This indicates that neither the introduction of GO into the matrix or the degradation effect of both mediums affects the intermolecular covalent bonds which hold the matrix together. It is also worth noting that the samples which contained 0.5% wt. GO have a much broader peak, and there seems to be various peaks integrated into one, which indicates that a higher content of GO nanoplatelets can give the results a higher variability. From this point onwards, the effect of 0.5% wt. GO in the degraded samples will only be studied at pH1, since the samples immersed at pH 13 degraded fully before 148 hours.

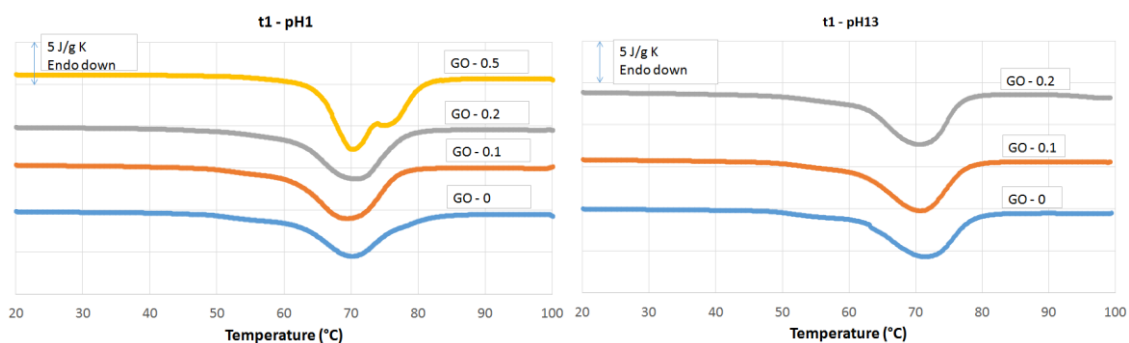


Figure 59. Endothermic DSC curves for the first heating scan after 143 hours of degradation at pH 1 and pH 13.

Table 12. Crystallinity,  $\chi$ , and melting temperature,  $T_m$ , determined during the first scan for the samples after 143 hours in, left - pH1 medium, right - pH13 medium.

$t_1$ - pH1	$\chi$ (%)	$T_m$ (°C)	$t_1$ - pH13	$\chi$ (%)	$T_m$ (°C)
PCL/GO - 0	49.85	70.76	PCL/GO - 0	48.75	70.66
PCL/GO - 0.1	54.24	69.10	PCL/GO - 0.1	50.47	70.07
PCL/GO - 0.2	53.67	70.22	PCL/GO - 0.2	51.91	69.83
PCL/GO - 0.5	65.35	72.18			

The trend in which the crystallinity of the samples increases with an increasing content of GO is also seen after 148 hours of degradation, although the increase is stronger when the samples are degraded in an acid medium. This could be due to the fast degradation which takes place in pH 13, which can heavily affect the structural composition of the samples, whilst at pH 1 the samples hardly degraded and therefore the original crystals present in the samples are practically untouched. Theoretically, since the amorphous phase has a higher chain mobility and the crystalline phase is tightly packed together, the amorphous phase is degraded first. This may affect the degree of crystallinity at pH 13 due to the high rate of degradation. Once again, the melting point ( $T_m$ ) is not affected neither by the composition of the samples or the medium in which they were immersed.

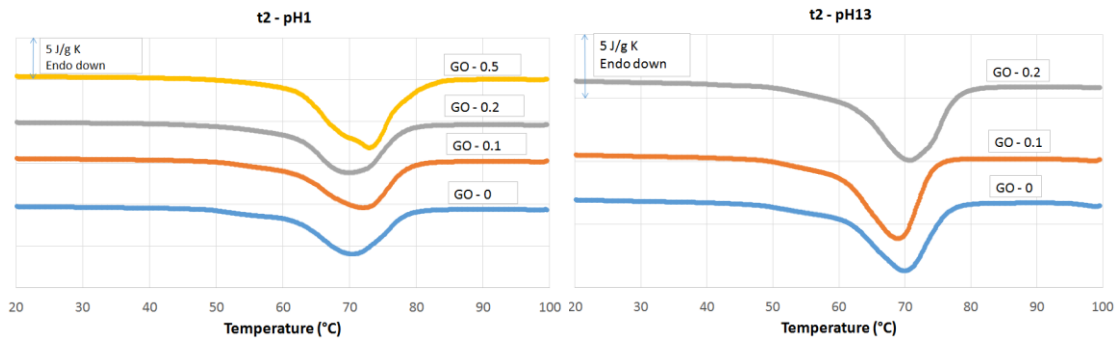


Figure 60. Endothermic DSC curves for the first heating scan after 284 hours of degradation at pH 1 and pH 13.

Table 13. Crystallinity,  $\chi$ , and melting temperature,  $T_m$ , determined during the first scan for the samples after 284 hours in, left - pH1 medium, right - pH13 medium.

$t_2$ - pH 1	$\chi$ (%)	$T_m$ (°C)	$t_2$ - pH 13	$\chi$ (%)	$T_m$ (°C)
PCL/GO - 0	49.56	69.82	PCL/GO - 0	69.63	69.96
PCL/GO - 0.1	53.52	71.24	PCL/GO - 0.1	46.96	68.31
PCL/GO - 0.2	54.87	69.66	PCL/GO - 0.2	52.47	69.37
PCL/GO - 0.5	73.93	72.59			

After 284 hours of the start of the degradation, the degree of crystallinity at pH 1 still increases significantly with an increase of content of GO, whilst the results obtained at pH 13 are very variable. This is due to the effect of degradation on the polymeric matrix. Once again, the fusion temperature is barely affected by the effect of the pH of the degradation medium and the content of GO.

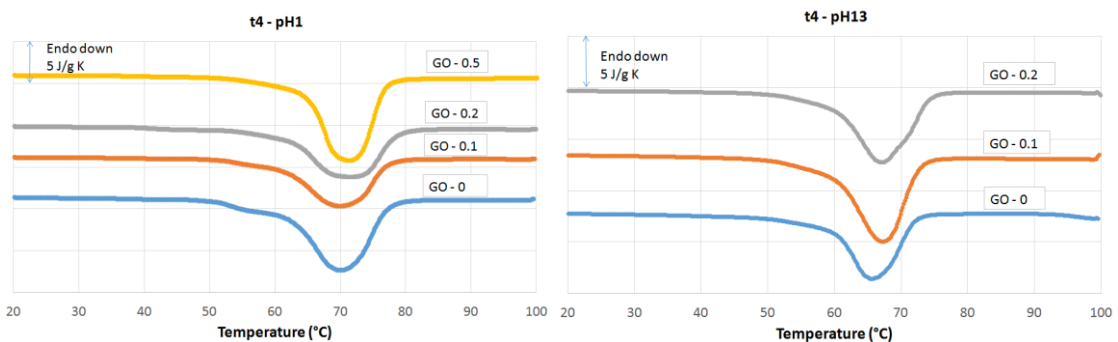


Figure 61. Endothermic DSC curves for the first heating scan after 889 hours of degradation at pH 1 and pH 13.



Table 14. Crystallinity,  $\chi$ , and melting temperature,  $T_m$ , determined during the first scan for the samples after 889 hours in, left - pH1 medium, right - pH13 medium.

$t_4$ - pH1	$\chi$ (%)	$T_m$ (°C)	$t_4$ - pH13	$\chi$ (%)	$T_m$ (°C)
PCL/GO - 0	49.88	69.09	PCL/GO - 0	48.12	65.05
PCL/GO - 0.1	49.21	69.15	PCL/GO - 0.1	54.98	66.28
PCL/GO - 0.2	55.31	69.72	PCL/GO - 0.2	50.75	66.58
PCL/GO - 0.5	66.95	69.35			

**t5 - pH1**

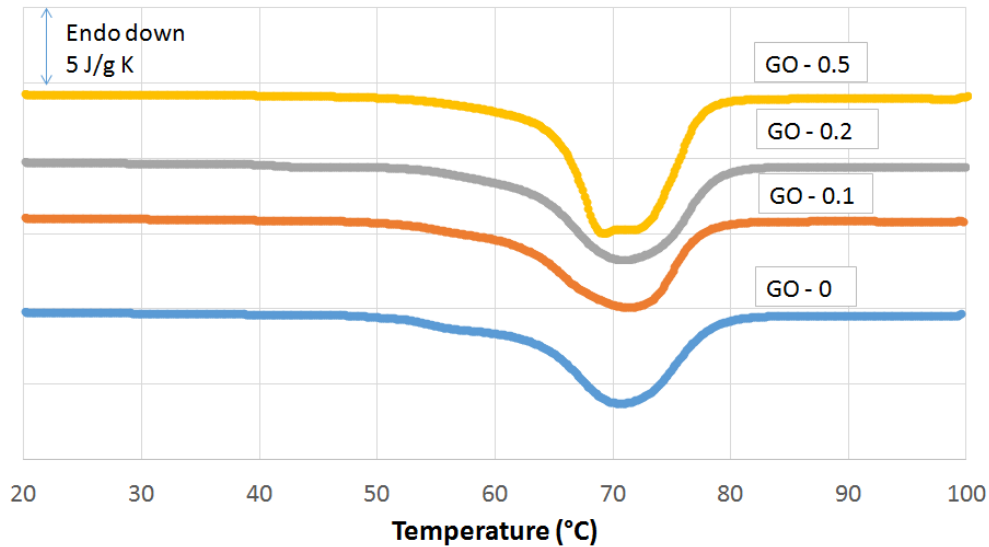


Figure 62. Endothermic DSC curves for the first heating scan after 1298 hours of degradation at pH 1 and pH 13.

Table 15. Crystallinity,  $\chi$ , and melting temperature,  $T_m$ , determined during the first scan for the samples after 1298 hours in, left - pH1 medium, right - pH13 medium.

$t_5$ - pH 1	$\chi$ (%)	$T_m$ (°C)
PCL/GO - 0	50.86	69.81
PCL/GO - 0.1	50.75	70.47
PCL/GO - 0.2	56.04	69.72
PCL/GO - 0.5	65.27	70.18

As the degradation continues, the effect of 0.1% wt. GO in the hybrids barely affects the crystallinity of the sample at pH 1, as appreciated in tables 14 and 15. However, the crystallinity of the hybrids continues to increase significantly with an ascending content in GO at the same medium. In the case of the samples degraded in an alkaline medium, the results obtained for the crystallinity of the samples continue to show a high variability due to the non-uniform superficial erosion which takes place.

In conclusion, an increase in the content of GO in the PCL/GO hybrids significantly increases the crystallinity of the original samples and those immersed in pH1, whilst those immersed in pH 13 have highly variable results due to the effect of the degradation. Furthermore, when observing the peaks corresponding to 0.5% wt. GO there generally

seems to be various peaks integrated into one, which is likely due to the fact that the DSC characterization was accomplished using three replicates of the same properties to obtain higher reliability in the results. Therefore, a content of 0.5% wt. GO in the PCL/GO hybrid created a variability in the crystallinity of the sample. Finally, the effect of the composition and degradation mediums did not seem to have any effect on the melting temperature of the samples.

In figures 63 - 66, the effect of degradation times are studied for fixed compositions in both degradation mediums.

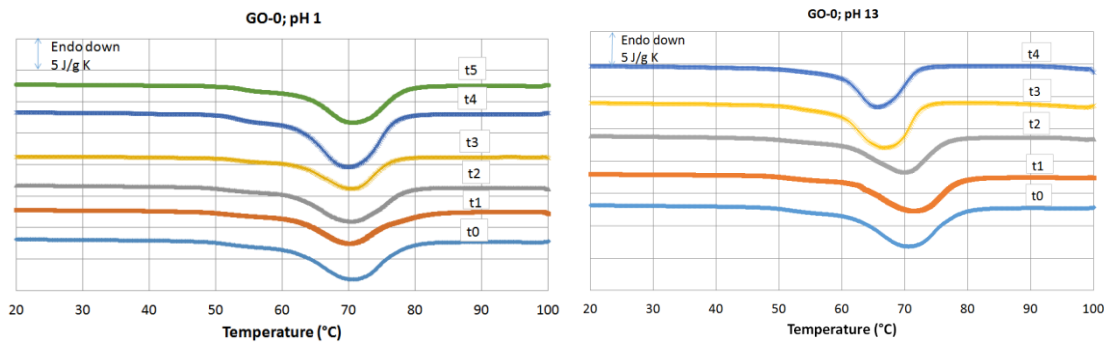


Figure 63. Endothermic DSC curves for the first heating scan for neat PCL.

Table 16. Crystallinity,  $\chi$ , and melting temperature,  $T_m$ , determined during the first scan for neat PCL at varying degradation times.

pH 1	$\chi$ (%)	$T_m$ (°C)
t0	52.39	70,34
t1	49.85	70.76
t2	49.56	69.82
t3	51.93	70.73
t4	49.88	69.09
t5	50.86	69.81

pH 13	$\chi$ (%)	$T_m$ (°C)
t0	52.39	70,34
t1	48.75	70.66
t2	69.63	69.96
t3	50.81	66.03
t4	48.12	65.05

Degradation time does not seem to affect the crystallinity of neat PCL, as the results shown in figure 63 and table 16 do not follow any trend. The fusion temperature does not vary significantly for the samples degraded in pH1. However, the samples degraded at pH13 show a decrease in their melting point after 284 hours. Since the degradation in this medium is very fierce, the intermolecular bonds which hold the polymeric matrix together are affected, and therefore the energy (temperature) necessary to break the bonds is reduced. The crystallinity of the samples immersed in the basic medium is very variable, due to the previously mentioned effect of the non-uniform degradation.

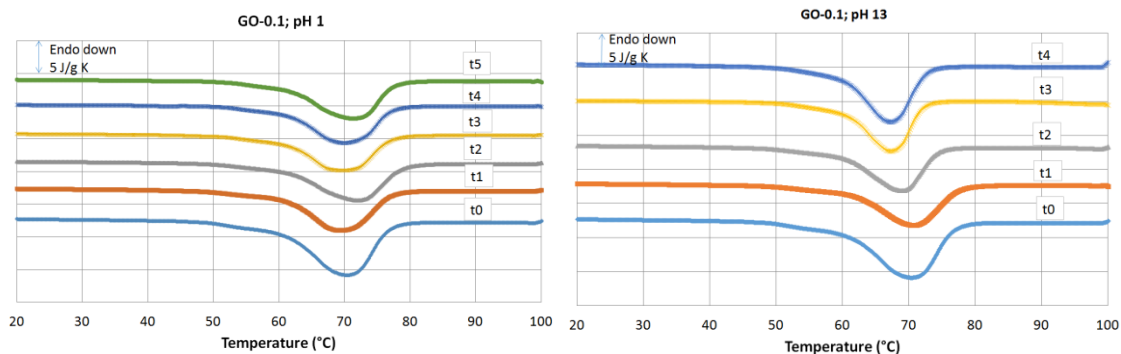


Figure 64. Endothermic DSC curves for the first heating scan for PCL/GO-0.1% wt.

Table 17. Crystallinity,  $\chi$ , and melting temperature,  $T_m$ , determined during the first scan for PCL/GO-0.1% wt. at varying degradation times.

pH 1	$\chi$ (%)	$T_m$ (°C)
t0	51.90	70.13
t1	54.24	69.10
t2	53.52	71.24
t3	52.47	69.71
t4	49.21	69.15
t5	50.75	70.47

pH 13	$\chi$ (%)	$T_m$ (°C)
t0	51.90	70.13
t1	50.47	70.07
t2	46.96	68.31
t3	47.51	66.67
t4	54.98	66.28

The results obtained from figure 64 and table 17 show a similar trend as the samples of neat PCL.

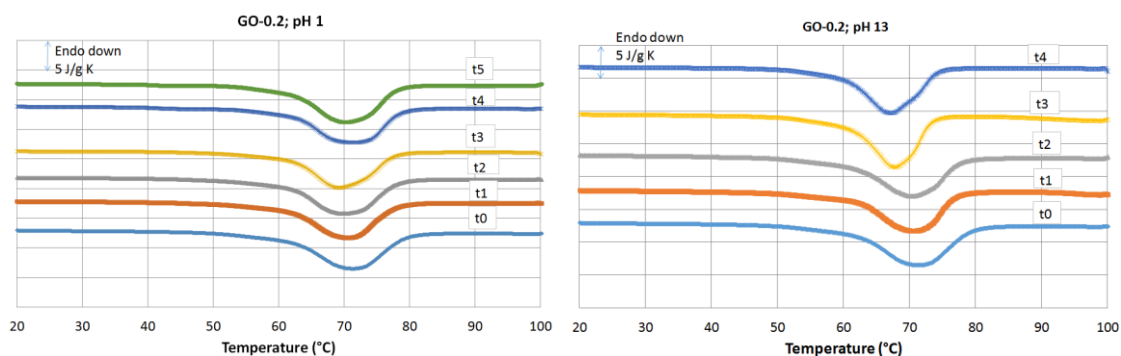


Figure 65. Endothermic DSC curves for the first heating scan for PCL/GO-0.2% wt.

Table 18. Crystallinity,  $\chi$ , and melting temperature,  $T_m$ , determined during the first scan for PCL/GO-0.2% wt. at varying degradation times.

	$\chi$ (%)	$T_m$ (°C)	pH 13	$\chi$ (%)	$T_m$ (°C)
t0	57.97	70.92	t0	57.97	70.92
t1	53.67	70.22	t1	51.91	69.83
t2	54.87	69.66	t2	52.47	69.37
t3	53.28	69.62	t3	51.55	67.04
t4	55.31	69.72	t4	50.75	66.58
t5	56.04	69.72			

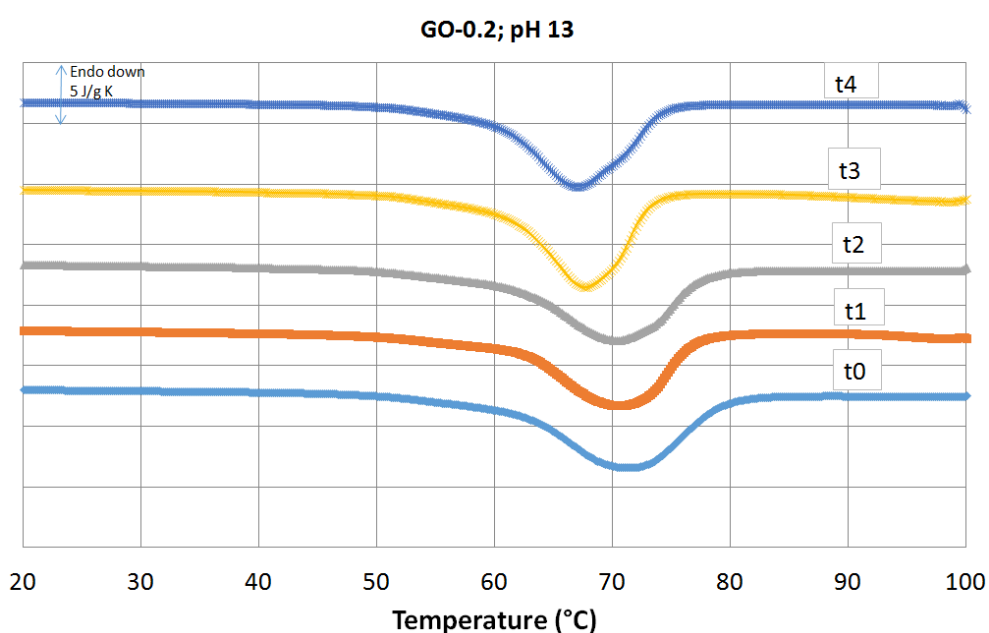


Figure 66. Endothermic DSC curves for the first heating scan for PCL/GO-0.5% wt.

Table 19. Crystallinity,  $\chi$ , and melting temperature,  $T_m$ , determined during the first scan for PCL/GO-0.5% wt. at varying degradation times.

	$\chi$ (%)	$T_m$ (°C)
t0	67.17	69.01
t1	65.35	72.18
t2	73.93	72.59
t3	69.26	69.40
t4	66.95	69.35
t5	65.27	70.18

The effect of degradation time on neat PCL is similar in the hybrid PCL/GO samples. Degradation time does not affect the crystallinity of the samples in either of the degradation mediums. Similarly, as degradation time increases the melting point of the

samples in pH1 is not affected. However, the fusion temperature ( $T_m$ ) of the samples immersed in a basic medium decreases from 284 hours onwards, as is the case of neat PCL.

In conclusion, the only significant trend observed when fixing composition and comparing the degradation mediums and degradation time is that the melting point of the samples immersed in a basic medium is decreased after a certain degradation time.

#### 5.2.4 X-Ray Diffraction

The X-ray diffraction profiles for the different hybrid samples of PCL/GO (0%, 0.1%, 0.2% and 0.5%) submitted to no degradation ( $t_0$ ) and 618 hours ( $t_3$ ) of degradation in a pH13 medium are shown in Figure 67. The objective was to study how different quantities of GO and degradation times affected the morphological structure and the crystal size of the hybrids. The diffraction pattern showed characteristic PCL peaks at  $2\theta=21.3^\circ$  and  $23.6^\circ$  for neat PCL before degradation, which correspond to (1 1 0) and (2 0 0) crystallographic planes, respectively (Peng, Han, & other, 2010). The diffraction pattern of neat PCL after having being submitted to 617,67 hours ( $t_3 = 25,7$  days) of degradation at pH13 showed very little variation, with characteristic PCL peaks at  $2\theta=21.0^\circ$  and  $23.3^\circ$ . It was concluded that the degradation time to which the PCL samples were submitted hardly affected the morphological structure and the crystal size of the matrix.

Furthermore, the analyzed samples which contained different quantities of GO did not appear to show any significant variation with the results obtained with those of neat PCL. Figure 68 below corresponds to the XRD profile of pure GO, where the diffraction pattern showed peaks at  $2\theta=10.0^\circ$  and  $42.2^\circ$ . However, these peaks could not be observed in figure 67 when analyzing the PCL/GO samples, and no other characteristic peaks appeared in the scanning range, which lead us to conclude that the incorporation of such small amounts of GO to the PCL matrix didn't affect the morphological structure of the overall hybrid matrix. Furthermore, when comparing the degradation times of PCL/GO hybrids containing the same quantity of GO, there was no pattern observed between those samples which had not been submitted to degradation and those that had. This backed up the initial results obtained which compared the changes on the morphological structure of neat PCL after having been submitted to degradation.

In conclusion, the addition of such small amounts of GO to the polymer matrix did not imply a change in the morphological structure or the crystal size of the original polymer. It is likely that if there had been larger amounts of GO added to the matrix there would have been new peaks observed corresponding to those of GO. It is also possible that due to the small amounts of GO present in the matrix the equipment wasn't able to effectively analyze the crystallite size present inside the matrix of the different studied hybrids.

Furthermore, submitting the samples to approximately 26 days (617,67 hours) of degradation did not significantly change the diffraction spectra, so it was also concluded that there were no visible significant results to be acquired from the studied XRD patterns. Therefore, all the hybrids, independent of their content of GO or degradation times, were arranged in such a way that they formed (1 1 0) and (2 0 0) crystallographic planes, and from the results obtained, the crystallite size was also not affected by both variables.

More extensive results could have been obtained if the scanning of the hybrids would have been carried out in a range which reached 45°, since there are characteristic peaks of the GO powder scanning profile (peak at  $2\theta = 42.2^\circ$ ) which are impossible to observe in the scanned range.

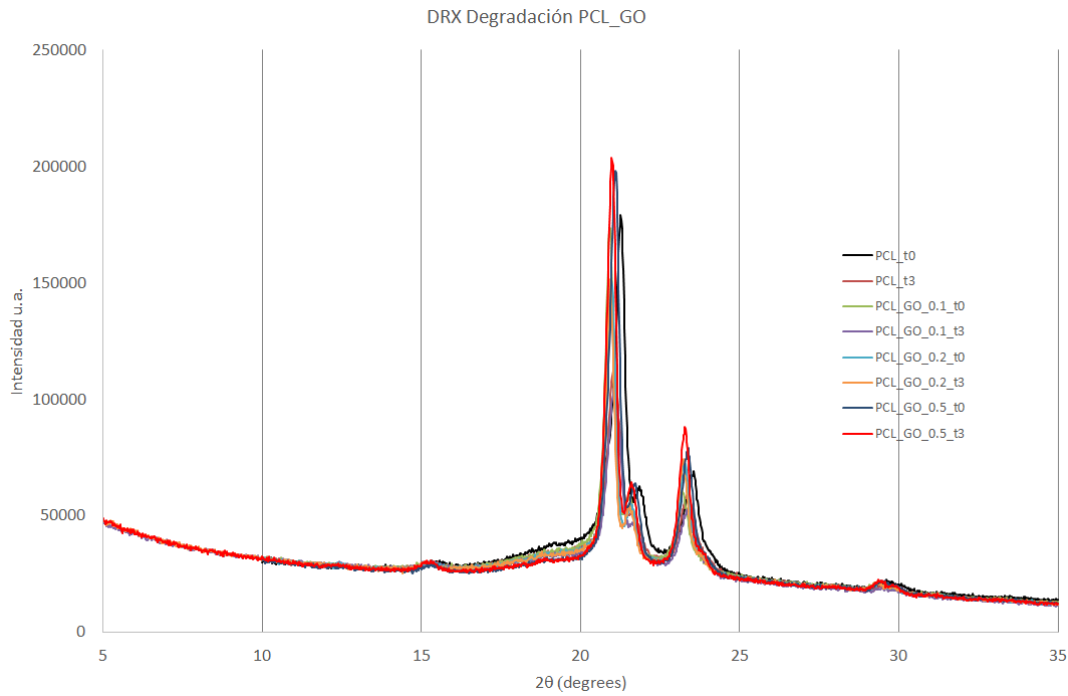


Figure 67. X-ray diffraction of different samples of PCL/GO hybrids containing different quantities of GO, as well as neat PCL, at different degradation times.

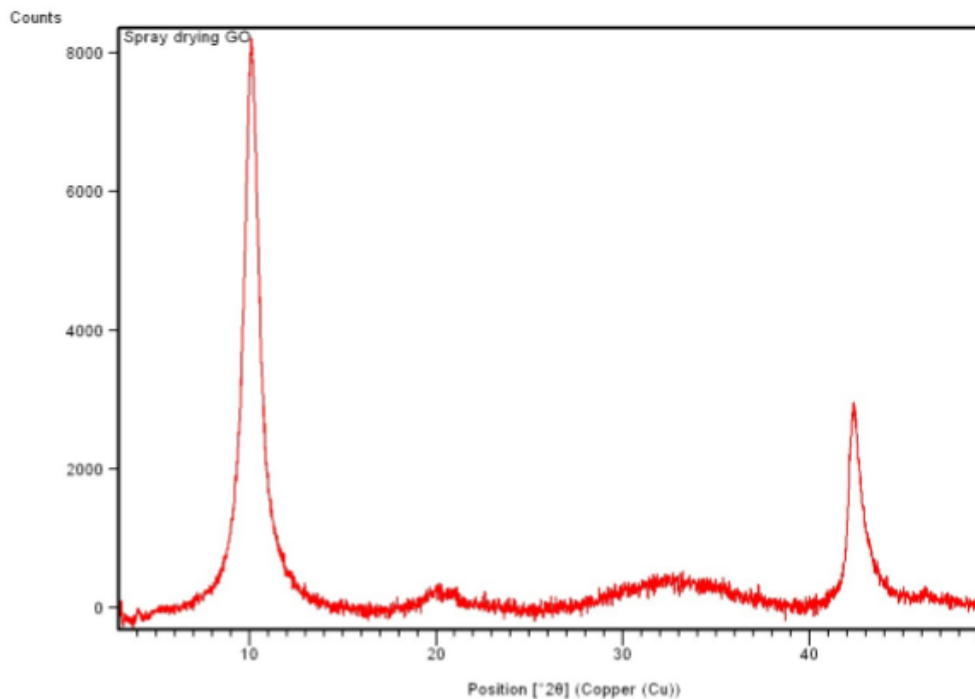


Figure 68. X-ray diffraction profile of pure GO powder. Characteristic GO powder peaks can be observed at  $2\theta=10.0^\circ$  and  $42.2^\circ$

## 6 CONCLUSIONS

### Degradation study:

- The degradation medium to which the samples were submitted substantially affected the kinetics of degradation; in fact, none of the materials degraded at pH1, whilst the opposite occurs in the reference article published by Sailema et al. (Sailema-Palate, Vidaurre, & others, 2016). This may be because the molecular weight used in this article,  $M_n$  70000 - 90000, is superior to the one used in the reference,  $M_n$  = 43000 - 50000.
- In a basic medium, the degradation accelerates when the content of GO increases; this can be attributed to the GO sheets intercalating in the polymer matrix, creating on one hand a matrix-GO interphase which is bigger in size, which enables the entrance of the degradation medium, and on the other hand, decreasing the size of the PCL crystals, and therefore facilitating the degradation.
- The series of synthesized hybrids demonstrates that the degradation can be adjusted in function of the GO content.

### Water uptake:

- In an alkaline medium, there is no significant differences in the quantity of water absorbed by the different materials, since there is a high variability between the samples.
- In an acid medium the samples do not present any water absorption, which is in consonance with the low degradation which they suffered.

### SEM:

- The results obtained from SEM are consistent with the degradation study and the water uptake. In basic medium, the degradation seems to be autocatalyzed by the by-products of degradation and it increases with an increasing content of GO.

### DSC:

- The change in crystallinity has been analyzed with a changing content of GO. As can be observed in section '5.2.3 - DSC', the quantity of GO has a clear influence in the crystallinity of the hybrids; with an increasing GO content there is an increase in crystallinity. This can be explained due to the fact that GO acts as a nucleation anchor point for the PCL crystals. Neat PCL has a crystallinity of 52.30% whilst PCL containing only 0.5% of GO increased it up to 67.17%. Furthermore, the double peak which appears in the fusion is very interesting, since it indicates two differentiated populations with two different average crystal sizes.
- There is not a great change observed in the crystallinity of the materials as the degradation time progresses in an acid medium, however, in the basic medium crystallinity tends to decrease with time, which contradicts the results obtained by different authors.

XRD:

- No clear conclusions can be reached from the evolution of the crystallinity through X-ray analysis, since the sensibility of the equipment did not detect such small quantities of GO.

In conclusion,

- A series of PCL/GO hybrid materials have been created to be used in potential applications as biomaterials.
- It has been demonstrated that the incorporation of GO substantially affects the degradation kinetics, endowing the system with a higher versatility in applications such as drug liberation vehicles.



## 7 REFERENCES

- Aharoni, S. (1998). Increased glass transition temperature in motionally constrained semicrystalline polymers. *Polym. Adv. Technol.* , 9, 169-201.
- Albertsson, A., & Karlsson, S. (1997). Controlled degradation by artificial and biological processes. *Macromolecular design of polymeric materials* , 739-780.
- Ali, S., Zhong, S., & other. (1993). Mechanisms of polymer degradation in implantable devices. I. Poly( $\epsilon$ -caprolactone). *Biomaterials* , 648-656.
- Barbucci, R. (2002). Integrated Biomaterials Science. *Springer US* .
- Bei, J., Li, J., & others. (1997). Polycaprolactone-poly(ethylene-glycol) block copolymer. IV: biodegradation behaviour in vitro and in vivo. *Polym. Adv. Technol.* , 8, 693-696.
- Bergsma, J. (1995). Late degradation tissue response to poly( $\epsilon$ -lactide) bone plates and screws. *Biomaterials* , 25-31.
- Bhattarai, N., Gunn, J., & Zhang, M. (2010). Advanced Drug Delivery Reviews. 83-99.
- Bhaw-Luximon, A., Jhurry, D., & other. (2001). *Polymer* , 42, 9651-9656.
- Bian, Q., Tian, H., & others. (2015). Effect of graphene oxide on the structure and properties of poly(vinyl alcohol) composite films. *Polymer Science Series A* , 836.
- Böstman, O., Hirvensalo, E., & others. (1990). Foreign-body reactions to fracture fixation implants of biodegradable synthetic polymers. *The Journal of Bone and Joint Surgery* , 72, 592.
- Brodie EA, e. a. (1860). Sur le poids atomique de graphite. *Annales de Chimie et de Physique* , 466-472.
- Bushnell, B. D., McWilliams, A. D., Whitener, G. B., & Messer, T. M. (2008). The Journal of Hand Surgery. 1081-1087.
- Cai, B., Chang, Y., & other. (2008). Thermoreversible gel-sol behavior of biodegradable PCL-PEG-PCL triblock copolymer in aqueous solutions. *Journal of Biomedical Materials Research - Part B Applied Biomaterials* , 165-175.
- Cai, B., Chang, Y., & other. (2008). Thermoreversible gel-sol behavior of biodegradable PCL-PEG-PCL triblock copolymer in aqueous solutions. *Journal of Biomedical Materials Research - Part B Applied Biomaterials* , 165-175.
- CG., P. (1990). Poly- $\epsilon$ -caprolactone and its copolymers. *biodegradable polymers as drug delivery systems* , 71-120.
- Chen, C., & Cai, G. (2010). Chitosan-poly( $\epsilon$ -caprolactone)-poly(ethylene glycol) graft copolymers: synthesis, self-assembly, and drug release behaviour. *J. Biomed. Mater. Res. A* , 116-124.

- Chen, C., & Cai, G. o. (2010). Chitosan-poly(epsilon-caprolactone)-poly(ethylene glycol) graft copolymers: synthesis, self-assembly, and drug release behaviour. *J. Biomed. Mater. Res. A* , 116-124.
- Chen, D., Bei, J., & other. (2000). Polycaprolactone microparticles and their biodegradation. *Polymer Degradation and Stability* , 67, 455-459.
- Chen, D., Bei, J., & others. (2000). Polycaprolactone microparticles and their biodegradation. *Polym. Degrad. Stab.* , 67, 455-459.
- Chen, H., Müller, M., & others. (2008). Mechanically strong, electrically conductive, and biocompatible graphene paper. *Advanced Materials* , 3557-3561.
- Chen, K., Shi, B., & others. (2015). Binary Synergy Strengthening and Toughening of Bio-Inspired Nacre-like Graphene Oxide/Sodium Alginate Composite Paper. *ACS Nano* , 8165-8175.
- Chiari, C., Koller, U., & other. (2006). A tissue engineering approach to meniscus regeneration in a sheep model. *Osteoarthritis and Cartilage* , 1056-1065.
- Chiari, C., Koller, U., & others. (2006). A tissue engineering approach to meniscus regeneration in a sheep model. *Osteoarthritis and Cartilage* , 1056-1065.
- Choi, J. S., Yang, H.-J., Kim, B. S., Kim, J. D., Kim, J. Y., Yoo, B., y otros. (2009). *Journal of Controlled Release* , 2-7.
- Corrales, T., Catalina, F., Peinado, C., & Allen, N. (2003). *Journal of Photochemistry and Photobiology A: Chemistry*. 103-114.
- Correa-Duarte, M., Wagner, N., & other. (2004). Fabrication and biocompatibility of carbon nanotube-based 3D networks as scaffolds for cell seeding and growth. *Nano Letters* , 2233-2236.
- Coulembier, O., Degée, P., & other. (2006). From controlled ring-opening polymerization to biodegradable aliphatic polyester: Especially poly(beta-malic acid) derivatives. *Progress in Polymer Science (Oxford)* , 723-747.
- Crescenzi, V., Manzini, G., & other. (1972). Thermodynamics of fusion of poly-beta-propiolactone and poly-epsilon-caprolactone. comparative analysis of the melting of aliphatic polylactone and polyester chains. *European Polymer Journal* , 449-463.
- Crescenzi, V., Manzini, G., Calzolari, G., & Borri, C. (1972). Thermodynamics of fusion of poly-beta-propiolactone and poly-epsilon-caprolactone. comparative analysis of the melting of aliphatic polylactone and polyester chains. *European Polymer Journal* , 449-463.
- D., C., S.H., H., & Y., I. (1995). Degradation of high molecular weight poly(L-lactide) in alkaline medium. *Biomaterials* , 833-843.

- Dash, T. K., & Konkimalla, V. B. (2012). Polycaprolactone based formulations for drug delivery and tissue engineering: A review. *Journal of Controlled Release* , 15-33.
- Drury, J. L., & Mooney, D. J. (2003). *Biomaterials*. 4337-51.
- Drury, J., & Mooney, D. (2003). *Biomaterials*. 4337-51.
- El-Sherbiny, I. M., & Yacoub, M. H. (2013). *Global Cardiology Science & Practice* 2013. 316-42.
- Estelle, J., Vidaurre, A., & other. (2008). Physical characterization of polycaprolactone scaffolds. *Journal Mater. Sci. Mater. Med.* 19 , 189-195.
- Fertier, L., Koleilat, H., Stemmelen, M., Giani, O., Joly-Duhamel, C., Lapinte, V., y otros. (2013). *Progress in Polymer Science*. 932-962.
- Friess, W. (1998). *European Journal of Pharmaceutics and Biopharmaceutics* , 113-136.
- Gaharwar, A., Sant, S., & other. (2013). *Nanomaterials in Tissue Engineering: Fabrication and Applications*.
- Ginde, R., & Gupta, R. (1987). In vitro chemical degradation of poly(glycolic acid) pellets and fibers. *Journal of Applied Polymer Science* , 2411-2429.
- Gopferich, A., Karydas, D., & others. (1995). Predicting drug release from cylindrical polyanhydride matrix discs. *European Journal of Pharmaceutics and Biopharmaceutics* , 81-87.
- Gorna, K., & Gogolewski, S. (2002). in vitro degradation of novel medical biodegradable aliphatic polyurethanes based on epsilon-caprolactone and pluronics with various hydrophilicities. *Polym. Degrad. Stab.* , 113-122.
- Grinstff, M. W., Carnahan, M. A., Fleming, P. S., Hatchell, D. L., Luman, N. R., Morgan, M. T., y otros. (2001). *Abstracts of Papers of the American Chemical Society*. 222.
- Grizzli, I., Garreau, H., & others. (1995). Hydrolytic degradation of devices based on poly(DL-lactic acid) size-dependance. *Biomaterials* , 305-311.
- Guinier, A. (1963). X-ray diffraction. 121.
- Gunatillake, P., Mayadunne, R., & other. (2006). Recent developments in biodegradable synthetic polymers. *Biotechnonology Annual Review* , 12, 301-347.
- Guo, B., Glavas, L., & others. (2013). *Progress in Polymer Science*. 1263-1286.
- Harrison, K., & Jenkins, M. J. (2004). The effect of crystallinity and water absorption on the dynamic mechanical relaxation behaviour of polycaprolactone. *Polym. Int.* , 53, 1298-1304.
- Hayashi, T. (1994). Biodegradable polymers for biomedical uses. *Progress in Polymer Science* , 663-702.

- He, Y., Kilsby, S., & other. (2013). Processing biodegradable polycaprolactone through 3D printing. *24th International SFF Symposium - An Additive Manufacturing Conference, SFF 2013* , 200-214.
- Hill, J., Carothers, W., & other. (1934). Studies of Polymerization and Ring Formation. XXIII. 1  $\epsilon$ -Caprolactone and its Polymers. *Journal of the American Chemical Society* , 455-457.
- Hoffman, A. S. (2001). Advanced Drug Delivery Reviews. 1869-1880.
- Huang, H., Oizumi, S., & other. (2007). Avidin-biotin binding-based cell seeding and perfusion culture of liver-derived cells in a porous scaffold with a three-dimensional interconnected flow-channel network. *Biomaterials* , 3815-23.
- Huang, S. (1985). Biodegradable polymers. *Encyclopedia of polymer science and engineering* , 220-243.
- Hull, D., & Clyne, T. (1996). An introduction to Composite materials. *Cambridge University Press* .
- Hull, D., & Clyne, T. W. (1996). An introduction to Composite materials. *Cambridge University Press* .
- Hummers W, O. R. (1958). Preparation of graphitic oxide. *Journal of the American Chemical Society* , 1339.
- Hutmacher, D. (2001). Scaffold design and fabrication technologies for engineering tissues - state of the art and future perspectives. *Biomaterial Science Polymers* , 107-124.
- Jedlinski, Z., Walach, W., & other. (1991). Die Makromolekulare Chemie. 2051-2057.
- Jing, X., & Ming, H. (2014). Preparation of thermoplastic polyurethane/graphene oxide composite scaffolds by thermally induced phase separation. *Polymer Composites* , 1408-1417.
- Jing, X., Mi, H., & others. (2014). Preparation of thermoplastic polyurethane/graphene oxide composite scaffolds by thermally induced phase separation. *Polymer Composites* , 1408-1417.
- Kai, W., Hirota, Y., & others. (2008). Thermal and mechanical properties of poly( $\epsilon$ -caprolactone)/graphite oxide composite. *Journal of Applied Polymer Science* , 1395-1400.
- Khan, F., & Ahmad, S. R. (2013). Macromolecular Bioscience. 395-421.
- Khor, E., & Lim, L. Y. (2003). Biomaterials. 2339-2349.
- Klug, H. (1967). X-ray diffraction procedures. *New York: Wiley* .
- Komura, M., H., K., Kanamori, Y. T., Suzuki, K., Sugiyama, M., Nakahara, S., y otros. (2008). *Journal of Pediatric Surgery* , 43, 2141-2146.
- Krane, S. (2008). Amino Acids. 703-710.

- Kricheldorf, H., & Langanke, D. (2002). *Polymer* , 43, 1973-1977.
- Kulkarni, R., Moore, E., & other. (1971). *Journal of Biomedical Materials Research* , 5, 169-181.
- Labet, M., & Thielemans, W. (2009). Synthesis of polycaprolactone: a review. *Chemical Society Reviews* .
- Lam, C., Hutmacher, D., & al., J. S. (2009). Evaluation of polycaprolactone scaffold degradation for 6 months in vitro and in vivo. *Journal of Biomedical Materials Research Part A* , 906-919.
- Lam, C., Hutmacher, D., & other. (2008). Dynamics of in vitro polymer degradation of polycaprolactone-based scaffolds: accelerated versus simulated physiological conditions. *Biomedical materials* , 034108.
- Lee, K. Y., & Mooney, D. J. (2001). Chemical Reviews. 1869-1880.
- Lee, K., Kim, H., & other. (2003). Characterization of nano-structured poly( $\epsilon$ -caprolactone) nonwoven mats via electrospinning. *Polymer* , 1287-1294.
- Lenz, W., & Marchessault, H. (2004). Biomacromolecules. 1-8.
- Leone, G., & Barbucci, R. (2009). Polysaccharide Based Hydrogels for Biomedical Applications - Hydrogels. *Springer Milan* , 25-41.
- Li, Z., Leung, M., & other. (2010). Biomaterials. 404,412.
- Lindblad Margaretha, S., Sjöberg, J., & other. (2007). Hydrogels from Polysaccharides for Biomedical Applications. *Materials, Chemicals, and Energy from Forest Biomass, American Chemical Society.* , 954, 404-412.
- Liu, X., Wang, X.-M., Chen, Z., Cui, F.-Z., Liu, H.-Y., Mao, K., y otros. (2010). Part B: Applied Biomaterials. *Journal of Biomedical Materials Research* , 72-79.
- Liu, Z., Robinson, J., & others. (2008). PEGylated nanographene oxide for delivery of water-insoluble cancer drugs. *Journal of the American Chemical Society* , 10876-10877.
- Lowery, J., Datta, N., & Rutledge, G. (2009). Effect of fiber diameter, pore size and seeding method on growth of human dermal fibroblasts in electrospun poly( $\epsilon$ -caprolactone) fibrous mats. *Biomaterials* , 31, 491-504.
- Luciani, A., Coccoli, V., & other. (2008). PCL microspheres based functional scaffolds by bottom-up approach with predefined microstructural properties and release profiles. *Biomaterials* , 4800-4807.
- Luo, H., Meng, X., & other. (2010). Enzymatic degradation of supramolecular materials based on partial inclusion complex formation between alpha-cyclodextrin and poly( $\epsilon$ -caprolactone). *The journal of physical chemistry B* , 4739-45.

- Lv, Q., Wu, D., & others. (2015). Crystallization of Poly( $\epsilon$ -caprolactone) composites with graphite nanoplatelets: Relations between nucleation and platelet thickness. *Thermochimica Acta* , 25-33.
- M., P., M., M., J., B., T., T., T, W., & al., S. J. (2009). Erratum to "in vivo implantation implantation of 2,2'-bis(oxazoline)-linked poly-epsilon-caprolactone: proof for enzyme sensitive surface erosion and biocompatibility". *European Journal of Pharmaceutical Science* , 310.
- M.H., H., S.M., L., D.W., H., J., C., & M., V. (2006). Degradation characteristics and poly(epsilon-caprolactone)-based copolymers and blends. *Applied polymer science* , 1681-1687.
- Mansur, H. S., Curti, E., & other. (2013). *Journal of Materials Chemistry B*. 1696-1711.
- Mark, H. F., & Kroschwitz, J. I. (1985). *Encyclopedia of polymer science and engineering*. Wiley .
- Marrazzo, C., Maio, E., & other. (2008). Conventional and nanometric nucleating agents in poly( $\epsilon$ -caprolactone) foaming: Crystals vs. bubbles nucleation. *Polymer Engineering and Science* , 336-344.
- Matsuni, T., Nakamura, T., Kuremoto, K.-i., Notazawa, S., Nakahara, T., Hashimoto, Y., y otros. (2006). *Dental Materials Journal*. 138-144.
- Matthew, J., Vincent, C., & others. (2009). Honeycomb carbon: a review of graphene. *Chem. Rev.* , 132-145.
- Meinig, R. P., Rahn, B., & others. (1996). *Journal of Orthopaedic Trauma*. 178-90.
- Mondrinos, M., Dembzyński, R., & other. (2006). Porogen-based solid freeform fabrication of polycaprolactone-calcium phosphate scaffolds for tissue engineering. *Biomaterials* , 4399-4408.
- Mondrinos, M., Dembzyński, R., & other. (2006). Porogen-based solid freeform fabrication of polycaprolactone-calcium phosphate scaffolds for tissue engineering. *Biomaterials* , 4399-4408.
- Nair, L. S., & Laurencin, C. T. (2006). *Tissue Engineering I: Scaffold systems for Tissue Engineering*. 47-90.
- Nair, L., & Laurencin, C. (2007). Biodegradable polymers as biomaterials. *Prog. Polym. Sci.* , 762-798.
- Nordtveit, R. J., Varum, K. M., & Smidsrod, O. (1996). *Carbohydrate Polymers*. 163-167.
- Okada, M. (2002). Chemical syntheses of biodegradable polymers. *Progress in Polymer Science (Oxford)* , 87-133.
- Okada, M. (2002). *Progress in Polymer Science*. 87-133.

- Paredes, J., & Villar-Rodil, S. e. (2008). Graphene oxide dispersions in organic solvents. *Langmuir* , 10560-10564.
- Pawar, S., Kumar, S., & others. (2015). Enzymatically degradable EMI shielding materials derived from PCL based nanocomposites. *RSC Advances Journal* , 17716.
- Peng, H., Han, Y., & other. (2010). Morphology and thermal degradation behaviour of highly exfoliated CoAl-layered double hydroxide/polycaprolactone nanocomposites prepared by simple solution intercalation. . *Thermochimica Acta* , 1-7.
- Pitt, C. (1990). Poly-ε-caprolactone and its copolymers. *biodegradable polymers as drug delivery systems* , 71-120.
- Pitt, C., Chasalow, F., & others. (1981). Aliphatic Polyesters. 1. Degradation of poly(epsilon-Caprolactone) in vivo. *Journal of Applied Polymer Science* , 3779-3787.
- Pitt, G., Gratzl, M., & others. (1981). Aliphatic polyesters 2. The degradation of poly-D,L lactide poly-epsilon capro lactone and their co polymers in-vivo. *Biomaterials* , 215-220.
- R., C., & R., R. (2002). Biodegradable polymers. *Progr Polym Sci* , 87-133.
- Rao, C., Sood, A., & others. (2009). Graphene: The New Two-Dimensional Nanomaterial. *A journal of the Gesellschaft Deutscher Chemiker* , 7752-7777.
- Ratner, B. (2013). A history of biomaterials. *Biomaterials in Science: An Introduction to Materials: Third Edition* , xli-liiii.
- Rinaudo. (2006). 1. M. *Progress in Polymer Science* , 603-632.
- Rinaudo, M. (2012). *Progress in Polymer Science*. 106-126.
- Riva, R. R., des Rieux, A., Duhem, N., Jerome, C., & Preat, V. (2011). *Advances in Polymer Science*. 19-44.
- S. Stankovich, R. P. (2006). Synthesis and exfoliation of isocyanate-treated graphene oxide nanoplatelets. *Carbon* , 282-6.
- S., K., & S., R. (2006). Rheological behavior of starch-polycaprolactone (PCL) nanocomposite melts synthesized by reactive extrusion. *Polymer Engineering and Science* , 650-658.
- S., L., & M., V. (1995). Biodegradation of aliphatic polyesters. *Degradable polymers: Principles and Applications* , 43-87.
- Sailema-Palate, P., Vidaurre, A., & others. (2016). A comparative study on Poly(epsilon-caprolactone) film degradation at extreme pH values. *Polymer degradation and stability* , 118-125.
- Sayyar, S. (2014). The development of graphene/biocomposites for biomedical applications. 20-36.

- Schuerch, C. (1972). The chemical synthesis and properties of polysaccharides of biomedical interest. *Fortschritte der Hochpolymeren-Forschung, Springer Berlin Heidelberg* , Vol. 10, 173-194.
- Sheikh, F., & Barakat, N. (2009). Novel self-assembled amphiphilic poly(epsilon-caprolactone)-grafter-poly(vinyl alcohol) nanoparticles: hydrophobic and hydrophilic drugs carrier nanoparticles. *Journal of Material Science Mater. Med.* , 821-831.
- Sheikh, F., Barakat, N., & other. (2009). Novel self-assembled amphiphilic poly(epsilon-caprolactone)-grafter-poly(vinyl alcohol) nanoparticles: hydrophobic and hydrophilic drugs carrier nanoparticles. *Journal of Material Science Mater. Med.* , 821-831.
- Shi, C., Zhu, Y., Ran, X., Wang, M., Su, Y., & Cheng, T. (2006). *Journal of Surgical Research*. 185-192.
- Shi, X., & Chang, H. (2012). Regulating cellular behavior on few-layer reduced graphene oxide films with well-controlled reduction states. *Advanced Functional Materials* , 751-759.
- Sivalingam, G., & Madras, G. (2003). (??-caprolactone), Thermal degradation of poly. *Polymer degradation and stability* , 11-16.
- Sivalingam, G., Karthik, R., & Madras, G. (2004). Blends of poly(poly(3-caprolactone) and poly(vinyl acetate): Mechanical properties and thermal degradation. *Polymer degradation stability* , 345.
- Song, J., Gao, H., & others. (2015). The preparation and characterization of polycaprolactone/graphene oxide biocomposite nanofiber scaffolds and their application for directing cell behaviours. *Carbon* , 1039-1050.
- Stankovic, S., Dikin, D. A., & others. (2006). Graphene-based composite materials. *nature* , 442, 282-286.
- Stankovich, S. (s.f.).
- Stankovich, S., Dikin, D. A., Piner, R. D., Kohlhaas, K. A., Kleinhammes, A., Jia, Y., y otros. (2007). Synthesis of graphene-based nanosheets via chemical reduction of exfoliated graphite oxide. *ELSEVIER* , 1558-1565.
- Staudenmaier, L. (1898). Verfahren zur darstellung der graphitsaure. *Berichte der Deutschen Chemischen Gesellschaft* , 1481-99.
- Storey, R., & Taylor, A. (1996). Effect of stannous octoate concentration on the ethylene glycol-initiated polymerization of epsilon-caprolactone. *Abstr Pap Am Chem Soc* , 114-120.
- Suggs, J., & Mikos, A. (1996). Synthetic biodegradable polymers for medical applications. *Physical properties of polymers handbook. New York: American Institute of Physics* , 615-624.



- Sun, H., Mei, L., & others. (2006). The in vivo degradation, absorption and excretion of PCL-based implants. *Biomaterials* , 27, 1735-1740.
- Szot, C., Buchanan, C., Gatenholm, P., Rylander, M., & Freeman, J. (2011). Investigation of cancer cell behaviour on nanofibrous scaffolds. *Mater. Sci. Eng.* , 37-42.
- T., H. (1994). Biodegradable polymers for biomedical uses. *Progress in Polymer Science* , 663-702.
- Taghizadeh, M., Abdollahi, R., & others. (2015). Crystallization behavior, thermal property and enzymatic degradation of PVP/amylose in the presence of graphene oxide nanosheets. *Polymer Degradation and Stability* , 53-61.
- Tapas, K., Sambhu, B., & others. (2010). Recent advances in graphene based polymer composites. *Progress in Polymer Science* , 1350-1375.
- Tian, H. Y., Tang, Z. H., & other. (2012). *Progress in Polymer Science*. 237-280.
- Tian, H., Tang, Z., & other. (2012). Biodegradable synthetic polymers: Preparation, functionalization and biomedical application. *Progress in Polymer Science (Oxford)* , 237-280.
- Tjong, S. (2012). *Polymer Composites with Carbonaceous Nanofillers: Properties and Applications*.
- Ulery, B. D., Nair, L. S., & Laurencin, C. T. (2011). *Journal of Polymer Science Part B: Polymer Physics* , 49, 832-864.
- Valence, S. D., Tille, J., & other. (2012). *Biomaterials*. 38-47.
- Van Vlierberghe, S., Dubruel, P., & Schacht, E. (2011). *Biomacromolecules*. 1387-1408.
- Venugopal, J., Low, S., Choon, A., & Ramakrishna, S. (2008). Interaction of cells and nonfiber scaffolds in tissue engineering. *Journal of Biomedical Mater. B Appl. Biomater.* , 84, 34-48.
- Vert, M. (2009). Degradable and bioresorbable polymers in surgery and in pharmacology: Beliefs and facts. *Journal of Materials Science: Materials in Medicine* , 20, 437-446.
- Vert, M., Li, S., & other. (1992). Bioresorbability and biocompatibility of aliphatic polyesters. *Journal of Materials Science: Materials in Medicine* , 432-446.
- Vidaurre, A., Crescenzo, V., & others. (1972). Thermodynamics of fusion of poly-beta-propiolactone and poly-epsilon-caprolactone - comparative analysis of melting of aliphatic polylactone and polyester chains. *European Polymer Journal* , 449-63.
- W.P., Y., F.S., D., W.H., J., J.Y., Y., & Y., X. (1997). In vitro degradation of poly(caprolactone), poly(lactide) and their block copolymers: influence of composition, temperature and morphology. *React. Funct. Polym.* , 161-168.

- Wan, C., & Chen, B. (2011). Poly( $\epsilon$ -caprolactone)/graphene oxide biocomposites: mechanical properties and bioactivity. *Biomedical Materials* .
- Wan, C., & Chen, B. (2012). Reinforcement and interphase of polymer/graphene oxide nanocomposites. *Journal of Materials Chemistry* .
- Wan, Y., Lu, X., & other. (2009). Thermophysical properties of polycaprolactone/chitosan blend membranes. *Thermochim. Acta* , 33-38.
- Wang, F., Li, Z., Khan, M., Tamama, K., Kuppusamy, P., Wagner, W. R., y otros. (2010). *Acta Biomaterialia*. 1978-1991.
- Williams, D. F. (1999). The Williams Dictionary of Biomaterials. *Liverpool University Press* .
- Woodroof, A., & Hutmacher, W. (2010). The return of a forgotten polymer-polycaprolactone in the 21st century. *Prog. Polym. Sci.* 35 , 1217-1256.
- Woodward, S., Brewer, P., & other. (1985). The intracellular degradation of poly( $\epsilon$ -caprolactone). *Journal of Biomedical Materials Research* , 437-444.
- Xue, R., Xin, X., & others. (2015). A systematic study of the effect of molecular weights of polyvinyl alcohol on polyvinyl alcohol-graphene oxide composite hydrogels. *Physical Chemistry Chemical Physics* , 5431-5440.
- Z., M., A., H., O., M., A., L., R., L., & J., S. (2008). Micelles of poly(-ethylene oxide)-b-poly(epsilon-caprolactone) as vehicles for the solubilization, stabilization, and controlled delivery of curcumin. *Journal of Biomedical Materials Res. A* , 300-310.
- Zein, I., Hutmacher, D., & other. (2002). Fused deposition modeling of novel scaffold architectures for tissue engineering applications. *Biomaterials* , 23, 1169-1304.
- Zhi, H., Jing, T., Bo, Y., Yong, X., & Qingling, F. (2009). *Biomedical Materials*.

## II. ATTACHMENTS

### 1 About the obtaining of the hybrid materials

#### 1.1 Selection of a suitable solvent

The first step of this project was to find a suitable solvent which was capable of dissolving PCL and of dispersing graphene oxide (GO) powder. It was of critical importance that the solvent could do both, since the next step would be to create a solution containing both PCL and GO. Due to their properties, polar non-halide solvents were used for this purpose. The three initial solvents investigated were Ethylene glycol, Dioxane and Acetonitrile.

Once the first step of the project had been planned, all the materials, machines and apparatus which were necessary for the project needed to be located in the lab. With everything located, having planned our method, and assuring that all apparatus and instruments used were perfectly clean to assure that nothing unwanted would intervene in our process (cleaned with ethanol and acetone, letting the acetone evaporate since cleaning with paper could contaminate with cellulose), we started the project as follows:

Firstly, to research the dispersion of GO in the solvent 3 vials containing GO were prepared. Then each of the solvents mentioned were added to each of them (each vial containing a different solvent), so we had the following mixtures - GO/Ethylene glycol, GO/Dioxane and GO/Acetonitrile. Secondly, to research the solubility of PCL in the solvents, 3 vials containing PCL were prepared, and following the same method as with GO, a different solvent was placed in each of them, so the following solutions were prepared - PCL/Ethylene glycol, PCL/Dioxane and PCL/Acetonitrile. All vials were tagged so that no future confusion would occur.

The vials which contained PCL were placed in an oven ( $T=37^{\circ}\text{C}$ ) for 1 hour and 30 minutes to analyze if the PCL dissolved in its respective solvents. The results are as follows:

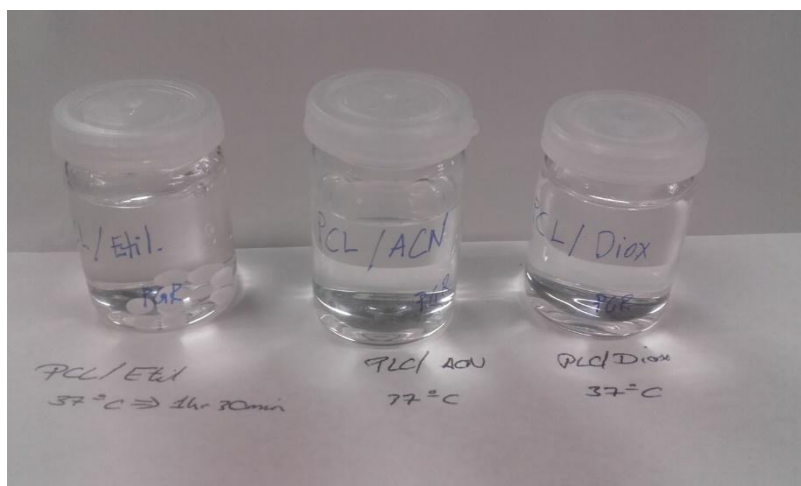


Figure \_: PCL/Ethylene glycol, PCL/Dioxane and PCL/Acetonitrile, in their respective vials, after 1hr. 30mins. in a  $37^{\circ}\text{C}$  oven.

As can be observed in Figure \_\_, PCL in Ethylene glycol did not dissolve. On the other hand, PCL did dissolve in Acetonitrile and Dioxane after being placed in the oven for 1 hour and 30 minutes.

The vials which contained GO were placed in an ultrasonic bath for 20 minutes to help the dispersion of the graphene oxide in each solvent. The results are as follows:

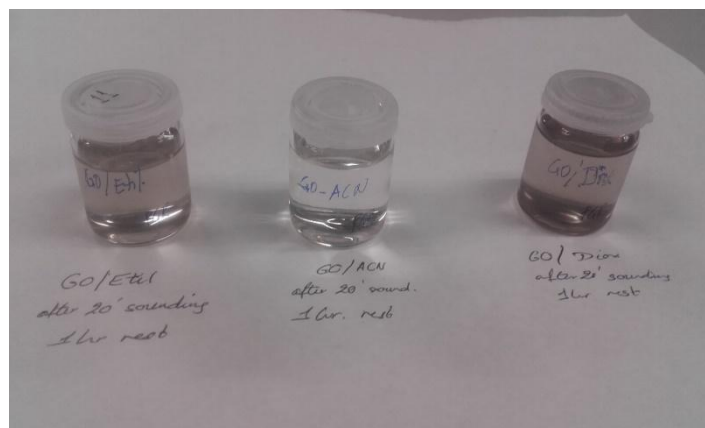


Figure \_\_: GO/Ethylene glycol, GO/Acetonitrile and GO/Dioxane, in their respective vials, after 20 mins. sonication.

After the sounding, the three vials were left to rest for one hour to see if the GO would sediment. As can be observed in figure\_\_, GO did not disperse at all in ACN - the GO sedimented to the bottom of the vial and the solution remained transparent. On the other hand, GO proved to disperse both in Ethylene glycol and Dioxane. In the case of Dioxane, a greyish solution could be observed, although a few grains of GO could be seen on the bottom of the vial, which proved that not all the GO has dispersed. For Ethylene glycol, GO proved to have dispersed in the solution - no sediments could be observed at the bottom of the vial after one hour of rest and the solution had adopted a greyish colour.

Guided by these results we concluded that the most suitable solvent for our project was Dioxane, since it managed to disperse GO and dissolve PCL. Ethylene glycol seemed to disperse GO very well, but didn't manage to dissolve PCL, and in the case of ACN the opposite happened - it managed to successfully dissolve PCL, but didn't seem to have the capability to disperse GO.

Later on in the investigation another two solvents were tested; N,N-dimethylformamide (DMF) and dimethylsiloxane (DMSO), but were discarded. The first seemed to dissolve PCL but the polymer seemed to become saturated in the solution, and the second, surprisingly due to its high polarity and corrosive properties, did not seem to dissolve the polymer at all after 3 days placed in an oven at 37°C.

## 1.2 Trial and error experiments previous to the final synthesis technique

The first step in order to create the hybrids was to investigate the best synthesis method for the desired PCL/GO samples. The objective was to create the following four samples (wt.% of GO in proportion to PCL):

1. Pure PCL (0% GO)
2. PCL + 0.1% GO
3. PCL + 0.2% GO
4. PCL + 0.5% GO

For the creation of the samples two separate methods were followed. Firstly, four solutions which we labelled as 'A' were created. These solutions contained PCL and were to be dissolved in Dioxane in an oven at 37°C inside four beakers.

Secondly, three solutions which we labelled as 'B' were created. These solutions contained different amounts of GO mixed with Dioxane and were to be inserted in an ultrasound bath for 20 minutes.

Once the four solutions which were tagged as 'A' had been created they were placed in an oven ( $T=37^{\circ}\text{C}$ ) for 24h. to allow the PCL to dissolve. Meanwhile, the solutions tagged as 'B' were to be sounded for 20 min. to disperse the GO in Dioxane, as shown in figure 19. Next, the different solutions were mixed by pouring 'B' into 'A' (the solutions which contained dissolved PCL were of a viscous nature, so as to lose the minimum amount of material we concluded that it was logical to pour 'B' - which maintained its liquid nature - into 'A'). The resulting mixtures were placed in an ultrasound bath and were left sounding in an ultrasound bath for 3 hours.



Figure 19. The mixture containing GO and Dioxane were placed in an ultrasound bath under an extraction hood.

The results of the sounding can be observed in Figure 20 below. The mixture labelled as PGR - 0 is pure PCL dissolved in Dioxane. In the other two remaining samples it is possible to appreciate how the GO in the upper phase started mixing with the lower PCL-rich phase.



Figure 20. Result of 20 min. of ultrasounding in PCL/GO/Dioxane mixture.

This initial part of the experiment proved to be useful to identify errors in the method of synthesis of the PCL/GO samples and to provide ideas of how to design a better method. Due to the different densities of both solutions (two phases were observed) they were mixed thoroughly with a dipstick to help mix the phases in order to get a homogenous solution. The final samples were left under an extraction hood for five days to give the solvent a chance to evaporate. To make sure that the sample did not get contaminated, they were covered with 'parafilm' and punctured with the help of a needle to create small holes so that the solvent could escape. Finally, after 5 days of rest the solvent still hadn't evaporated so the parafilm was taken off in order to let the solvent evaporate, which took more than two weeks. The resulting samples can be seen in figures 21 - 23 below.

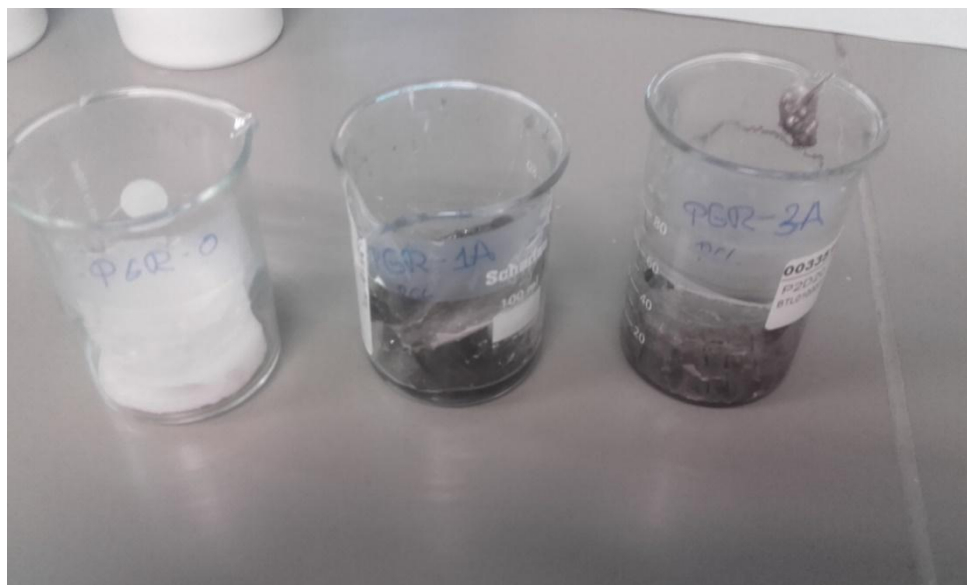


Figure 21. From left to right, the samples of pure PCL, PCL + 0.1%, and PCL + 0.5% GO. The sample containing 0.2% GO was lost.

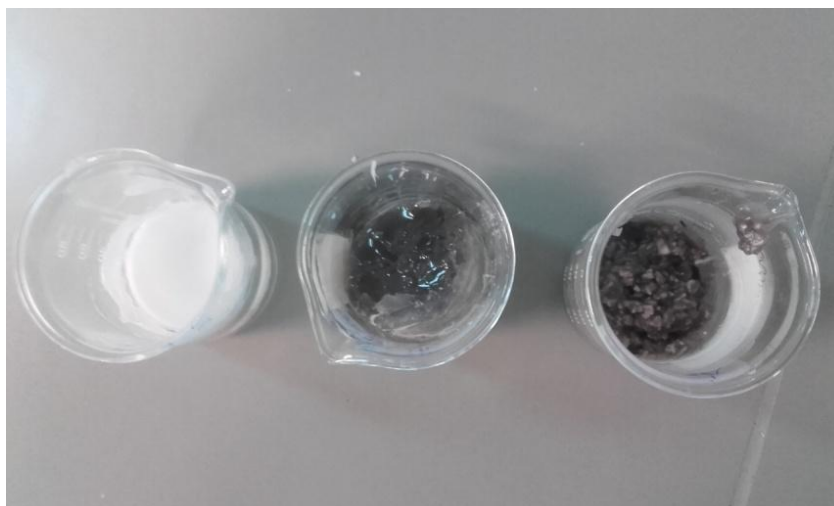


Figure 22. From left to right, the samples of pure PCL, PCL + 0.1%, and PCL + 0.5% GO. It can be appreciated that the solvent has not evaporated completely and that a homogeneous solution was not created for the PCL + 0.5% GO sample.

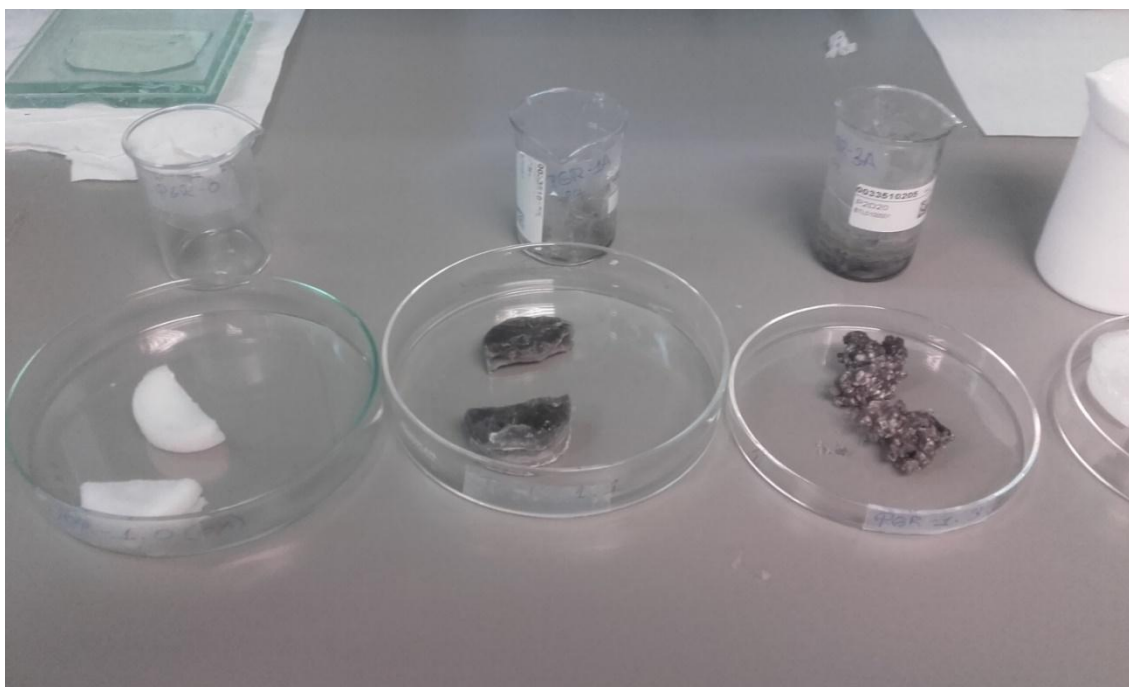


Figure 23. From left to right, the resulting samples of pure PCL, PCL + 0.1%, and PCL + 0.5% GO once all the solvent had evaporated.

It can be observed that the sample containing 0.5% GO didn't manage to produce a homogeneous distribution. Rather, it seemed to form zones of PCL separated by sheets of GO.

Following these results an improved method was devised by further designing the experiment to fix previous errors and using less materials to reduce costs, as GO is expensive. To do so, the quantity of materials used was calculated in relation with the size of four geometrically identical Teflon crystallizers. Their diameters were measured to calculate an average diameter and the mass of PCL needed was obtained from the volume

occupied by the sample in the crystallizer cup. Finally, a theoretical mass of 12.174g of PCL was needed. Four times the amount of solvent was used (48.69g) to assure that all the PCL dissolved without saturating, and the respective percentages in weight (wt.%) of GO in respect to PCL were prepared in the same way as previously.

The same methods were used to disperse the GO (22 minutes) and to dissolve the PCL as previously. When both procedures had finished, the respective containers were mixed inside the Teflon crystallizers and left sounding for four hours, having previously stirred the mixture with a dipstick. Since the solution of PCL inside the Dioxane is a very viscous mixture there were problems trespassing all of the PCL from the tumbler cups into the crystallizers, so for posterior methods the container used for the dissolving of PCL pellets would be the crystallizers. Once sounded, punctured parafilm was placed over the container and was left for 5 days. In that time the Dioxane did not get the chance to evaporate and a separation of the GO and PCL phases could be observed. In order to make the samples homogeneous they were thoroughly mixed once more, and the parafilm was taken off to help the solvent evaporate, and the samples were sounded for another 24:30 hours. As expected, the Dioxane evaporated much faster due to the vibration energy of the sounding, but air bubbles had been retained inside the sample. We thought that this could be due to the vibration of the sounding together with the fact that the solution became more viscous as the solvent evaporated, so the bubbles became trapped in the sample and couldn't escape the interphase. The resulting samples were left to evaporate without parafilm under the extraction hood to eliminate the rest of the Dioxane. The samples of pure PCL/GO can be seen in Figure \_.

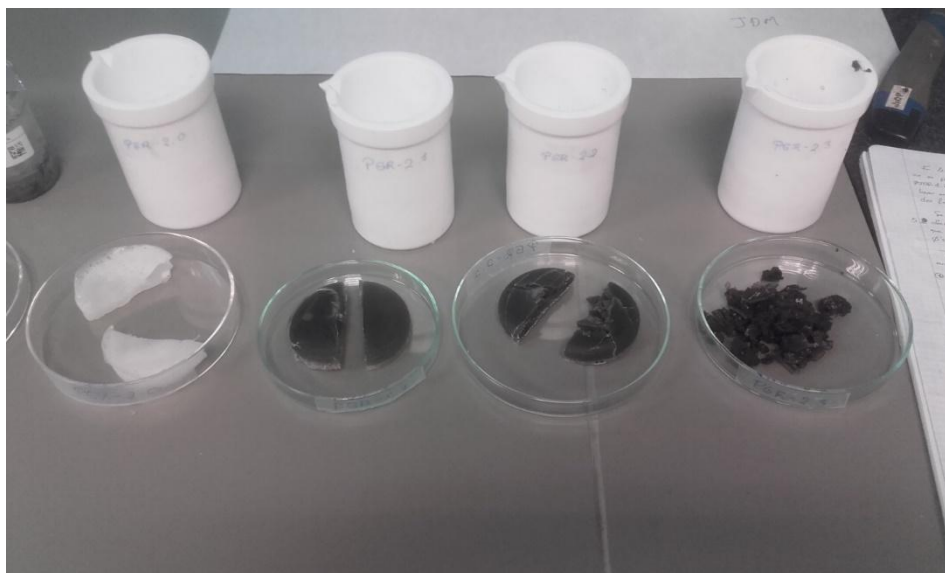


Figure \_. From left to right, the samples of pure PCL, PCL + 0.1% GO, PCL + 0.2% GO, PCL + 0.5% GO. It can be clearly appreciated that there are large hollow areas created by the formation of bubbles. We were going to try to eliminate the hollow areas by compression, but a better synthesis method which is described later was thought of. As before, the sample containing 0.5% GO was brittle and fell apart easily, and seemed to form areas of PCL surrounded by GO sheets which didn't hold together with each other.



## 2 Scanning Electron Microscopy (SEM) images

### 2.1.1.1 SEM photographs fixing sample composition and degradation medium

pH 1 (HCl)

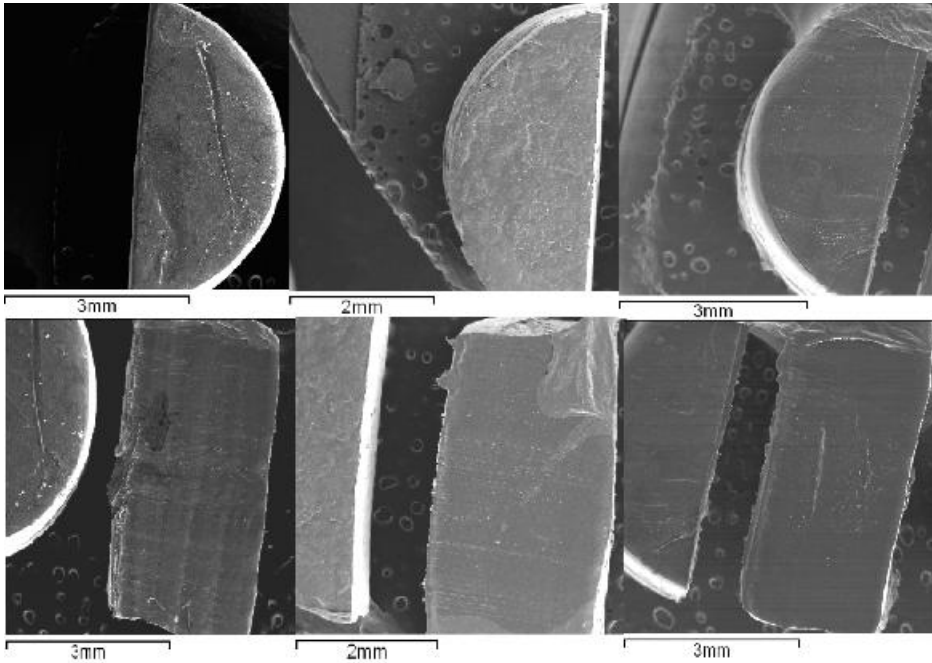


Figure \_. Superficial (top) and transversal section (bottom) SEM photos of neat PCL samples submitted to, from left to right, 0h(t0), 617.67h(t3) and 1297.67(t5) degradation hours respectively in a pH1 medium.

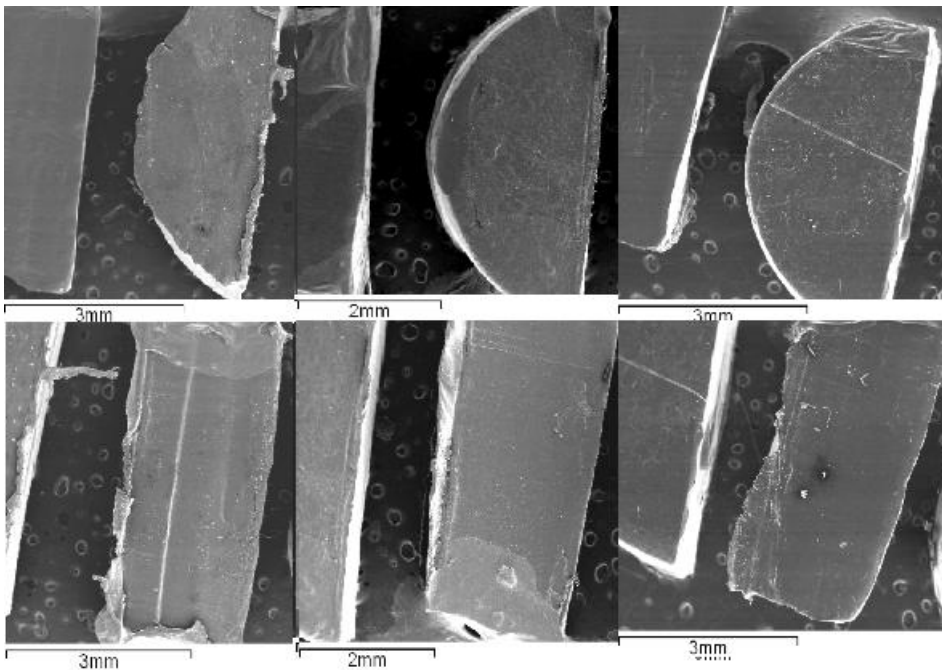


Figure \_\_. Superficial (top) and transversal section (bottom) SEM photos of PCL/GO-0.1 samples submitted to, from left to right, 0h(t0), 617.67h(t3) and 1297.67(t5) degradation hours respectively in a pH1 medium.

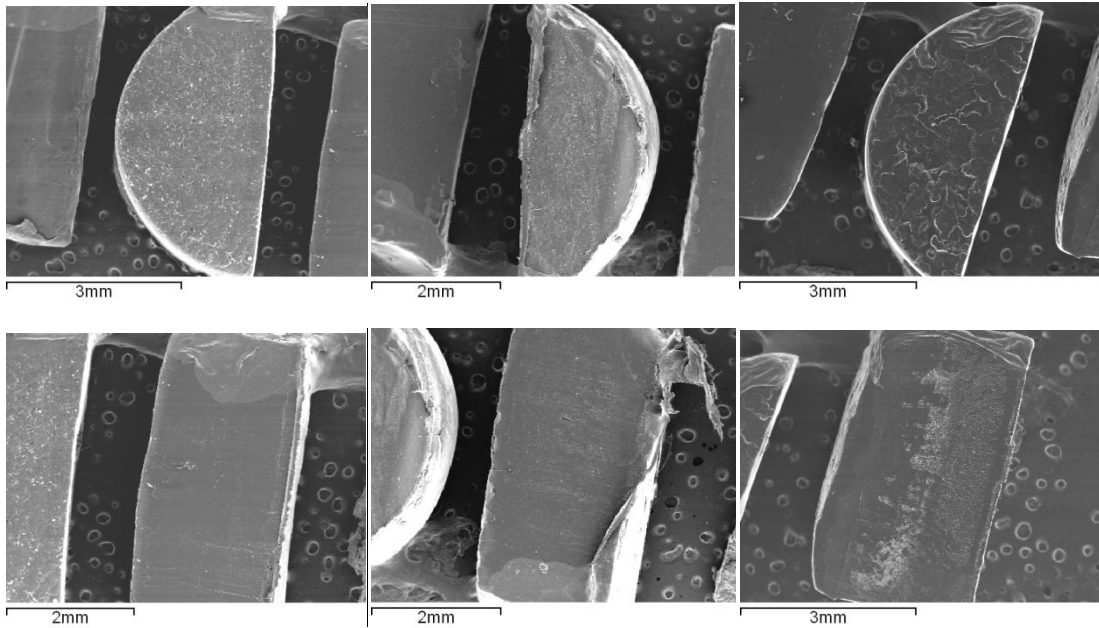


Figure \_\_. Superficial (top) and transversal section (bottom) SEM photos of PCL/GO-0.2 samples submitted to, from left to right, 0h(t0), 617.67h(t3) and 1297.67(t5) degradation hours respectively in a pH1 medium.

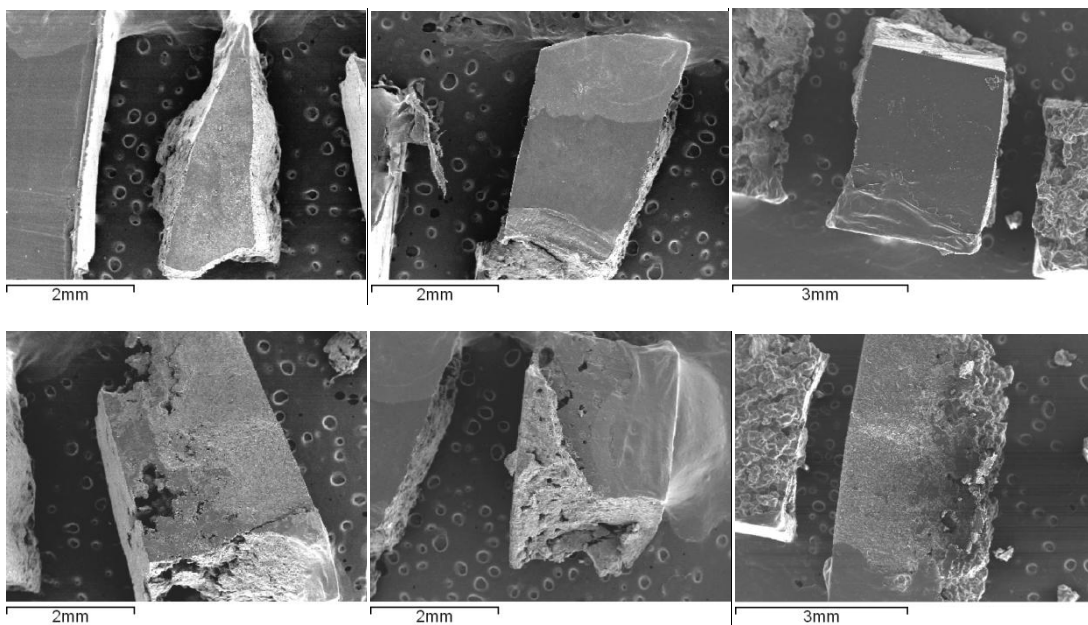


Figure \_\_. Superficial (top) and transversal section (bottom) SEM photos of PCL/GO-0.5 samples submitted to, from left to right, 0h(t0), 617.67h(t3) and 1297.67(t5) degradation hours respectively in a pH1 medium.

pH 13 (NaOH)

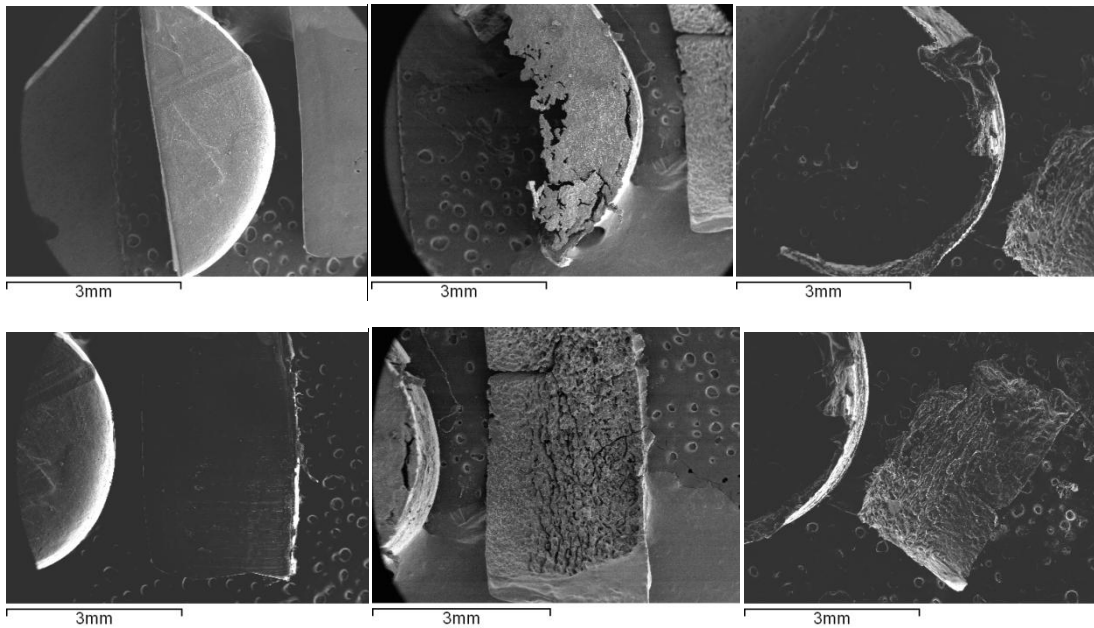


Figure \_\_. Superficial (top) and transversal section (bottom) SEM photos of neat PCL samples submitted to, from left to right, 0h (t0), 617.67h (t3) and 889.17(t4) degradation hours respectively in a pH13 medium.

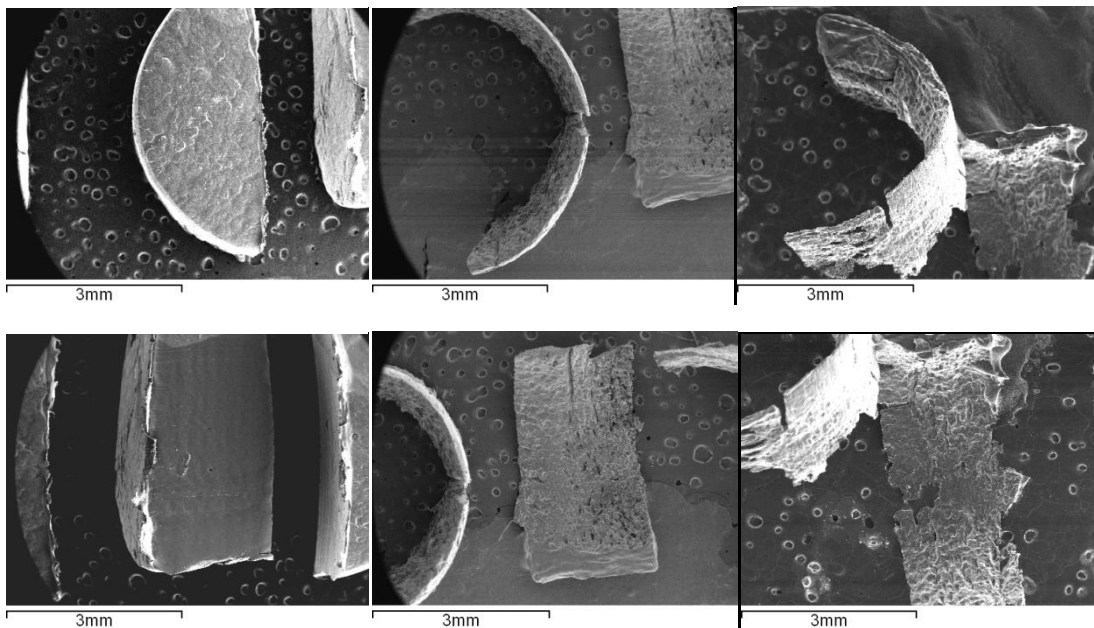


Figure \_\_. Superficial (top) and transversal section (bottom) SEM photos of PCL/GO-0.1 samples submitted to, from left to right, 0h (t0), 617.67h (t3) and 889.17(t4) degradation hours respectively in a pH13 medium.

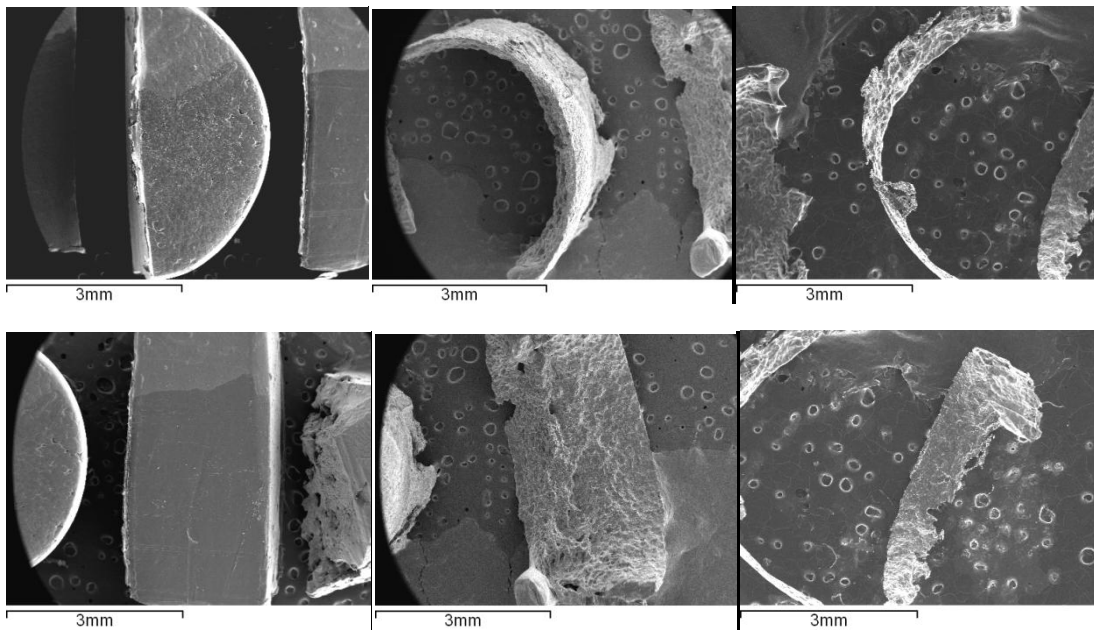


Figure \_\_. Superficial (top) and transversal section (bottom) SEM photos of PCL/GO-0.2 samples submitted to, from left to right, 0h (t0), 617.67h (t3) and 889.17(t4) degradation hours respectively in a pH13 medium.

**2.1.1.2 SEM photographs fixing degradation time and degradation medium**

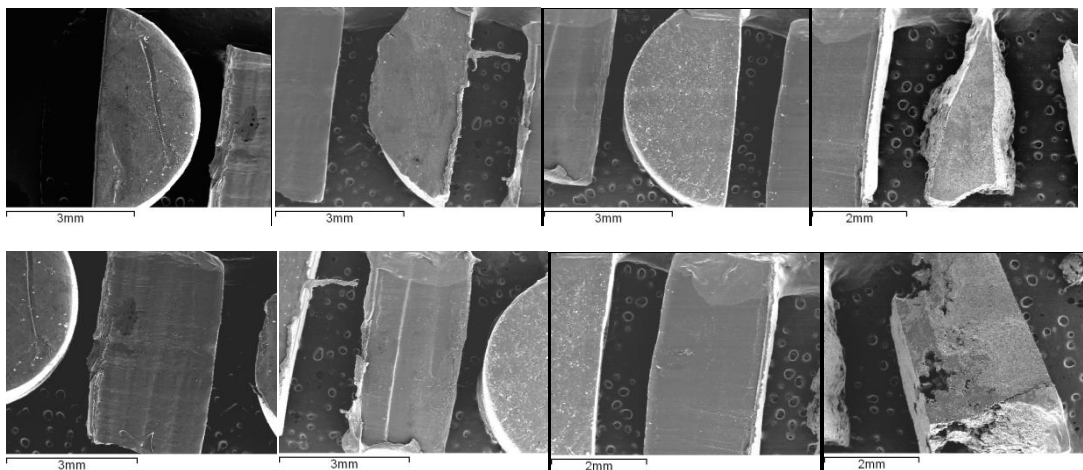


Figure \_\_. Superficial (top) and transversal section (bottom) SEM photos of PCL/GO samples containing different quantities of GO (0, 0.1, 0.2 & 0.5%) at t0.

pH 1

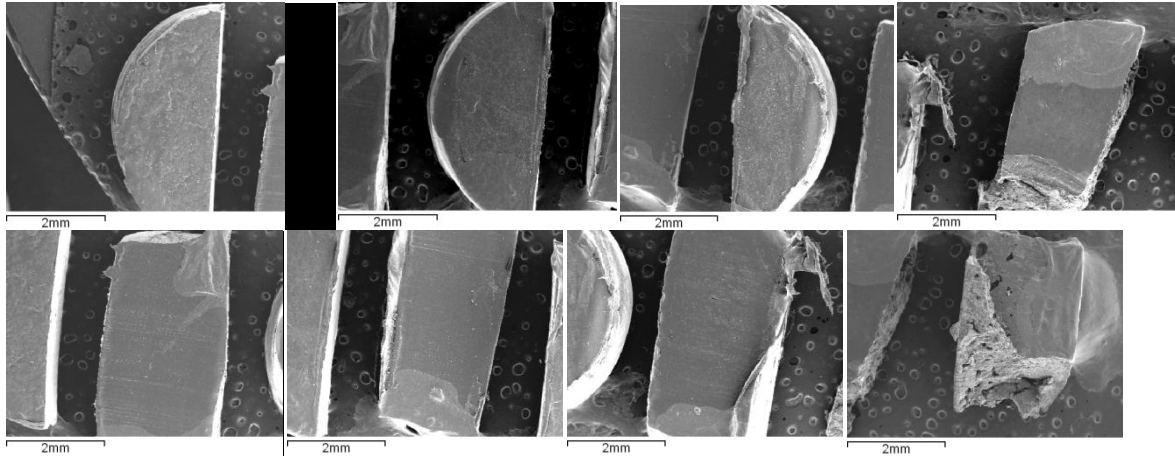


Figure 1. Superficial (top) and transversal section (bottom) SEM photos of PCL/GO samples containing different quantities of GO (0, 0.1, 0.2 & 0.5%) at t3.

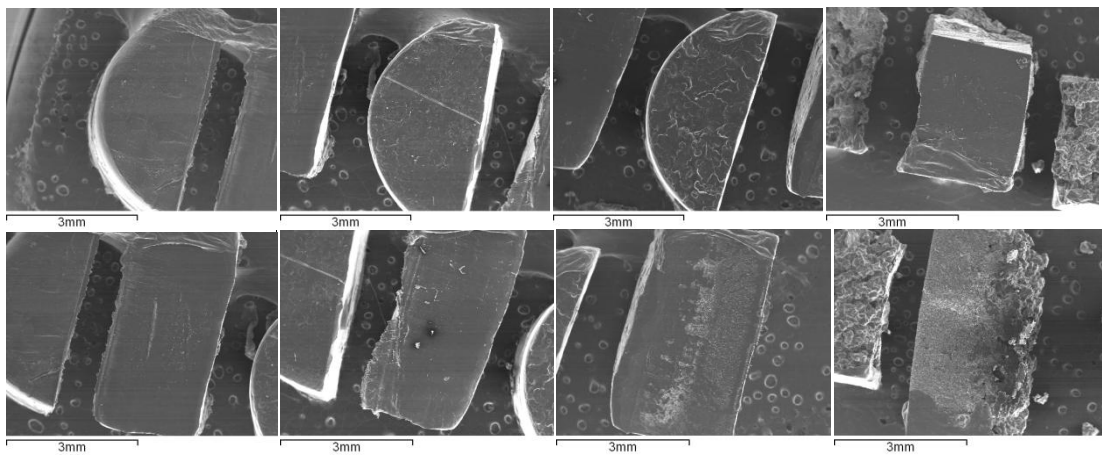


Figure 2. Superficial (top) and transversal section (bottom) SEM photos of PCL/GO samples containing different quantities of GO (0, 0.1, 0.2 & 0.5%) at t5.

pH 13 (NaOH)

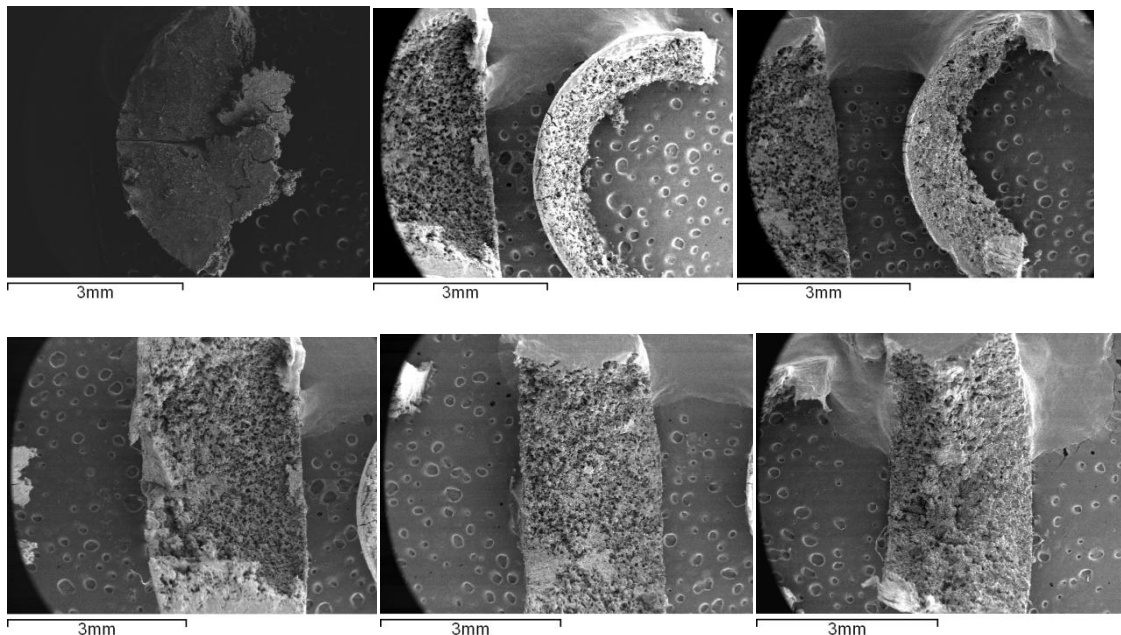


Figure 1. Superficial (top) and transversal section (bottom) SEM photos of PCL/GO samples containing different quantities of GO (0, 0.1, 0.2%) at t2.

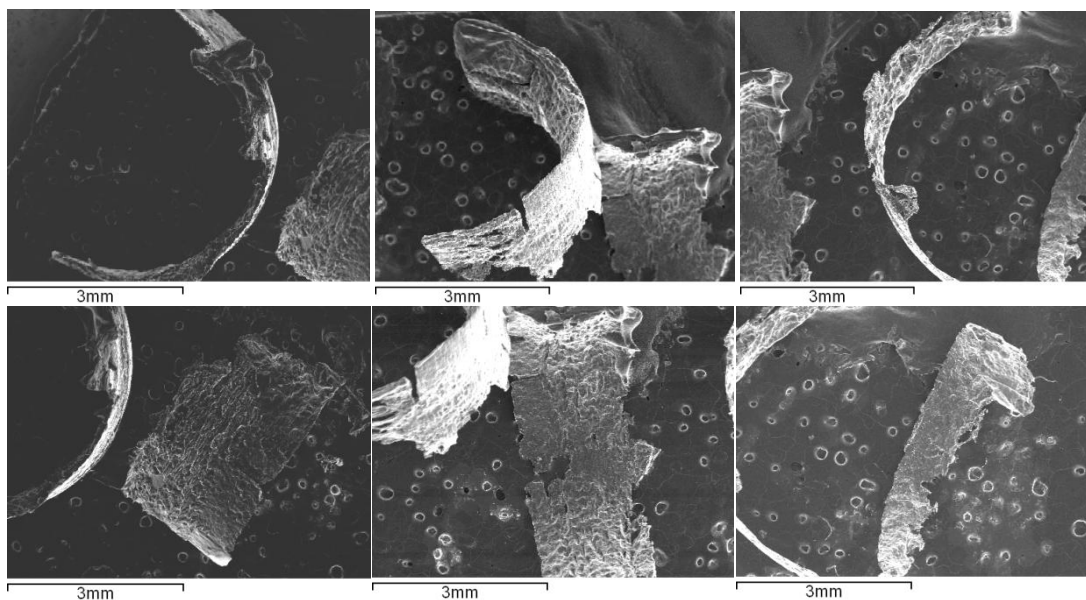
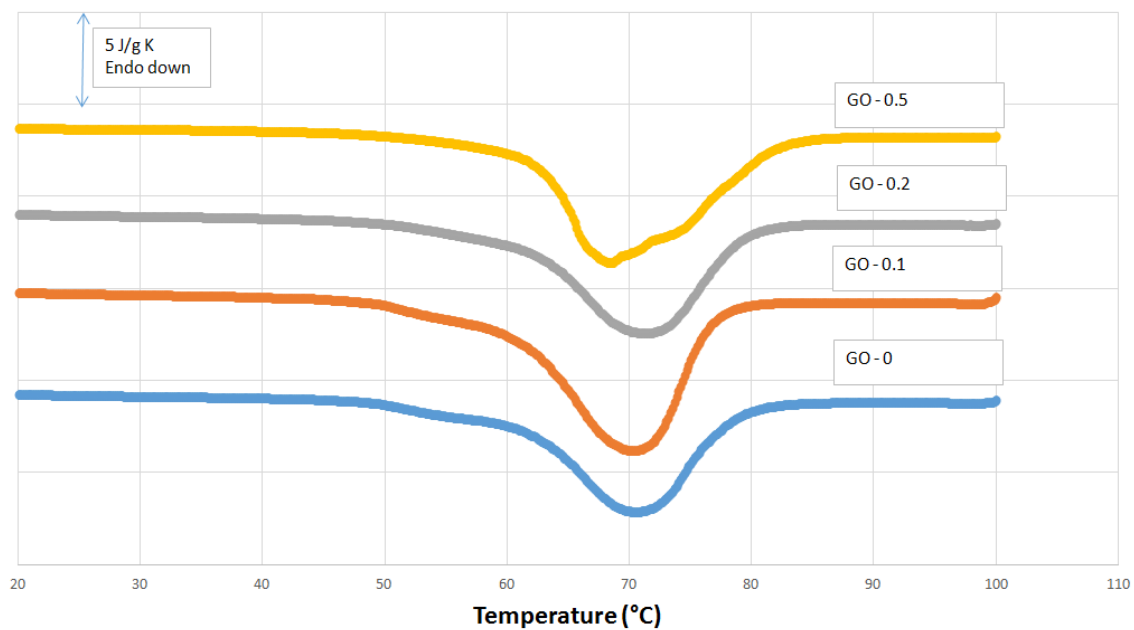


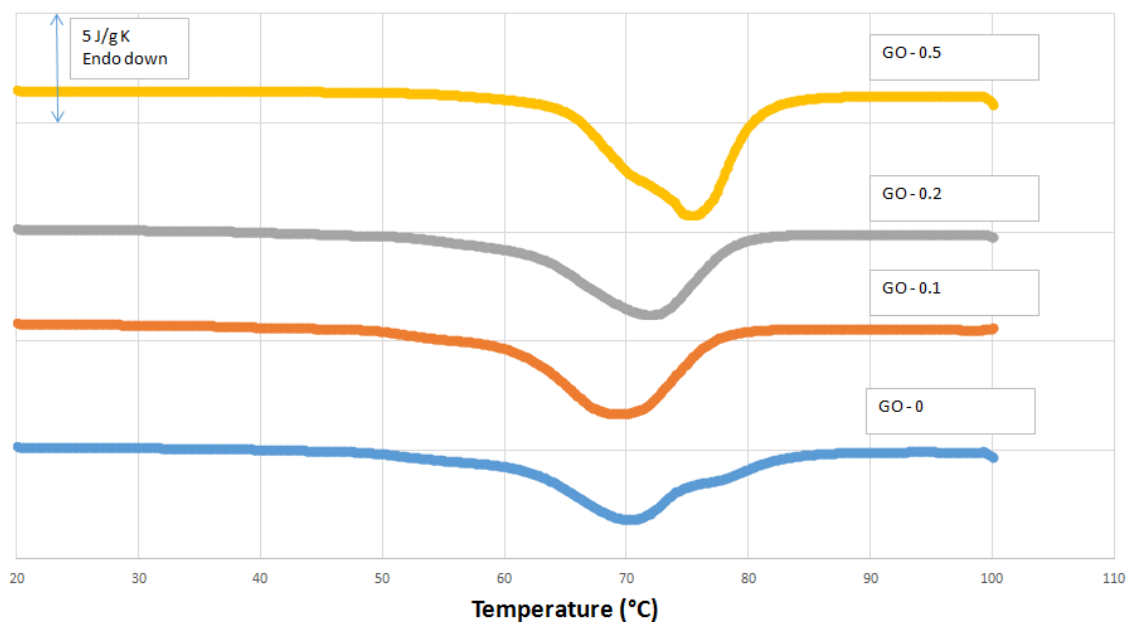
Figure 2. Superficial (top) and transversal section (bottom) SEM photos of PCL/GO samples containing different quantities of GO (0, 0.1, 0.2%) at t4.

### 3 Differential Scanning Calorimetry (DSC) Graphs.

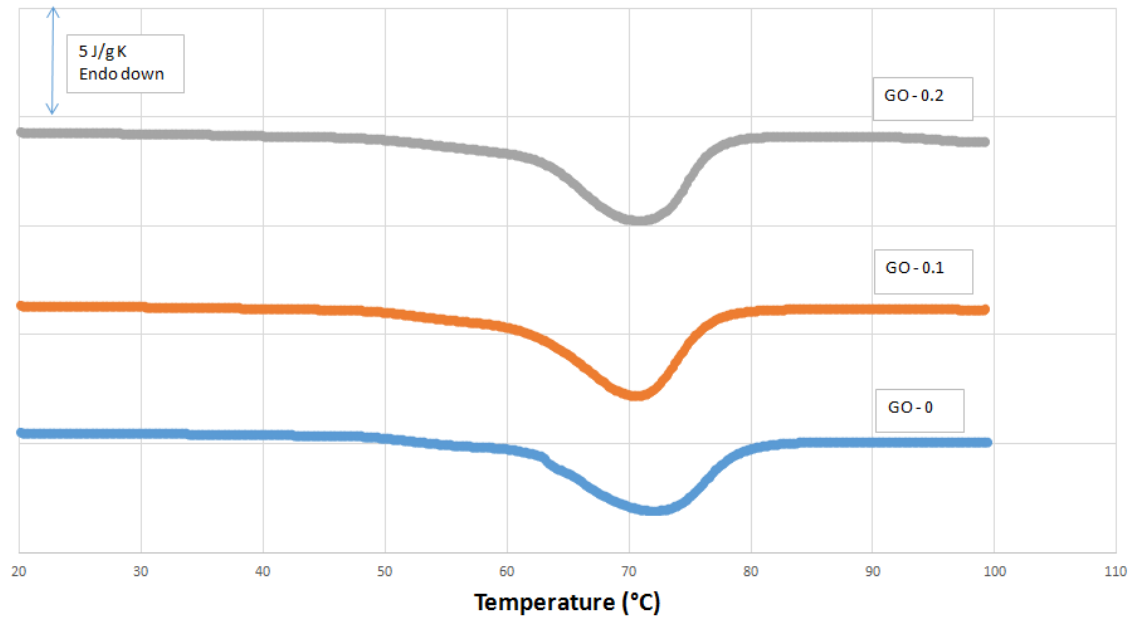
t0 - Before degradation



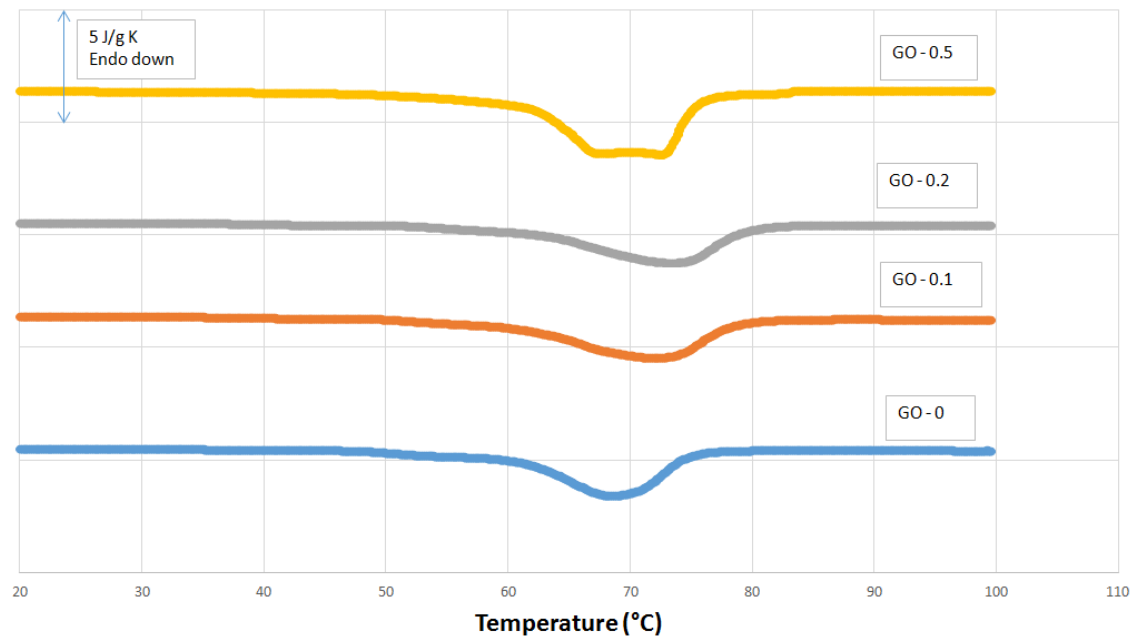
t1 - pH1



t1 - pH13

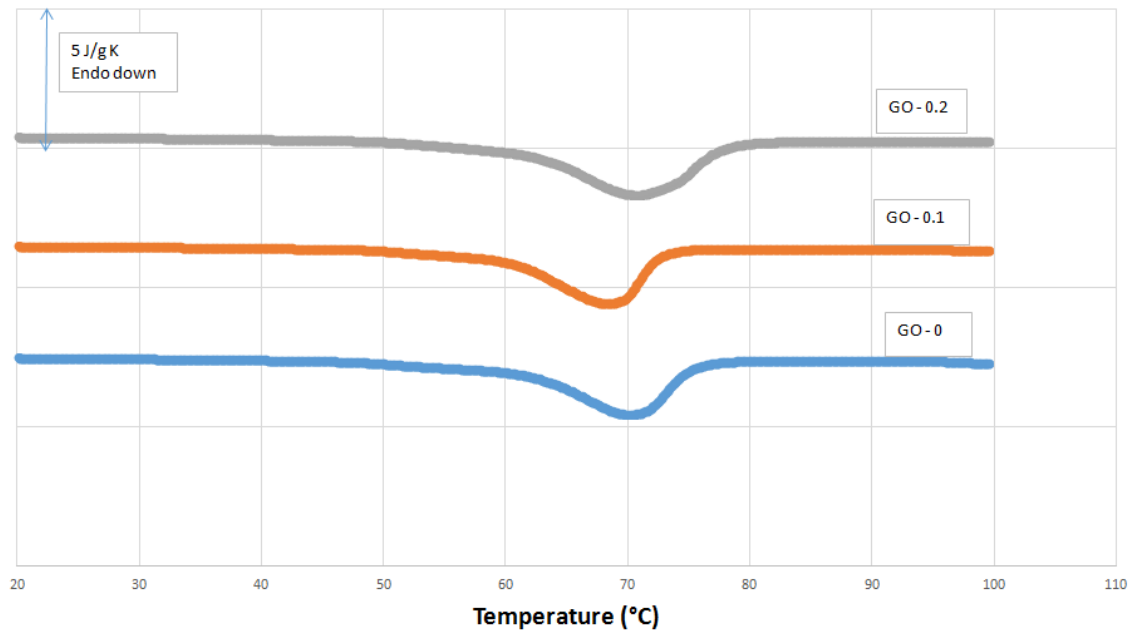


t2 - pH1

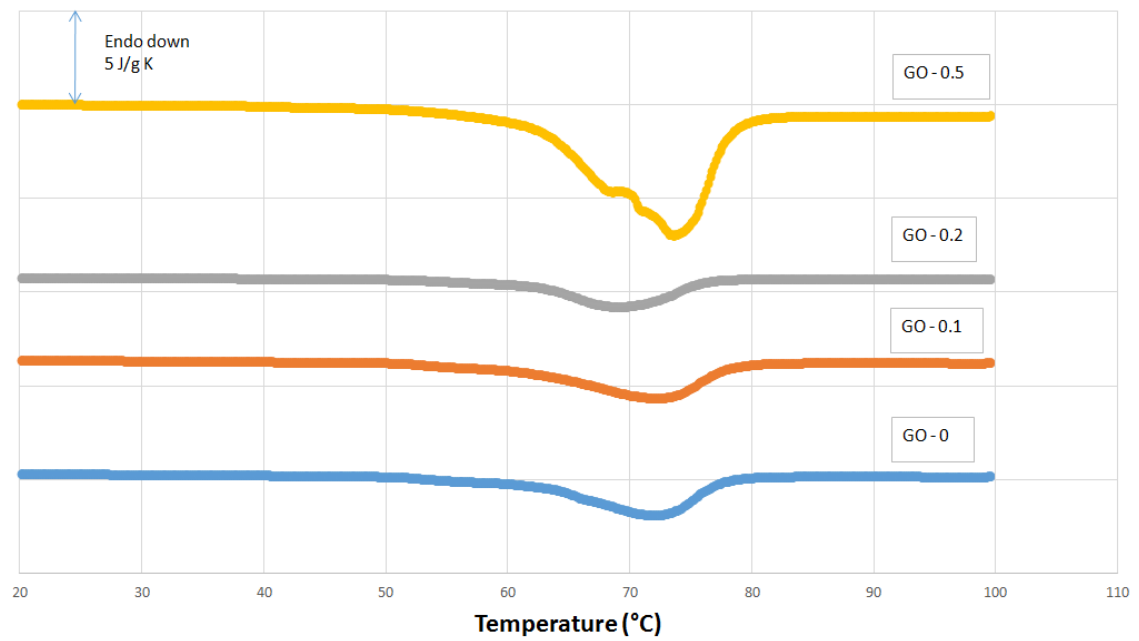




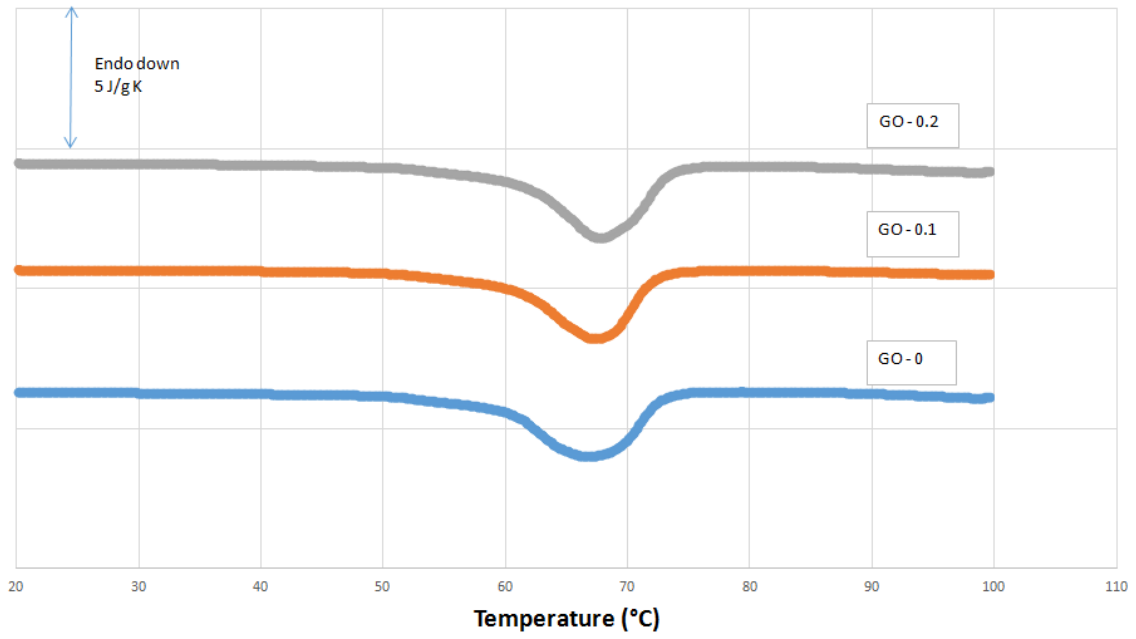
### t2 - pH13



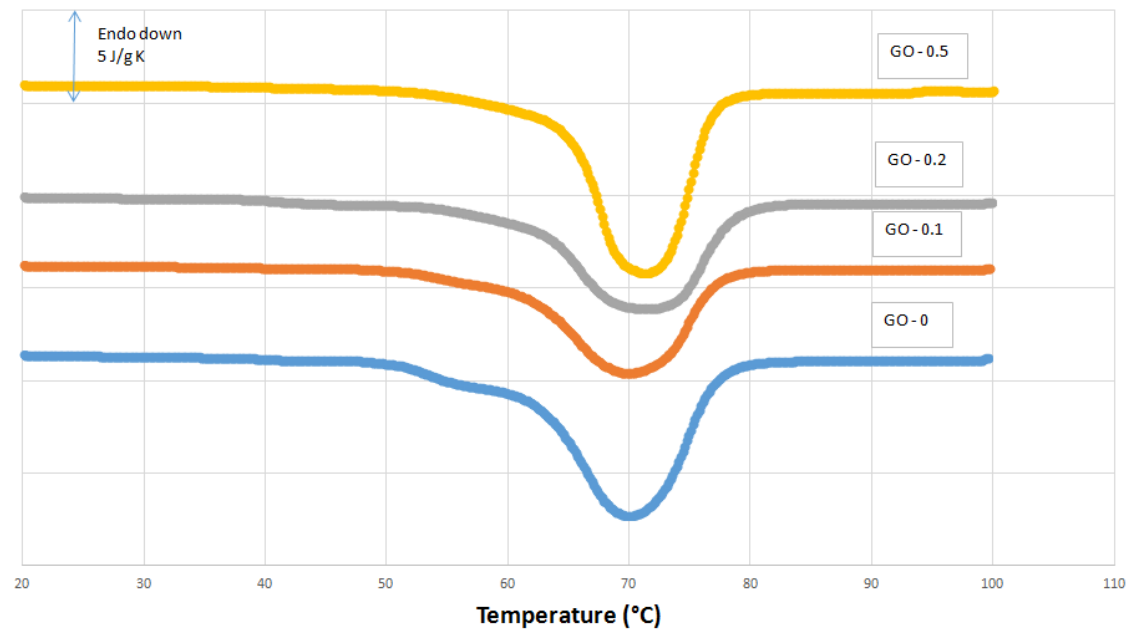
### t3 - pH1



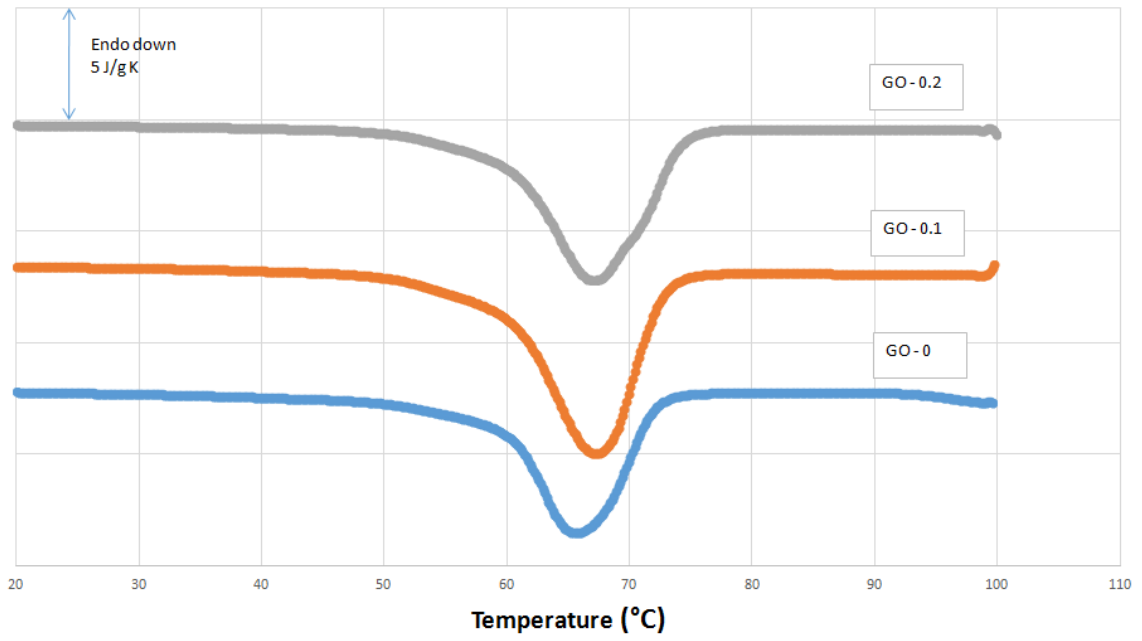
t3 - pH13



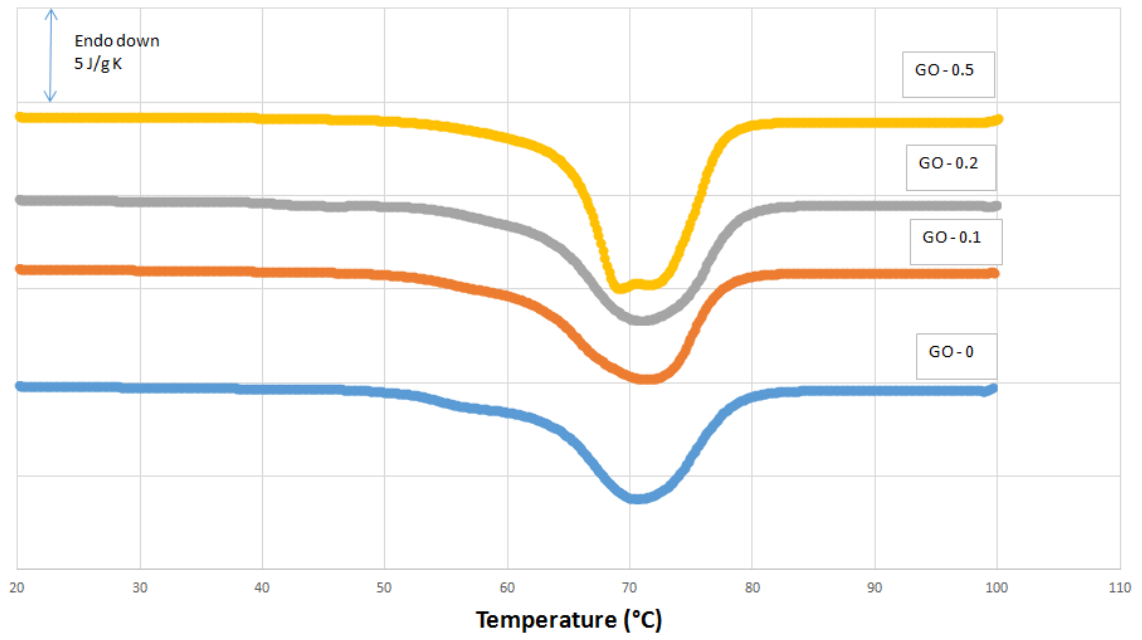
t4 - pH1



t4 - pH13



t5 - pH1



# SPECIFICATIONS INDEX

III.	SPECIFICATIONS .....	2
1	Project scope.....	2
2	General Specifications .....	2
2.1	General Open Specifications .....	2
2.1.1	Obligations and rights of the project designer.....	2
2.1.2	Authority of the Project Management .....	3
2.1.3	Laboratory Workbook .....	3
2.1.4	Project Details .....	3
2.2	General Economic Specifications .....	4
3	Technical Requirements .....	4
3.1	Technical Specifications .....	4
3.1.1	Technical Specifications of the Equipment.....	4
3.1.2	Technical Specifications of the Materials. ....	11
3.2	Waste Management and Correct Laboratory Protocols .....	18
IV.	ECONOMIC STUDY .....	20

# III. SPECIFICATIONS

## 1 Project scope

The present specifications have the objective of defining the economical conditions of this end of degree project, the policies and laws through which it is governed, its general and specific conditions, the techniques and apparatus used for its correct development, and the technical conditions of both the materials, and equipment used in the accomplishment of this project.

The development of this project takes place in the "Centro de Biomateriales e Ingeniería Tisular" (CBIT) in accordance with the requirements of the present specifications. In the laboratory in the CBIT reactive chemical substances and laboratory equipment will be used, so the specifications and preventive measures taken during the project will be defined in the following sections.

The policies and regulations through which this project is defined can be found in section 3. POLICIES.

## 2 General Specifications

### 2.1 General Open Specifications

They describe and regulate the relationship between the project designer and the project management.

#### 2.1.1 Obligations and rights of the project designer

##### 2.1.1.1 Obligations

The obligations which the project designer must comply to during the accomplishment of this project are as follows:

- To know and apply the current legislation which regulates the work which takes place in the laboratory.
- To understand the project in its full extension. This engulfs the need to acquire the corresponding knowledge in every area of the project.
- To follow the indications set by project management in its full extension.
- No changes should take place in the design of the project without the previous approval of project management.
- To know and apply the policies of waste management which originates from the use of chemical products in the laboratory.
- To inform project management and the laboratory technicians about any incident which may arise during the completion of the project.
- To correctly apply the appropriate safety measures when using chemical substances and laboratory equipment. To do so, the corresponding safety protocols must be

consulted, as well as the technical specifications of the substances and apparatus used.

- To respect the policies of academic honesty dictated by the ETSII, as well as respecting the policies which dictate how the project should be performed, presented and handed in. This engulfs the need to respect the copyright laws when writing the project.
- To respect the confidentiality of the project.

### **2.1.1.2 Rights**

The project designer has the following rights when undertaking the project:

- All equipment and materials needed for the completion of the investigation project must be supplied by project management in order to complete the project before the deadline whilst complying with the previously agreed imposed conditions.
- To dispose of the adequate installations to undertake the project. They must comply with the required security and hygiene measures.
- To dispose of the corresponding technical specifications of the laboratory apparatus and equipment in order to apply the necessary safety measures.
- To dispose of a list of the chemical products present in the laboratory, including their provider and costs.
- To receive the corresponding assistance to any technical problems which can arise in the completion of the project. The project designer may get assistance in fixing a problem, but the project designer must perform the corresponding changes according to the information given. In other words, the work must be done by the project designer.

### **2.1.2 Authority of the Project Management**

Project management is the highest authority in the execution of the project. It is in charge of designing, directing, controlling, and if necessary, correcting the work done by the project designer in order to complete the project in the agreed deadline, with the imposed conditions, quality and costs. The person in charge of the project management in the present end of degree project is Mr. Alberto José Campillo Fernández, and therefore is in charge of the full responsibilities of the project management.

### **2.1.3 Laboratory Workbook**

During the execution of the project, the project designer must keep an up to date laboratory workbook which contains all the details about the experiments which have taken place, the apparatus and materials used, any problems and modifications which have arisen, etc. The objective of this workbook is to perfectly define what has been done in the laboratory, so that if in the future an authorized person wants information on how the project took place, he can look it up in the workbook and all the information needed will be perfectly described and explained. The workbook must necessarily always stay in the laboratory.

### **2.1.4 Project Details**

According to the policies which are dictated by the ETSII, the time spent on the present end of degree project must be equal and must not surpass a total of 300 lecture hours, the

equivalent of 12 ECTS. These hours have to be distributed between laboratory work time and the time spent in the analysis of the results and the elaboration of this article, according to the agreement between the project designer and project management. The beginning of this project took place in February of 2017, and the work hours were organized so that the project must be handed in before the 7th of July of 2017. Therefore, the first part of this project were fully dedicated to the laboratory work, and the 300 hours were completed with the analysis of the obtained results and the elaboration of this article.

During this time, the project designer and the project management organized weekly meetings in order to control, correct and further design the initial experiment. Before handing in the project, the project management must correct any possible errors.

## **2.2 General Economic Specifications**

Due to the academic nature of this project, the project designer will not get any economical income for the work hours spent in the dedication of the project.

For the economic study of the project, the project designer has access to updated information contributed by the supplier of the materials and equipment. To obtain an economic study of the materials used, information about the unitary prices of all the materials used are specified. To obtain the economical study of the equipment, the price of its acquisition in the date of its acquisition are used.

In order to correctly complete the economical study, the corresponding percentages will be applied to the direct and indirect costs, value-added tax (VAT), general expenditure and industrial benefits

The full economical study of this project is defined in section IV. ECONOMICAL STUDY, of the present article.

## **3 Technical Requirements**

So to satisfy the technical requirements in the development of this project, certain policies, which are described in section I. 2. POLICIES, need to be obligatorily followed. These policies regulate the use of the materials and apparatus in the laboratory in order to keep a safe, hygienic and organized working space, as well as avoiding any hazard, and in case of such, indicating the guidelines to follow to minimize the damages.

### **3.1 Technical Specifications**

The technical specifications of the materials and equipment used seek to standardize and facilitate the development of the project by giving guidelines as to how to carry out the project.

#### **3.1.1 Technical Specifications of the Equipment**

In the following tables the technical characteristics of the laboratory equipment used is specified using the information provided by suppliers and manufacturers.

Name of the equipment	Analytical precision balance
Brand and model	XS105DU
Maximum weighing capacity	120g/41g
Readability	0.1 mg; 0.01 mg
Repeatability (2)	0.02 mg (5g)
Adjustment	Internal / FACT
Weighing plate dimensions	78 mm
Stabilization time	1.5 s
Repeatability (typical)	0.01 mg
Linearity $\pm$	0.2 mg
Dimensions (height x width)	322 mm x 263 mm



Name of the equipment	Universal precision stove
Brand and model	DIGITRONIC 1451 reference: 2005161
Dimensions (height x width x length) (cm)	70 x 95 x 72
Weight (kg)	74
Capacity	145
Interior dimensions (height x width x length) (cm)	50 x 58 x 50
Consumption (W)	2000
Temperature regulation	Digital with microprocessor
Heat distribution	Forced air



Maximum temperature range (°C)	250
Minimum temperature range (°C)	Room temperature + 5°C
Stability	±0.25°C, at 100°C
Homogeneity	±1°C, at 100°C
Set-point error	±2%, at working temperature
Resolution	1°C
Time to reach set-point 100°C (min)	17
Recovery time (min)	10
Air renewals per hour	12
Electrical power supply	115-230V 50-60Hz



Name of the equipment	Ultrasonic bath
Brand and model	USC 600 TH
Capacity (L)	5.4
Ultrasonic power eff. (W)	120
Heating power (W)	400
Internal dimensions (width x depth x height)	300 x 150 x 150
External dimensions (width x depth x height)	325 x 175 x 295
Category no.	142-0091
Frequency (kHz)	45

Tank heater	20...80°C
Digital timer (min)	1 - 99



Name of the equipment	Oil vacuum pump
Brand and model	Vacuubrand from SIGMA ALDRICH - RZ 2
Vacuum flow rate limit	2.2 - 2.5 m <sup>3</sup> /h
Ultimate vacuum (partial) without gas ballast (mbar)	4 x 10 <sup>-4</sup>
Ultimate vacuum (total) without gas ballast (mbar)	2 x 10 <sup>-3</sup>
Ultimate vacuum (total) with gas ballast (mbar)	1 x 10 <sup>-2</sup>
Dimensions (length x width x height) (mm)	308 x 122 x 160



Name of the equipment	Desiccator
Brand and model	Vacuo-Temp 4000474
Maximum vacuum	10 <sup>-2</sup> mmHg
Volume	3 L
Heating plate diameter	23,5 cm
Dimensions (height x width x length)	17 x 28 x 34 mm
Consumption	540 W
Weight	9 kg
Stability	±1°C

Precision

±1°C



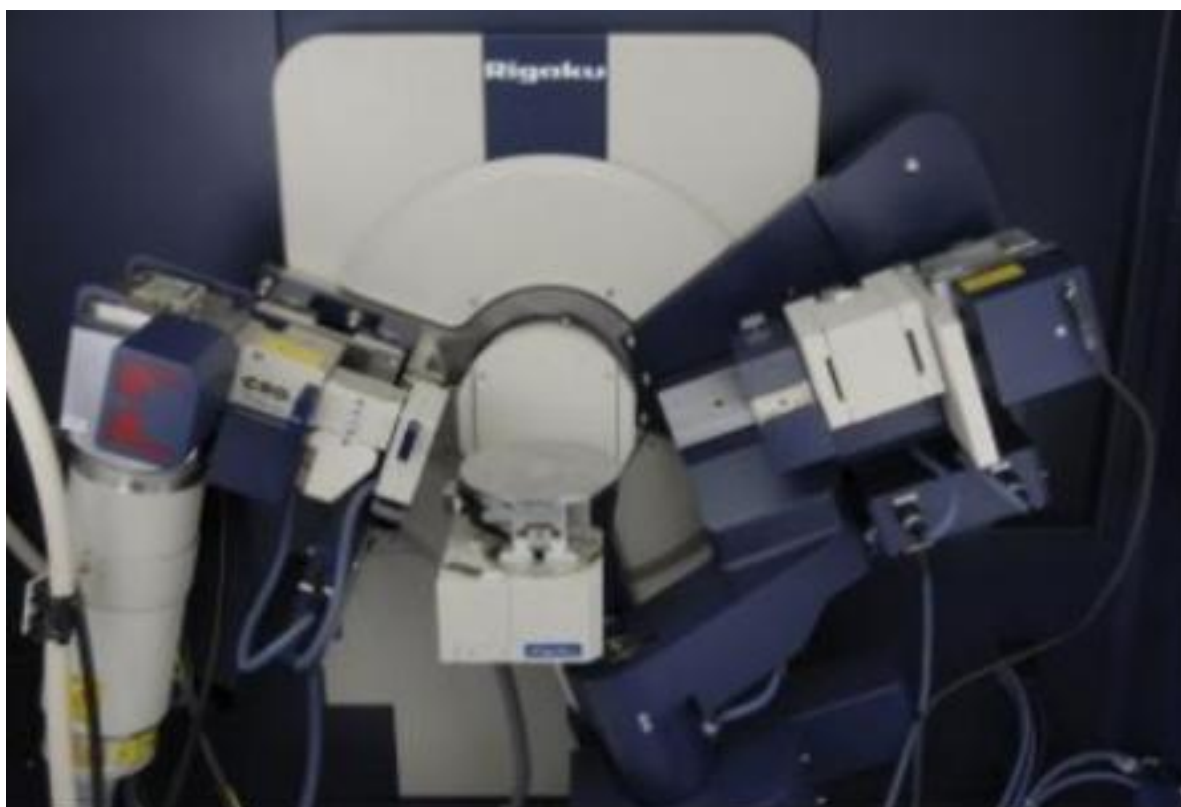
Name of the equipment	Differential scanning calorimeter	
Brand and model	Mettler Toledo DSC823e	
	200W	400W

Temperature range - liquid nitrogen cooling	(-150°C ... 500°C)	(-150°C ... 500°C)
Temperature accuracy	±0.2K	
Temperature precision	±0.02K	
Heating rate (RT ... 700°C)	0.01 ... 300K/min (continuously)	
Cooling rate	0.01 ... 50K/min	
Cooling time - liquid nitrogen (100°C ... -100°C)	15 min	
Minimum weight of samples in capsule (mg)	5	

Name of the equipment	Sample robot
Brand and model	TSO 801 RO
Sample capacity	34





Name of the equipment	X-ray diffractometer	
Brand and model	Rigaku Ultima IV	
X- ray generator	Maximum rated output (kW)	3
	Rated tube voltage (mA)	20 - 60
	Rated tube current	2.0 - 60
	Target	Cu (others:optional)
	Focus size (mm)	0.4 x 12 (others: optional)
Goniometre	Scanning mode	$\theta_s/\theta_d$ coupled or $\theta_s$ , $\theta_d$ independant
	Goniometre radius (mm)	285
	2 $\theta$ measuring range	(-3 to 162°) maximum
	Minimum step size	0.0001°
Detector	Detector	Scintillation counter
Dimensions	H x W x D (mm)	1600 x 1100 x 800
	Sample height (mm)	1050






### 3.1.2 Technical Specifications of the Materials.

In the following tables the technical characteristics of the chemical products used in the laboratory are specified using the information provided by the manufacturers and information gathered from the laboratory database.

Common Name				
Acetone				
Empirical formula	CAS	Supplier		
C <sub>3</sub> H <sub>6</sub> O	67-64-1	SCHARLAB		
Properties				
Molecular weight	Density	Viscosity	Solubility in water	vapour pressure
58.08 g/mol	0.790 g/cm <sup>3</sup>	0.31 mPas	100% miscible	233 hPa
Physical state	Melting T	Boiling T	Flash point	Decomposition T
Liquid	- 95°C	56°C	<-20°C	-
Recommendations				
Risks	- H (hazard) GHS statements: H225 - H319 - H336 - EUH66			
	- P (precautionary) GHS statements: P210 - P233 - P305+P351+P338			
Handling measures	- Open and handle container with care.			
	- Work with the ventilation system activated			
	- Do not inhale the substance			
	- Avoid the generation of vapours/aerosols			
	- Maintain far away from sources of ignition. No smoking			
	- Take measures against electro-static charges			
Storage measures	- Keep the container hermetically sealed			
	- Store in a ventilated and dry place			
	- Store far away from ignition and heat sources			
Pictograms				
	GHS02		GHS07	




Common Name		
Ethanol		
Empirical formula	CAS	Supplier
C <sub>2</sub> H <sub>6</sub> O	64-17-5	SCHARLAB



Properties				
Molecular weight	Density	Viscosity	Solubility in water	vapour pressure
46.07 g/mol	0.79 g/cm <sup>3</sup>	1.519 mm <sup>2</sup> /s	100% miscible	79 hPa
Physical state	Melting T	Boiling T	Flash point	Decomposition T
Liquid	- 114°C	78°C	-	-
Recommendations				
Risks	- H (hazard) GHS statements: H225 - H319			
	- P (precautionary) GHS statements: P210 - P233 - P241 - P280 - P305+P351+P338			
	- P501a			
Handling measures	- Store in tightly closed containers in a dry and cool environment			
	- Protect from heat and direct sunlight			
	- Ensure good ventilation of the room, even at ground level (vapours weigh more than air)			
	- Work with the ventilation system activated			
	- Maintain far away from sources of ignition. No smoking.			
Storage measures	- Take measures against electro-static charges			
	- Forsee watertight and solvent-resistant floors			
	- Keep container tightly closed			
Storage measures	- Store in a cool place			
	Pictograms	 <p>GHS02</p>		

Common Name				
Ethylene glycol				
Empirical formula	CAS	Supplier		
C <sub>2</sub> H <sub>6</sub> O <sub>2</sub>	107-21-1	SCHARLAB		
Properties				
Molecular weight	Density	Viscosity	Solubility in water	vapour pressure
62.068 g/mol	1.116 g/cm <sup>3</sup>	-	100% miscible	0.123 hPa
Physical state	Melting T	Boiling T	Flash point	Decomposition T
Liquid	-13°C	197°C	111°C	-
Recommendations				
Risks	- H (hazard) GHS statements: H302 - H373			
	- P (precautionary) GHS statements: P264 - P301+P312 - P314 - P330			
Handling measures	- No special precautions are necessary if used correctly			
Storage measures	- Store in a properly ventilated place, far away from heat and ignition sources			
	- Store under lock and key and with access restricted to technical experts			
Pictograms	 <b>GHS07</b>		 <b>GHS08</b>	





Common Name		
1,4 Dioxane		
Formula	CAS	Supplier
C4H8O2	123-91-1	FISHER


Properties				
Molecular weight	Density	Viscosity	Solubility in water	vapour pressure
88.11 g/mol	1.033 g/cm3	-	Miscible	27 mmHg (20°C)
Physical state	Melting T	Boiling T	Flash point	Decomposition T
Liquid	11.8°C	101.1°C	-	-
Recommendations				
Risks	- H (hazard) GHS statements: H225 - H319 - H335 - H351 - P (precautionary) GHS statements: P210 - P280 - P305 + P351 + P338-P370 + P378 - P403 + P235			
Handling measures	Wear personal protective equipment			
	Assure adequate ventilation			
	Handle in an inert atmosphere, keep away from naked flames, hot surfaces and sources of ignition			
	Do not inhale vapors			
	Avoid contact with eyes, skin or clothing.			
	Wear a particles mask when manipulating the substance			
	Avoid the accumulation of electrostatic charges			
	If peroxide formation is suspected, do not open or move the container			
	Use only non-sparking tools			
	To prevent ignition and vapors from discharging static electricity all metal parts used in the installations must be grounded			
Storage measures	Wash hands before breaks and immediately after use			
	Store at room temperature			
	Keep containers tightly closed in a cool, dry and well-ventilated place.			
	Store in an inert atmosphere			
	May form explosive peroxides			
	The containers should be marked with the opening date and should be tested periodically for the presence of peroxides.			
	If crystals form in a peroxidizable liquid peroxidation may occur and the product should			
Pictograms	Keep away from heat and sources of ignition			
	<div style="display: flex; justify-content: space-around; align-items: center;"> <div style="text-align: center;">   <b>GHS02</b> </div> <div style="text-align: center;">   <b>GHS07</b> </div> <div style="text-align: center;">   <b>GHS08</b> </div> </div>			

Common Name				
Acetonitrile				
Empirical formula	CAS		Supplier	
C <sub>2</sub> H <sub>3</sub> N	75-05-8		SCHARLAB	
Properties				
Molecular weight	Density	Viscosity	Solubility in water	vapour pressure
41.05 g/mol	0.786 g/cm <sup>3</sup>	0.343 mPa*s (25°C)	Miscible	27 mmHg (20°C)
Physical state	Melting T	Boiling T	Flash point	Decomposition T
Liquid	-45°C	82°C	-	-
Recommendations				
Risks	- H (hazard) GHS statements: H225 - H302 + H312 + H332-H319			
	- P (precautionary) GHS statements: P210-P261-P280-P305 + P351 + P338-P370 + P378-P403-P235			
Handling measures	Keep away from sources of ignition			
	Take measures to prevent electrostatic charge			
Storage measures	Store in a ventilated place away from heat and sources of ignition			
	Keep containers tightly closed in a cool, dry and well-ventilated place.			
Pictograms	 GHS02		 GHS07	

Common Name				
Poly( $\epsilon$ -caprolactone)				
Empirical formula	CAS	Supplier		
(C <sub>6</sub> H <sub>10</sub> O <sub>2</sub> ) <sub>n</sub>	24980-41-4	SIGMA-ALDRICH		
Properties				
Molecular weight	Density	Viscosity	Solubility in water	vapour pressure
variable	1.145 g/cm <sup>3</sup>	-	-	-
Physical state	Melting T	Boiling T	Flash point	Decomposition T
Solid	59-64°C	-	-	350°C
Recommendations				
Risks	Not dangerous			
Handling measures	Must have adequate extraction in places where dust is formed			
	Normal preventive fire protection provisions			
Storage measures	Keep container tightly closed in a dry and well-ventilated place.			
	Store in a cool place			
Pictograms	-			

Common Name				
Graphene Oxide powder				
Formula	CAS	Supplier		
GO	7782-42-5	GRAPHENE A		
Properties				
Molecular weight	Density	Viscosity	Solubility in water	vapour pressure
198.22 g/mol	1.051 g/cm <sup>3</sup>	-	-	<0.1 mmHg (21.1°C)
Physical state	Melting T	Boiling T	Flash point	Decomposition T
Solid	-	98-100°C	-	-
Recommendations				
Risks	May cause irritation to eyes, skin and respiratory tract. May contain impurities of carcinogenic compounds.			
Handling measures	Ensure adequate ventilation during handling			
	Wear personal protective equipment whilst handling with the product			
Storage measures	Store in tightly labeled closed containers, away from heat sources			
	Avoid formation and accumulation of dust			
Pictograms	-			

Common Name				
Hydrochloric acid				
Empirical formula	CAS	Supplier		
HCl	7647-01-0	SIGMA-ALDRICH		
Properties				
Molecular weight	Density	Viscosity	Solubility in water	vapour pressure
36.458 g/mol	-	-	Miscible	-
Physical state	Melting T	Boiling T	Flash point	Decomposition T
Liquid	-114°C	49,44°C	-	100°C
Recommendations				
Risks	H (hazard) GHS statements: H290+H314+H335			
	P (precautionary) GHS statements: P260 - P280 - P303 +P361 + P353-P304 + P340 + P310-P305 + P351 + P338			
Handling measures	Do not inhale			
	Avoid contact with eyes, skin and clothes			
Storage measures	May produce pressure, open with care			
Pictograms	<div style="display: flex; justify-content: space-around; align-items: center;"> <div style="text-align: center;">  <p>GHS05</p> </div> <div style="text-align: center;">  <p>GHS07</p> </div> </div>			

Common Name				
Sodium Hydroxide				
Empirical formula	CAS	Supplier		
NaOH	1310-73-2	SIGMA-ALDRICH		
Properties				
Molecular weight	Density	Viscosity	Solubility in water	vapour pressure
39.997 g/mol	2.13 g/cm <sup>3</sup>	-	1110g/L (°C)	<18 mmHg (20°C)
Physical state	Melting T	Boiling T	Flash point	Decomposition T
Solid	-318°C	1388°C	-	-
Recommendations				
Risks	H (hazard) GHS statements: H290 + H314			
	P (precautionary) GHS statements: P280-P303 + P361 + P353-P304 + P340 + P310-P305 + P351 + P338			
Handling measures	Do not inhale			
	Avoid contact with eyes, skin and clothes			
Storage measures	May produce pressure, open with care			
Pictograms				

### 3.2 Waste Management and Correct Laboratory Protocols

The correct management of the waste products (which are practically any remaining substance or equipment which cannot be cleaned or recovered directly in the lab) is of crucial importance in order to meet the requirements specified in the legal policies. Therefore, there are certain guidelines which need to be followed in order to correctly treat the waste products, and these guidelines vary depending on their nature. Furthermore, in order to maintain health and safety protocols in the lab, various precaution measures need to be taken.

- The liquid residues are stored in bottles and need to be correctly identified through a label. Under no circumstances will a residue bottle be left unidentified. In the case of finding an untagged bottle, it will be notified to the laboratory technician.
- When manipulating any hazardous residues (carcinogen, corrosive, etc.) the use of the appropriate gloves is obligatory.
- Any waste product which has been in contact with monomers or any hazardous substance shall be carefully placed in a Zip bag and placed in the corresponding recycling container.

- The solvents used in the laboratory (including acetone and ethanol) are classified into halogenated and non-halogenated solvents, and must be deposited in their respective labelled containers. In this project all the solvents used were non-halogenated, and were therefore all placed in the corresponding container. Furthermore, the carcinogenic products must be placed in their own respective container.
- Before disposing of any acidic or basic solutions, they must be previously neutralized with the help of the laboratory technician.
- Any broken glass or paper which has been in contact with monomers or carcinogenic products must be sealed in a Zip bag and placed in the respective container for its posterior recycling. There are separate containers for glass and paper.
- When working with a chemical substance whose properties are unknown, contact with the laboratory technician in first place to avoid any possible hazards both to the personal health of the project designer and to any laboratory staff in the proximity.
- When working with any irritant, harmful, carcinogenic, etc. product it is obliged to work under an extraction hood. In the case of the more dangerous chemical products like monomers or carcinogenic products, a gas mask must be used. In the case of working with particles, a particle mask must be worn.
- When working in the lab - even if not in contact with any chemical substance - the use of a lab coat is obliged. When working with any chemical substance, its properties need to be known in order to wear the corresponding personal protection (gloves, mask, etc.).

## IV. ECONOMIC STUDY

### 1. Project staff

Nº	Code	Unit	Description	Unitary Price (€)	Quantity	Cost (€)
1	P.PD	hr	Project Director	24,00	39	936,00
3	P.LT	hr	Laboratory Technician	12,60	11	138,60
4	P.CE	hr	Chemical engineer	18,00	300	5400,00
					Total	6474,60

### 2. Equipment

Nº	Code	Unit	Description	Unitary Price (€)	Quantity	Cost (€)
1	E.APB	hr	Analytical precision balance	0,20	26	5,20
2	E.UPS	hr	Universal precision stove	0,98	1773,5	1738,03
3	E.UB	hr	Ultrasonic bath	0,11	32,16	3,54
4	E.OVP	hr	Oil vacuum pump	0,19	4,84	0,92
5	E.D	hr	Desiccator	0,09	1797	161,73
6	E.DSC	hr	Differential scanning calorimeter	0,55	80	44,00
7	E.SR	hr	Sample robot	0,12	80	9,60
8	E.XRD	hr	X-ray diffractometer	0,51	3	1,53
10	E.E	hr	Encapsulator	0,10	1,5	0,15
11	E.SEM	hr	Scanning electron microscope	1,49	13	19,37
12	E.F	hr	Fridge	0,08	24	1,92
13	E.PHM	hr	pH-meter	0,12	1	0,12
					Total	1986,11

### 3. Materials

Nº	Code	Unit	Description	Unitary Price (€)	Quantity	Cost (€)
1	M.vial20	unit	20 mL vial	0,10	3	0,30
2	M.CE	unit	Clamping equipment	13,00	4	52,00
3	M.TC	unit	Teflon Crystallizer	22,00	4	88,00
4	M.PD	unit	Petri dish	1,33	4	5,32
5	M.AT	unit	Aluminium tweezers	2,00	1	2,00
6	M.DSS	unit	Double spoon spatula	4,95	1	4,95
7	M.FSS	unit	Flat spoon spatula	4,21	1	4,21
8	M.ISO20	unit	20mL ISO bottle	5,31	3	15,93
9	M.ISO1000	unit	1L ISO bottle	6,99	2	13,98
10	M.PP	unit	Pasteur pipette 1000µL	11,50	1	11,50
11	M.B	unit	100mL beaker	0,50	3	1,50
12	M.MR	unit	Mixing rod	0,39	1	0,39
13	M.vial10	unit	10 mL vials	0,10	480	48,00
14	M.VL	unit	10 mL vial lid	0,01	168	1,68

15	M.SSS	unit	Stainless steel microspatula	7,65	1	7,65
16	M.WG	unit	Watch glass	2,99	1	2,99
17	M.CT	unit	Cable tie	0,10	168	16,80
18	M.AC	unit	Aluminium Capsules	2,83	123	348,09
19	M.N	unit	Needle	0,10	1	0,10
20	M.FP	unit	Filter paper	0,05	9	0,45
21	M.H	unit	Hammer	15,00	1	15,00
22	M.T5	unit	5mm troquel	1,55	1	1,55
23	M.TB	unit	Troquel base	20,00	1	20,00
24	M.LND	unit	Liquid Nitrogen Dewar 150L	50,00	4	200,00
25	M.AP	unit	Aluminium platform	5,10	4	20,40
26	M.C	unit	Cutter	1,30	2	2,60
27	M.PF	unit	Parafilm	38,00	0,5	19,00
28	M.CP	unit	Paper roll	2,00	1	2,00
29	M.LC	unit	Laboratory coat	15,50	1	15,50
30	M.LG	unit	Latex gloves box	5,85	1	5,85
31	M.NG	unit	Nitrile gloves box	7,29	0,4	2,92
32	M.LG	unit	Laboratory glasses	8,00	1	8,00
33	M.GM	unit	Gas mask	40,30	1	40,30
34	M.DM	unit	Dust mask	10,00	1	10,00
35	M.ZB	unit	Zip bags	0,20	20	4,00
36	R.PCL	gr	Poly(ε-caprolactone)	7,84	143	1121,12
37	R.GO	gr	Graphene oxide	58,00	0,283	16,41
38	R.D	L	1,4 Dioxane	70,30	0,333	23,41
39	R.ACN	L	Acetonitrile	70,36	0,018	1,27
40	R.EG	L	Ethylene glycol	63,60	0,018	1,14
41	R.DW	L	Distilled water	0,20	20	4,00
42	R.A	L	Acetone	9,00	2	18,00
43	R.E	L	Ethanol	32,40	2	64,80
44	R.HA	L	Hydrochloric acid	85,90	0,02	1,72
45	R.SH	kg	Sodium hydroxide pellets	106,00	0,03	3,18
					Total	2248,01



## 4. Decomposed Prices

### Chapter 1. Sample synthesis

Subchapter 1.1 Selection of a suitable solvent					
Code	Quantity	Unit	Description	Unitary Price (€)	Cost (€)
M.vial20	3	unit	20 mL vial	0,10	0,30
R.D	0,02	L	1,4 Dioxane	70,30	1,41
R.ACN	0,02	L	Acetonitrile	70,36	1,41
R.EG	0,02	L	Ethylene glycol	63,60	1,27
E.UB	0,33	hr	Ultrasonic bath	0,11	0,04
E.UPS	1,5	hr	Universal precision stove	0,98	1,47
M.DSS	1	unit	Double spoon spatula	4,95	4,95
M.SSS	1	unit	Stainless steel microspatula	7,65	7,65
R.GO	0,03	gr	Graphene oxide	58,00	1,74
R.PCL	3	gr	Poly( $\epsilon$ -caprolactone)	7,84	23,52
M.CE	4	unit	Clamping equipment	13,00	52,00
P.CE	2	hr	Chemical engineer	18,00	36,00
	2	%	Direct costs		2,64
				Total	134,39

Subchapter 1.2 Trial and error experiments and final synthesis technique					
Code	Quantity	Unit	Description	Unitary Price (€)	Cost (€)
R.GO	0,253	mg	Graphene oxide	58,00	14,67
M.SSS	1	unit	Stainless steel microspatula	7,65	7,65
M.ISO20	3	unit	20mL ISO bottle	5,31	15,93
E.UB	31,83	hr	Ultrasonic bath	0,11	3,50
M.CE	4	unit	Clamping equipment	13,00	52,00
E.APB	1	hr	Analytical precision balance	0,20	0,20
M.WG	1	unit	Watch glass	2,99	2,99
R.PCL	140	gr	Poly( $\epsilon$ -caprolactone)	7,84	1097,60
M.TC	4	unit	Teflon Crystallizer	22,00	88,00
M.DSS	1	unit	Double spoon spatula	4,95	4,95
E.UPS	72	hr	Universal precision stove	0,98	70,56
M.PF	0,5	unit	Parafilm	38,00	19,00
M.MR	1	unit	Mixing rod	0,39	0,39
E.OVP	4,67	hr	Oil vacuum pump	0,19	0,89
E.D	240	hr	Desiccator	0,09	21,60
E.F	24	hr	Fridge	0,08	1,92
M.PD	4	unit	Petri dish	1,33	5,32
P.CE	20	hr	Chemical engineer	18,00	360,00
P.LT	3	hr	Laboratory Technician	12,60	37,80
	2	%	Direct costs		36,10
				Total	1841,07

---

### Subchapter 1.3 Degradation of the samples

Code	Quantity	Unit	Description	Unitary Price (€)	Cost (€)
M.AT	1	unit	Aluminium tweezers	2,00	2,00
M.PP	1	unit	Pasteur pipette 1000 $\mu$ L	11,50	11,50
M.vial10	168	unit	10 mL vials	0,10	16,80
M.VL	168	unit	10 mL vial lid	0,01	1,68
M.WG	1	unit	Watch glass	2,99	2,99
E.APB	5	hr	Analytical precision balance	0,20	1,00
E.UPS	1700	hr	Universal precision stove	0,98	1666,00
M.CT	56	unit	Cable tie	0,10	5,60
M.FP	2	unit	Filter paper	0,05	0,10
M.H	1	unit	Hammer	15,00	15,00
M.T5	1	unit	5mm troquel	1,55	1,55
M.TB	1	unit	Troquel base	20,00	20,00
M.ISO1000	2	unit	1L ISO bottle	6,99	13,98
R.HA	0,02	L	Hydrochloric acid	85,90	1,72
R.SH	0,03	kg	Sodium hydroxide pellets	106,00	3,18
R.DW	0,58	L	Distilled water	0,20	0,12
E.PHM	0,5	hr	pH-meter	0,12	0,06
P.CE	20	hr	Chemical engineer	18,00	360,00
	2	%	Direct costs		42,47
				Total	2165,74

## Chapter 2. Physicochemical characterization

---

### Subchapter 2.1 Weight loss and equilibrium water content

Code	Quantity	Unit	Description	Unitary Price (€)	Cost (€)
M.AT	1	unit	Aluminium tweezers	2,00	2,00
M.WG	1	unit	Watch glass	2,99	2,99
E.APB	10	hr	Analytical precision balance	0,20	2,00
M.FP	7	unit	Filter paper	0,05	0,35
M.vial10	168	unit	10 mL vials	0,10	16,80
R.DW	1	L	Distilled water	0,20	0,20
E.OVP	0,17	hr	Oil vacuum pump RZ2	0,19	0,03
E.D	1557	hr	Desiccator Vacuo-Temp	0,09	140,13
P.CE	10	hr	Chemical engineer	18,00	180,00
	2	%	Direct costs		6,89
				Total	351,39

---

Subchapter 2.2 Scanning electron microscopy

Code	Quantity	Unit	Description	Unitary Price (€)	Cost (€)
M.vial10	56	unit	10 mL vials	0,10	5,60
E.SEM	13	hr	Scanning electron microscope	1,49	19,37
M.C	1	unit	Cutter	1,30	1,30
M.AP	4	unit	Aluminium platform	5,10	20,40
P.LT	3	hr	Laboratory Technician	12,60	37,80
P.CE	16	hr	Chemical engineer	18,00	288,00
	2	%	Direct costs		7,45
				Total	379,92

---

Subchapter 2.3 Differential scanning calorimetry

Code	Quantity	Unit	Description	Unitary Price (€)	Cost (€)
			Differential scanning calorimeter		
E.DSC	80	hr	Mettler Toledo	0,55	44,00
E.SR	80	hr	Sample robot	0,12	9,60
M.LND	4	unit	Liquid Nitrogen Dewar 150L	50,00	200,00
M.C	1	unit	Cutter	1,30	1,30
E.APB	10	hr	Analytical precision balance	0,20	2,00
M.AC	123	unit	Aluminium Capsules	2,83	348,09
M.N	1	unit	Needle	0,10	0,10
M.AT	1	unit	Aluminium tweezers	2,00	2,00
E.E	1	hr	Encapsulator	0,10	0,10
P.LT	2	hr	Laboratory Technician	12,60	25,20
P.CE	8	hr	Chemical engineer	18,00	144,00
	2	%	Direct costs		15,53
				Total	791,92

---

Subchapter 2.4 X-ray calorimetry

Code	Quantity	Unit	Description	Unitary Price (€)	Cost (€)
E.XRD	3	hr	X-ray diffractometer	0,51	1,53
P.LT	3	hr	Laboratory Technician	12,60	37,80
	2	%	Direct costs		0,79
				Total	40,12

## Chapter 3. Laboratory health and safety

Subchapter 3.1 Washing of apparatus					
Code	Quantity	Unit	Description	Unitary Price (€)	Cost (€)
R.DW	5	L	Distilled water	0,20	1,00
R.A	2	L	Acetone SCHARLAB	9,00	18,00
R.E	2	L	Ethanol SCHARLAB	32,40	64,80
M.CP	1	unit	Paper roll	2,00	2,00
P.CE	3	hr	Chemical engineer	18,00	54,00
	2	%	Direct costs		2,80
				Total	142,60

Subchapter 3.2 Waste treatment					
Code	Quantity	Unit	Description	Unitary Price (€)	Cost (€)
M.ZB	20	unit	Zip bags	0,20	4,00
	2	%	Direct costs		0,08
				Total	4,08

## Chapter 4. Meetings and project accomplishment

Subchapter 4.1 Project planning and management					
Code	Quantity	Unit	Description	Unitary Price (€)	Cost (€)
P.PD	8	hr	Project Director	24,00	192,00
P.CE	8	hr	Chemical engineer	18,00	144,00
	2	%	Direct costs		6,72
				Total	342,72

Subchapter 4.2 Project monitoring and control meetings					
Code	Quantity	Unit	Description	Unitary Price (€)	Cost (€)
P.PD	21	hr	Project Director	24,00	504,00
P.CE	21	hr	Chemical engineer	18,00	378,00
	2	%	Direct costs		17,64
				Total	899,64

Subchapter 4.3 Revision and corrections					
Code	Quantity	Unit	Description	Unitary Price (€)	Cost (€)
P.PD	10	hr	Project Director	24,00	240,00
P.CE	10	hr	Chemical engineer	18,00	180,00
	2	%	Direct costs		8,40
				Total	428,4

Subchapter 4.4 Project accomplishment					
Code	Quantity	Unit	Description	Unitary Price (€)	Cost (€)
P.CE	182	hr	Chemical engineer	18,00	3276,00
	2	%	Direct costs		65,52
				Total	3341,52

## Chapter 5. Personal protective equipment and security

### Subchapter 5.1 Personal protection equipment

Code	Quantity	Unit	Description	Unitary Price (€)	Cost (€)
M.LC	1	unit	Laboratory coat	15,50	15,50
M.LG	2	unit	Latex gloves box	5,85	11,70
M.NG	0,4	unit	Nitrile gloves box	7,29	2,92
M.LG	1	unit	Laboratory glasses	8,00	8,00
M.GM	1	unit	Gas mask	40,30	40,30
M.DM	1	unit	Dust mask	10,00	10,00
	2	%	Direct costs		1,77
				Total	90,18

## 5. Project budget by chapters

### Chapter 1 - Sample synthesis

Code	Description	Cost (€)
1.1	Selection of a suitable solvent	134,39
1.2	Trial and error experiments and final synthesis technique	1841,07
1.3	Degradation of the samples	2165,74

### Chapter 2 - Physicochemical characterization

Code	Description	Cost (€)
2.1	Weight loss and equilibrium water content	351,39
2.2	Scanning electron microscopy	379,92
2.3	Differential scanning calorimetry	791,92
2.4	X-ray diffractometer	40,12

### Chapter 3 - Laboratory health and safety

Code	Description	Cost (€)
3.1	Washing of apparatus	142,60
3.2	Waste treatment	4,08

### Chapter 4 - Meetings and project accomplishment

Code	Description	Cost (€)
4.1	Project planning and management	342,72
4.2	Project monitoring and control meetings	899,64
4.3	Revision and corrections	428,40
4.4	Project accomplishment	3341,52

### Chapter 5 - Personal protective equipment and security

Code	Description	Cost (€)
5.1	Personal protective equipment	90,18

## 6. Budget of material and contractual execution

Code	Description	Cost (€)
Chapter 1	Sample synthesis	4141,20
Chapter 2	Physicochemical characterization	1563,35
Chapter 3	Laboratory health and safety	146,68
Chapter 4	Meetings and project accomplishment	5012,28
Chapter 5	Personal protective equipment and security	90,18
<b>Budget of material execution</b>		<b>10953,68</b>
7% overhead and tax charges		766,76
0% industrial benefit		0
<b>Sum</b>		<b>11720,44</b>
21% VAT		2461,29
<b>Budget for contractual execution</b>		<b>14181,73</b>

The budget for contractual execution ascends to the price of fourteen thousand, one hundred and eighty one Euros and seventy three Eurocents.